Universidad de Oviedo

Programa de Doctorado en Biomedicina y Oncología Molecular

Tesis Doctoral

Study of the immune response in the context of antitumor therapeutic strategies

Seila Lorenzo Herrero

Oviedo, 2019

Universidad de Oviedo

Programa de Doctorado en Biomedicina y Oncología Molecular

Tesis Doctoral

Study of the immune response in the context of antitumor therapeutic strategies

Seila Lorenzo Herrero

Oviedo, 2019

Directores:

Segundo González Rodríguez y Alejandro López Soto

Universidad de Oviedo
Universidá d'Uviéu
University of Oviedo

RESUMEN DEL CONTENIDO DE TESIS DOCTORAL

1.- Título de la Tesis	
Español/Otro Idioma: Estudio de la respuesta inmunitaria en el contexto de estrategias terapéuticas antitumorales	Inglés: Study of the immune response in the context of antitumor therapeutic strategies

2.- Autor	
Nombre: Seila Lorenzo Herrero	DNI/Pasaporte/NIE:
Programa de Doctorado: Biomedicina y Oncología Molecular	
Órgano responsable: Instituto Universitario de Oncología del Principado de Asturias (IUOPA)	

RESUMEN (en español)

En la presente Tesis, hemos estudiado diferentes estrategias terapéuticas antitumorales con el objetivo de determinar su eficacia en el tratamiento del cáncer. En la primera parte del trabajo, hemos empleado muestras de pacientes con leucemia linfática crónica (LLC), un cáncer hematológico de linfocitos B caracterizado por una acentuada inmunosupresión, para estudiar el interés terapéutico de nuevos compuestos en esta malignidad. Hemos observado que EC-7072, un análogo de mitramicina A, cuenta con actividad antileucémica *ex vivo* independiente de la presencia de alteraciones citogenéticas típicamente asociadas a resistencia a terapia. Cabe destacar que el compuesto no afectó marcadamente a poblaciones inmunes sanas [linfocitos T y células *natural killer* (NK)]. Experimentos adicionales mostraron que EC-7072 provoca una desregulación notable de la vía de señalización de *B cell receptor* (BCR), que es crucial para la supervivencia de las células leucémicas. Por ello, EC-7072 podría constituir una nueva terapia dirigida en LLC. A continuación, dada la importancia de la vía del BCR en LLC, hemos estudiado su implicación en la supresión de la respuesta inmune. La activación de la señalización por BCR en linfocitos B sanos produjo una reducción en la expresión de NKG2D, un receptor activador clave expresado tanto en células NK como en linfocitos T $CD8^+$ mediada por factores solubles. En consonancia, se detectó una disminución de la capacidad citotóxica de células NK enfrentadas a células tumorales, estableciendo un vínculo entre la activación de los linfocitos B y la supresión de respuestas efectoras antitumorales. El bloqueo de la señalización inducida por los factores solubles que median este efecto podría constituir una nueva estrategia para potenciar la activación del sistema inmune en malignidades de linfocitos B. En la segunda parte del trabajo, hemos analizado el efecto de compuestos antimitóticos, empleados de forma convencional como quimioterápicos antitumorales, en el perfil inmunogénico de las células cancerígenas *in vitro*. Tras el tratamiento con estos compuestos, se observó una inducción de la expresión de ligandos activadores de las células NK, que se correlacionó con un estímulo de la lisis de células tumorales mediada por esta población inmune. Este efecto estaba producido principalmente por la activación de ATM y, de forma secundaria, por vías de señalización del llamado estrés de retículo endoplasmático. En conjunto, nuestros hallazgos ponen de manifiesto que la inducción de la hiperploidía en células tumorales favorece su reconocimiento y eliminación por el sistema inmune, fundamentalmente por las células NK, abriendo las puertas a tratamientos que modulan la ploidía tumoral como agentes inmunoestimuladores en pacientes con cáncer.

Universidad de Oviedo
Universidá d'Uviéu
University of Oviedo

RESUMEN (en Inglés)

In the Thesis herein, we have studied distinct antitumor therapeutic approaches with the aim to unravel their potential efficacy in cancer treatment. In the first part of this work, we have studied samples from patients with chronic lymphocytic leukemia (CLL), a B-cell hematologic malignancy characterized by an intense immunosuppression, to unveil novel drugs with potential therapeutic interest for this cancer. We found that EC-7072, an analog of mithramycin A, displays high antileukemic activity in CLL *ex vivo* independently of cytogenetic alterations typically associated to treatment resistance. Interestingly, the compound did not markedly affect healthy immune subsets (T cells and natural killer (NK) cells). Further investigation unraveled that EC-7072 exerted a profound dysregulation of the B cell receptor (BCR) signaling pathway, which is central for leukemia cell survival. Thus, EC-7072 may represent a novel targeted treatment in CLL. Afterwards, given the importance of the BCR pathway in CLL, we evaluated its role in immunosuppression. Stimulation of BCR signaling in healthy B cells downregulated surface expression of NKG2D, a key NK cell activating receptor, on NK cells and $CD8^+$ T cells via soluble factors. In agreement, NK cell cytotoxicity against tumor cells was hindered in these conditions, establishing a link between B cell activation and suppression of cytotoxic antitumor immune responses. Therefore, disruption of the molecular events activated by soluble factors mediating this effect might constitute a novel strategy to boost immune responses in B-cell malignancies. On the second part of this work, we have analyzed the impact of antimitotic drugs, which are conventionally employed in anticancer chemotherapies, on the immunogenic profile of tumor cells *in vitro*. An upregulation in the tumor expression of NK cell activating ligands was observed upon treatment with the compounds studied, which correlated with increased NK cell-mediated elimination of cancer cells. This upregulation was mainly driven by ATM activation and partially mediated by endoplasmic reticulum stress signaling pathways. Overall, these data bring to light that inducing hyperploidy in tumor cells favors their immune recognition and clearance, mainly by NK cells, opening a window for treatments modulating cancer cell ploidy as immunotherapeutic agents for cancer treatment.

SR. PRESIDENTE DE LA COMISIÓN ACADÉMICA DEL PROGRAMA DE DOCTORADO EN BIOMEDICINA Y ONCOLOGÍA MOLECULAR

INTRODUCTION

Cancer and immune system: an overview

The term *cancer* comprises a group of malignancies characterized by abnormal and uncontrolled growth of certain cells within the body. There are more than 200 types of cancer registered to date and they are traditionally classified by cell and/or tissue of origin, being lung and breast cancer the most prevalent cancers worldwide (Bray et al., 2018). Cancer is the leading cause of death in a great number of countries and its incidence is rapidly increasing throughout the globe with 18.1 million new cases registered in 2018 (Bray et al., 2018). A wide collection of environmental risk factors are associated to cancer development, from exposure to carcinogens to alcohol consumption, obesity or even viral infections. Although the environment and lifestyle are crucial factors in tumor incidence, it should be pointed that around 5-10% of tumors are caused by inherited genetic mutations, such is the case of mutations in *BRCA1* and *BRCA2* genes, associated to breast and ovarian cancer (King, Marks, Mandell, & New York Breast Cancer Study, 2003).

Tumors usually arise from a localized tissue, yet, as a consequence of cancer progression, tumor cells can eventually invade surrounding healthy areas as well. Further, tumor cells can migrate from their niche to distant tissues in a process known as metastasis. The transformation of normal cells to highly malignant and actively dividing counterparts is still a field subjected to intense research. The causes of malignant transformation are variable depending on the tumor although it has been defined as a multistep process. Nonetheless, genetic alterations appear to play such a pivotal role in tumorigenesis that they are considered an enabling characteristic of cancer (Hanahan & Weinberg, 2011). Genomic instability and accumulation of DNA damage lead to mutant genotypes, some of which show selective advantages that favor tumorigenesis. In precancerous lesions, malignantly transformed cells acquire distinct functional capabilities, commonly known as hallmarks of cancer, that allow tumor establishment and development (Figure 1) (Hanahan & Weinberg, 2000, 2011).

These hallmarks generally promote the adaptation of the cellular homeostasis to support a highly proliferative state, which encompasses evading growth suppressors and modifying cell metabolism, among others. A classic example of metabolic reprogramming is the glycolytic switch suffered by tumor cells to cope with their increased bioenergetic demand. This metabolic signature, called the Warburg effect, favors aerobic glycolysis over oxidative phosphorylation (Pavlova & Thompson, 2016). Stressed and malignantly transformed cells are usually eliminated by intracellular control mechanisms that trigger programmed cell death via apoptosis. However, tumor cells develop strategies to overcome those proapoptotic responses, being the most common the loss of p53 tumor suppressor function, a central damage sensor (Kastenhuber & Lowe, 2017). Resistance to apoptosis is therefore a feature of many types of cancer, such as chronic lymphocytic leukemia, a hematological malignancy that will be further reviewed in this work (see *Chronic Lymphocytic Leukemia*).

Figure 1. The Hallmarks of Cancer. Functional capabilities acquired by tumor cells that are linked to cancer establishment and progression. Modified from Hanahan & Weinberg, 2011.

Tumor modifications linked to growth and progression advantages not only affect intrinsic cellular processes, but also take part in the crosstalk between the tumor and its surrounding microenvironment (e.g. inducing angiogenesis). The immune system plays a double-edged role in tumor formation and development and this crucial interplay has become part of the hallmarks of cancer (Figure 1). Premalignant lesions show high immune infiltration due to their disrupted homeostasis, which translates into activation of antitumor immune responses and chronic inflammation. Incipient tumors evolve different strategies to evade immune-mediated elimination, promoting, for example, T cell dysfunction via overexpression of ligands for inhibitory receptors like programmed cell death ligand 1 (CD274, best known as PD-L1) or cytotoxic T-lymphocyte-associated antigen 4 (CD152, best known as CTLA-4) (Wherry & Kurachi, 2015). NK cells become exhausted as well during tumor progression as a consequence of checkpoint receptor engagement (Sivori et al., 2019). This immune cell exhaustion is characteristic of the vast majority of tumors and is usually linked to general immunosuppression. During the last few years, this evasion strategy has prompted the development of a new antitumor therapeutic approach, known as immune checkpoint blockade (ICB), based on inhibitors of these regulatory checkpoints or their ligands. An overview of the current state of the management and treatment options in patients with cancer will be further reviewed (see *Anticancer therapies*). Contrastingly, proinflammatory immune cells contribute to tumor establishment by creating the ideal conditions for a protumoral niche, supporting neoplastic growth or modulating physiological processes like vascular remodeling (Grivennikov, Greten, & Karin, 2010). Presence of infiltrating tumor-associated macrophages, myeloid-derived suppressor cells (MDSCs) or regulatory T (Treg) cells potentiates tumor initiation. Concomitantly, mouse

models with attenuated innate immune cell functions exhibited restricted tumor growth and invasion, further supporting the relevance of inflammation as a protumoral process (de Visser, Eichten, & Coussens, 2006). Altogether, the complex interactions suffered by neoplastic cells throughout tumorigenesis and the functional capabilities they acquire conform the biology of the incipient tumor and influences its behavior at advanced stages.

Cell ploidy in cancer

Aside from the hallmarks of cancer, considered crucial for cancer progression, a typical feature of early-arising cancer cells is polyploidization, defined as an increase in the usual number of chromosomes by whole-number multiples (Davoli & de Lange, 2011; Gordon, Resio, & Pellman, 2012). Human cells are commonly diploid (2n), that is, they count with two genome copies. Still, some specialized cell types can be haploid (n), such as gametes, and tetraploid (4n) cells can be found in tissues with high proliferation rates, like liver and placenta. Actually, polyploidy (>2n) is a frequent trait of certain species, mainly plants. Polyploidization can be achieved by three different mechanisms: cell fusion, endoreplication, a version of the cell cycle in which the cell skips precise stages of the mitosis, and abortive cell cycle (Figure 2) (Storchova & Pellman, 2004). Anti-mitotic drugs, which were employed in the present work, can induce hyperploidy (>2n, a chromosome number higher than the normal diploid, not necessarily whole-multiple) via impairment of cytokinesis and subsequent abortion of the cell cycle.

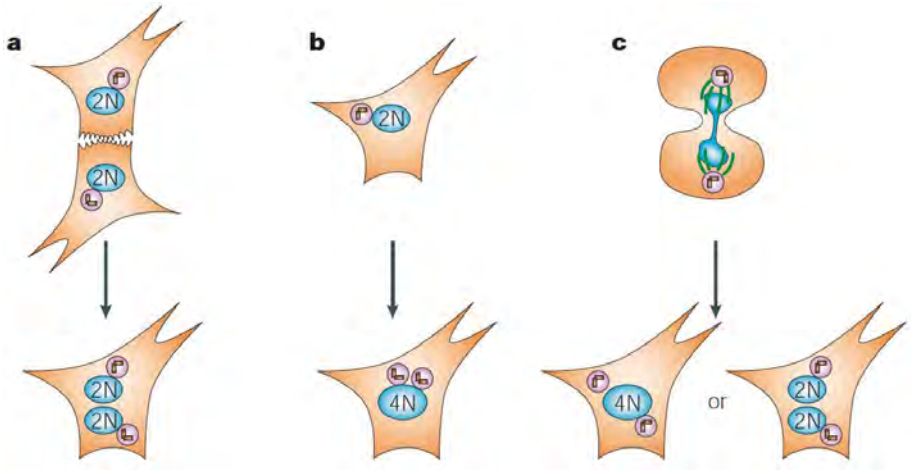

Figure 2. Main mechanisms of polyploidization. a. Cell fusion. **b.** Endoreplication. **c.** Abortive cell cycle. Modified from Storchova & Pellman, 2004. N: number of genome copies.

Changes in cell ploidy are not only a consequence of physiological processes, but have also been related to disease. Aberrant DNA content can lead to cell cycle arrest and finally trigger apoptosis to remove the stressed cell when the damage is beyond repair (Barnum & O'Connell, 2014). One of the stress response programs that are activated under these circumstances is p53 tumor suppressor

signaling, the so-called *guardian of the genome* due to its role as a stress signal integrator. Retinoblastoma (Rb) stands as another essential cell cycle checkpoint that controls genomic integrity. In the context of tumorigenesis, events such as inactivation of p53 or Rb lead to the appearance of tumor cells with complex karyotypes (>2n), usually tetraploids at first. These changes in the chromosome content translate into genomic instability, a hallmark that, in turn, favors tumor initiation and acquisition of other functional capabilities, as already mentioned. Loss of p53 is a classical feature of more than half of registered tumors and *TP53* is one of the most frequently mutated genes in cancer, once more highlighting its pivotal role as tumor suppressor (Ozaki & Nakagawara, 2011).

Recent work unraveled that DNA ploidy is greatly controlled by extrinsic mechanisms, mainly operated by the immune system (Senovilla et al., 2012). Tumor cells with extra chromosomes are more immunogenic, rendering them more susceptible to immune recognition and elimination. The control exerted by the immune system against tumors in general and specifically against tumor cells with complex karyotypes is an issue that will be further discussed in the present work (see *Cancer immunosurveillance*).

Cancer immunosurveillance

The immune system exerts a constant surveillance to defend the organism against foreign threats, such as infections, but also to avoid internal damage caused by cells undergoing stress or malignant transformation. The immune system is comprised by two different branches, innate and adaptive, that cooperate to accomplish this antitumor control. Innate cells are the first to arrive to the affected tissue and provide the necessary signals to recruit adaptive immune cells. Pre-malignant lesions normally display disrupted homeostasis that leads to cells stress, hence promoting immune cell infiltration and activation of inflammatory responses. At this point, the immune system and the nascent tumor establish a crosstalk that ultimately resolves in tumor clearance or tumor progression. This is widely-known as the *cancer immunoediting* process, since the immune system not only safeguards the organism against tumors, but also shapes the immunogenic profile of the tumor (Dunn, Bruce, Ikeda, Old, & Schreiber, 2002; Schreiber, Old, & Smyth, 2011). There are three consecutive phases within this immunoediting (Figure 3).

- Elimination. The innate and adaptive components of the immune system cooperate to eradicate incipient tumors before they become clinically visible. The mechanisms underpinning tumor clearance essentially encompass the recognition of danger signals derived from malignant transformation, such as the exposure of stress-induced molecules or tumor antigens on the surface of the cancer cell, that activate antitumor immune responses.

- Equilibrium. Resistant tumor clones can evade immune destruction during the elimination phase. As a result, the immune system interacts with the remaining tumor cells in a dynamic equilibrium, controlling tumor growth and *sculpting* its immunogenicity. During this dormant state, the genomic instability intrinsic to cancer favors the generation of new tumor cell variants with different immunogenic profiles. The immune system recognizes and removes the highly-immunogenic clones, therefore allowing the outgrowth of aggressive tumor variants with acquired immunoevasive mechanisms.
- Escape. Tumor clones resistant to immune detection overcome the immune control and emerge as visible tumors. Tumor escape is normally a consequence of the modifications produced in the tumor population by immunoediting, yet it can be favored by changes in the immune system in response to tumor-induced immunosuppression or external factors as well. Several mechanisms of immune evasion have been reported, including the downregulation of antigen presentation by major histocompatibility complex class I (MHC-I) molecules, a feature that activates natural killer (NK) cell-mediated antitumor responses and can actually be detrimental to tumor progression (see *The role of NK cells in cancer immunosurveillance*).

Effector immune cells take an active part in the immunoediting process, but other immune cell subsets intervene as well. NK cells, together with natural killer T (NKT) cells and dendritic cells (DCs) are the first line of defense, usually in charge of eradicating developing tumors and activating adaptive immune responses mediated by infiltrating effector $CD8^+$ and $CD4^+$ T cells. Contrastingly, Treg cells and MDSCs are two key subsets recruited by tumor cells due to their immunosuppressive properties. Tumor infiltration of these regulatory immune cells is detrimental to antitumor surveillance and facilitates the progression from equilibrium to tumor escape. Collectively, the intratumor balance of distinct immune subsets determine the evolution of the immunoediting process and can tip the scale towards tumor clearance or growth (Quezada, Peggs, Simpson, & Allison, 2011; Schreiber et al., 2011).

The role of NK cells in cancer immunosurveillance

NK cells are a subset of immune cells that play a central part in the innate immune response. Their primary function is to detect and eliminate damaged or stressed cells, such as those undergoing virus infections or malignant transformation (Vivier, Tomasello, Baratin, Walzer, & Ugolini, 2008). Accordingly, NK cells cooperate in the control of tumorigenesis, being capable of arresting tumor growth and, sometimes, leading to its complete eradication. Further, NK cells display a potent antimetastatic activity and can hamper tumor spreading and survival of disseminated cells (Lopez-Soto, Gonzalez, Smyth, & Galluzzi, 2017).

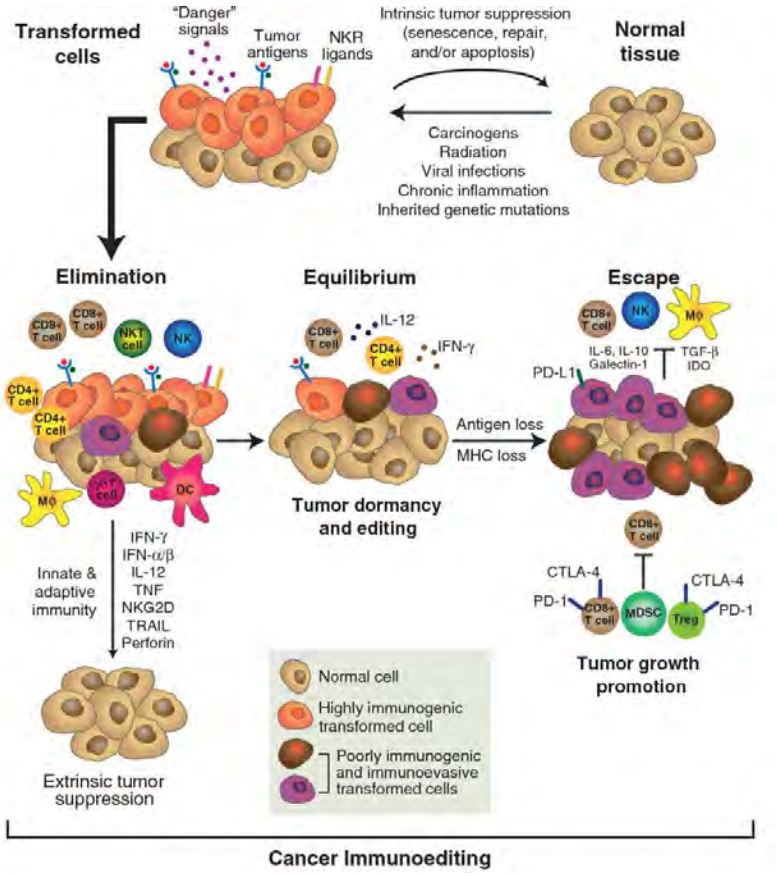

Figure 3. The three phases of cancer immunoediting. Early tumors establish a dynamic crosstalk with the immune system that consist of three subsequent steps. During the *elimination* phase, the immune control detects and eliminates the tumor before it is clinically detectable. If the immune system fails to destroy a fraction of the tumor cells, the immunoediting evolves to an *equilibrium* phase. Tumor growth is controlled and the immune system sculpts the immunogenicity of the tumor, eliminating the more immunogenic variants. At some point, tumor clones resistant to immune destruction *escape* immunosurveillance and progress into a clinically visible tumor. Obtained from Schreiber, Old & Smyth, 2011.

NK cells are characterized by their dynamic cytotoxic activity against misbehaving cells that relies on a process called *degranulation*. Preformed granules containing cytolytic proteins are stored in the cytoplasm of NK cells and, upon recognition of a target cell, are released into the immunological synapse established. The cytolytic proteins, mainly perforin and granzymes, are responsible for triggering the apoptotic cell death of the target. At the same time, activated NK cells secrete cytokines (e.g. IFN-γ, TNF-α) that stimulate adaptive immune responses.

Unlike T and B lymphocytes, NK cells do not exert antigen-driven responses. The activation state of NK cells is dictated by a tight balance of signals provided by an array of inhibitory and activating surface receptors (Pegram, Andrews, Smyth, Darcy, & Kershaw, 2011). Accordingly, the induction of NK cell function is achieved via two different scenarios (Figure 4).

- *Missing self*. NK cell inhibitory receptors recognize self-molecules ubiquitously expressed in healthy tissues, preventing inappropriate NK cell activation and ensuring the protection of healthy cells (Figure 4a). These transmembrane receptors signal through intracellular immunoreceptor tyrosine-based inhibitory motifs (ITIMs), located in the cytoplasmic tail of the molecule. There are two main families of NK cell inhibitory receptors: killer immunoglobulin-like receptors (KIR), which selectively bind to classical MHC class I molecules, and CD94-NKG2 heterodimer receptors, which recognize non-classical MHC molecules (Sivori et al., 2019). Among the latter, CD94-NKG2A is the only member with inhibitory potential, since CD94-NKG2C and -E bear no ITIMs (Borrego, Masilamani, Marusina, Tang, & Coligan, 2006). Additionally to classical receptors, NK cells are inhibited through engagement of co-inhibitory receptors as well, like PD-1 or CD96. Downregulation or loss of surface expression of MHC molecules is a prototypical evasion strategy acquired by arising tumors, partially induced by the selective pressure caused by effector T cell action. In this case, NK cells stop receiving inhibitory signals and unfold their cytotoxic potential, killing the tumor cell (Figure 4b) (Morvan & Lanier, 2016).

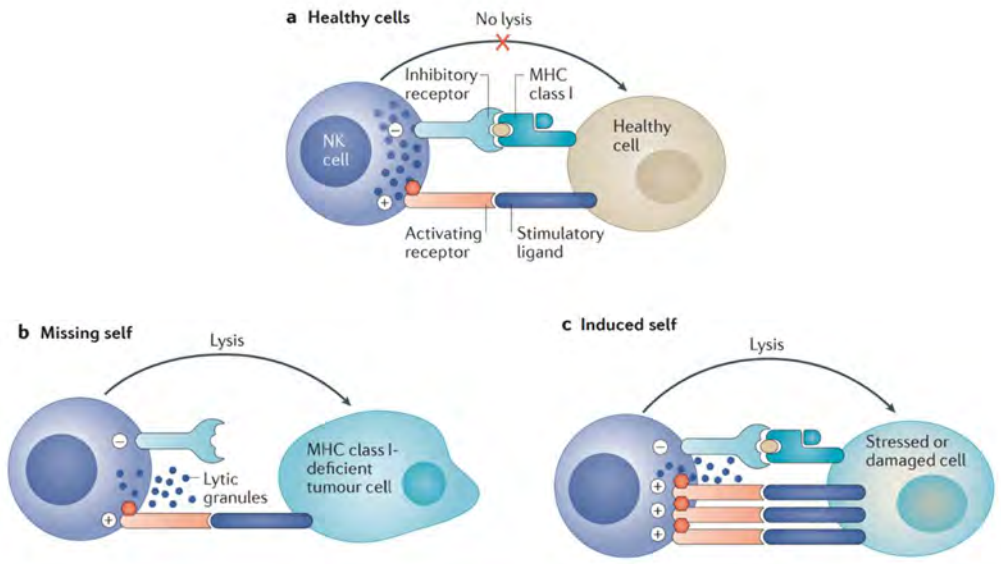

Figure 4. Regulation of NK cell activation. NK cell function is controlled by a delicate balance of signals transduced by a collection of inhibitory and activating receptors. **a.** Healthy cells provide inhibitory signals through their MHC-I molecules and express low or non-existent levels of stimulatory ligands, therefore avoiding NK cell detection. **b.** Loss of MHC-I molecules, a strategy commonly acquired by tumor cells to avoid T cell recognition, triggers NK cell activation, owing to the lack of inhibitory signals. **c.** Ligands for NK cell activating receptors are upregulated in conditions of cell stress, including tumorigenesis, thus NK cell inhibition is overcome upon encounter with these tumor cells, promoting NK cell-mediated lysis. Modified from Morvan & Lanier, 2016.

- *Induced self*. NK cells can be activated through activating receptors if they receive a strong signal that overcomes their inhibition (Figure 4c). These receptors transduce the activating signals

through interaction with specific adaptor proteins containing immunoreceptor tyrosine-based activating motifs (ITAMs). NK cells express a wide repertoire of activating receptors that interact with specific ligands present on the surface of stressed, damaged and transformed cells (Table 1) (Sivori et al., 2019). Tumorigenesis is linked to induced expression of activating ligands, rendering tumor cells more susceptible to NK cell-mediated clearance, whereas healthy cells usually express low levels of these surface molecules, further protecting them from NK cell attack.

Table 1. Natural killer cell activating receptors and their ligands.

Receptor	*CD name*	*Confirmed ligands*
NKG2D	CD314	MICA/B, ULBP1-6
DNAM-1	CD226	Nectin-2 (CD112), PVR (CD155)
NKp30	CD337	B7-H6
NKp44	CD336	unknown
NKp46	CD335	unknown

Natural killer group 2, member D (KLRK1, best known as NKG2D) probably stands as the best-characterized NK cell receptor and has a crucial role in cancer immunosurveillance. Apart from NK cells, it is expressed by the vast majority of $CD8^+$ T cells, γδ T cells and NKT cells and by some subsets of $CD4^+$ T cells (Raulet, 2003). In humans, NKG2D signals via the adaptor protein DNAX-activating protein of 10 kDa (DAP10), followed by recruitment of phosphatidylinositol 3-kinase (PI3K) and the complex Grb2-Vav1 (Upshaw et al., 2006). The human NKG2D receptor recognizes a collection of ligands that are structurally related to MHC-I molecules and comprise two families: the MHC class I chain-related protein A (MICA) and B (MICB) family, and the UL16-binding proteins (ULBPs) family, with six members (ULBP1-6) (Huergo-Zapico, Acebes-Huerta, Lopez-Soto, et al., 2014; Lopez-Soto, Huergo-Zapico, Acebes-Huerta, Villa-Alvarez, & Gonzalez, 2015). Several stress conditions have been reported to regulate the expression of NKG2D ligands (NKG2DLs), such as DNA damage (via ATM or ATR checkpoint kinases) or heat shock (via HSF1 transcription factor) (Lopez-Soto et al., 2015). A great number of signaling pathways triggered in response to stress are activated during tumorigenesis as well, hence providing a strong activating signal that allows the NK cell-mediated recognition and lysis of tumor cells (Raulet, Gasser, Gowen, Deng, & Jung, 2013). In advanced tumors, epithelial-mesenchymal transition (EMT) also stimulates NKG2DL expression on tumor cells, facilitating the control of metastasis by NK cells (Lopez-Soto et al., 2017; Lopez-Soto et al., 2013). *In vivo* studies showed that NKG2D-deficient mouse models had enhanced incidence of spontaneous tumors and accelerated tumor progression, further supporting the relevance of NKG2D in the control of tumor initiation (Guerra et al., 2008). Nonetheless, recent data in hepatocellular carcinoma models suggests that NKG2D might play a double-edged role in

inflammation-driven tumors, favoring a proinflammatory microenvironment and contributing to tumor growth (Sheppard et al., 2017).

DNAX accessory molecule-1 (DNAM-1) is another major receptor in NK cells that is also present in certain subsets of T cells and myeloid cells. Unlike NKG2D, crosslinking of DNAM-1 directly recruits Grb2 to transduce the activation signal to downstream effectors (Zhang et al., 2015). The human DNAM-1 ligands discovered so far are Nectin-2 and poliovirus receptor (PVR). Upregulation of these molecules has been reported in certain tumors and *Cd226*$^{-/-}$ mice suffer accelerated tumor growth, collectively evidencing that NK cell-mediated antitumor responses are also dictated by DNAM-1 signaling (Gilfillan et al., 2008; Iguchi-Manaka et al., 2008; Lakshmikanth et al., 2009). Similar to NKG2DLs, the expression of Nectin-2 and PVR is regulated by classical stress response pathways (Cerboni et al., 2014; Soriani et al., 2014; Soriani et al., 2009).

The other major group of NK cell activating receptors is known as natural cytotoxicity receptors (NCRs) and consist of three members: NKp30, NKp44 and NKp46. Each receptor has a different signaling cascade that initiates with coupling to FcεRI-γ (for NKp30 and NKp46) or DAP12 (for NKp44) adaptor proteins. Up to date, B7-H6 is the only described ligand for NKp30, whereas NKp44 and NKp46 ligands are less well characterized (Brandt et al., 2009). Still, NCRs can interact with molecules from diverse origin, such as pathogen-derived proteins, like neuraminidases, or cellular proteins exposed on the surface, like vimentin (Kruse, Matta, Ugolini, & Vivier, 2014; Sivori et al., 2019). B7-H6 expression has been detected in different types of cancer and certain tumor-associated proteins have been found to bind to NCRs (e.g. BAT3 to NKp30, PCNA to NKp46 and NKp44L to NKp44), which correlates with the abrogation of NK cell-mediated tumor cell lysis detected in the presence of anti-NCR blocking antibodies (Baychelier et al., 2013; Brandt et al., 2009; Kruse et al., 2014; Pende et al., 1999; Pogge von Strandmann et al., 2007). This data suggests that signaling through NCRs contributes to the antitumor function of NK cells.

Despite the integrated network of activating signals that can induce NK cell-mediated killing, tumor cells have developed evasion mechanisms to promote NK cell dysfunction and circumvent the immune vigilance. The release of soluble ligands for NK cell receptors has emerged as one of the favorite immunosuppressive strategies acquired by tumors (Groh, Wu, Yee, & Spies, 2002; Pesce et al., 2015; Reiners et al., 2013; Salih, Rammensee, & Steinle, 2002). Shedding of NKG2DLs is accomplished by metalloproteases typically upregulated in tumorigenesis, a feature shared by B7-H6 that reduces the levels of exposed ligand (Schlecker et al., 2014; Waldhauer et al., 2008; Waldhauer & Steinle, 2006). In general, it has been reported that engagement of NKG2D by soluble isoforms of its ligands induces endocytosis and lysosomal degradation of the receptor, limiting NK cell activation (Groh et al., 2002; Song, Kim, Cosman, & Choi, 2006). Besides, downregulated

NKp30 expression correlated with high levels of soluble B7-H6 in several tumors, suggesting that engagement of soluble ligands might have a common impact on all NK cell receptors (Pesce et al., 2015; Semeraro et al., 2015).

Immunogenic cell death and tumor cell ploidy

Studies in tumor mouse models unveiled that certain chemotherapeutic agents triggered a modality of apoptotic cell death that, in turn, stimulated immune responses (D. R. Green, Ferguson, Zitvogel, & Kroemer, 2009; Zitvogel, Kepp, & Kroemer, 2011). Accordingly, the efficacy of these therapies rely on the antitumor potential of the immune system. Tumor cells succumbing to immunogenic cell death (ICD) expose intracellular proteins on the cell surface that act as *eat-me* signals, facilitating their uptake by DCs and subsequent antigen presentation to effector T cells (Figure 5) (D. R. Green et al., 2009). Upon treatment with IDC inducers, tumor cells particularly expose the endoplasmic reticulum (ER)-resident chaperone calreticulin (CRT) in a preapoptotic stage, followed by secretion of ATP and release of the nuclear protein high-mobility group box 1 (HMGB1) in advanced apoptotic stages. This soluble molecules act as *find-me* signals, recruiting professional phagocytes (Figure 5) (Kroemer, Galluzzi, Kepp, & Zitvogel, 2013; Obeid et al., 2007; Panaretakis et al., 2008). The exposure of CRT is caused by chemotherapy-induced ER stress, which is linked to increased phosphorylation of eukaryotic initiation factor 2α (eIF2α), one of the central effectors of the unfolded protein response (UPR) triggered upon ER stress (Garg et al., 2012; Panaretakis et al., 2009).

In the same line, hyperploid tumor cells exhibit elevated levels of ER stress, which translates in the exposure of CRT on the cell surface, mimicking the effect of ICD inducers and eliciting the engulfment of the tumor cell by phagocytes (Zanetti & Mahadevan, 2012). In fact, a seminal work from Senovilla *et al*. described that immunocompetent mice display reduced cancer development upon injection of hyperploid tumor cells than mice challenged with the diploid counterparts (Senovilla et al., 2012). Contrastingly, immunodeficient mice had similar tumor incidence independent of the ploidy of the tumor cells injected, corroborating that malignant cells with complex karyotypes are subjected to a strong immunosurveillance.

Cancer therapies

The adaptations suffered by pre-malignant and tumor cells along cancer development, together with the editing exerted by the immune system, shape tumor biology in a unique manner. Consequently, tumor behavior is highly dependent on its background, making each type of cancer a

disease on its own and complicating the design of therapeutic approaches with broad-spectrum clinical effectivity.

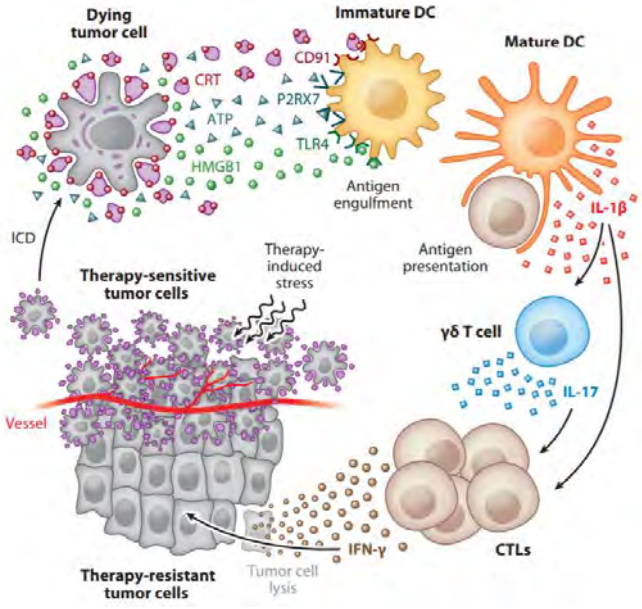

Figure 5. Hallmarks of immunogenic cell death in cancer. As a consequence of treatment with ICD inducers, tumor cells expose CRT on the surface, which is mediated by the activation of ER stress responses. This takes places in a preapoptotic stage and favors the phagocytosis of tumor cells by DCs. During the apoptotic process, tumor cells undergoing ICD release ATP and HMGB1 to the extracellular space, acting as chemoattractants to phagocytes. Collectively, antigen-loaded DCs stimulate antitumor T cell-mediated responses, which can ultimately lead to the eradication of the tumor. Obtained from Kroemer, Galluzi, Keep & Zitvogel, 2013.

Traditionally, cancer treatment has been based on methods that roughly target tumor cells, primarily represented by radiotherapy, chemotherapy and surgery. These approaches not always eliminate the whole tumor and the remaining cancer cells, typically resistant to treatment, can evolve into a more aggressive tumor. The lack of specificity is another major handicap in conventional anticancer treatments. Chemotherapeutic agents, for example, rely on the high proliferation rates of tumor cells, interfering with cell division or DNA synthesis, thus affecting healthy tissue as well and producing significant toxicity. Consequently, surgical resection still remains the most effective and tolerated option for the management of the majority of localized tumors.

Over the past decade, the field of cancer treatment has expanded towards the development of targeted therapies, which take advantage of intrinsic characteristics of the tumor and/or try to boost the immune system. As an illustration of the first, the small molecule inhibitor imatinib (Gleevec®), which selectively targets the BCR-ABL fusion protein, a hallmark harbored by the majority of patients with chronic myeloid leukemia (CML), has achieved long-lasting clinical responses and

improved overall survival rates, thus becoming the first-line treatment option for patients with CML (Moen, McKeage, Plosker, & Siddiqui, 2007). On the other hand, cancer immunotherapy stands out as an extensively studied and highly effective alternative to conventional cancer treatments. These targeted strategies seek the activation of antitumor immune responses in order to destroy the tumor and include approaches like monoclonal antibodies and adoptive cell transfer. Monoclonal antibodies (mAb) are a versatile therapeutic tool that act as markers, favoring tumor recognition by effector immune subsets, and/or hamper receptor-ligand interactions and, therefore, signal transduction (Figure 6). On one hand, mAbs can promote antibody-dependent cell-mediated cytotoxicity (ADCC). NK cells recognize the Fc regions of the antibodies when they are bound to antigens on the surface of tumor cells and release lytic proteins that kill the tumor cell (Figure 6a). This type of mAbs can frequently activate complement-dependent cytotoxicity as well. Nowadays, a wide myriad of ADCC-inducing mAbs is approved for the management of patients with cancer, like rituximab (anti-CD20) for non-Hodgkin's lymphoma or trastuzumab (anti-HER2) for breast cancer (Kimiz-Gebologlu, Gulce-Iz, & Biray-Avci, 2018). mAbs can also modulate immune activation via blockade of regulatory checkpoints, a clinical strategy commonly known as ICB therapy that aims to overcome T cell and NK cell exhaustion and stimulate effective antitumor responses (Figure 6b). CTLA-4 blocking antibodies were one of the first immune checkpoint inhibitors clinically developed, followed by antibodies targeting the PD-L1/PD-1 axis, some of which are currently approved for the treatment of certain types of cancer owing to their promising clinical results (Wei, Duffy, & Allison, 2018). Recent studies have unveiled the inhibitory role of other proteins expressed by tumor-reactive effector immune cells and the therapeutic potential of inhibiting these molecules is being assessed in pre-clinical and clinical trials (Park, Kuen, & Chung, 2018). These newly targeted checkpoints include molecules such as lymphocyte-activation gene 3 (LAG-3) (Andrews, Marciscano, Drake, & Vignali, 2017; Wierz et al., 2018), natural killer group 2, member A (NKG2A) (Andre et al., 2018; Sun et al., 2017) or T cell immunoreceptor with Ig and ITIM domains (TIGIT) (Guillerey et al., 2018; Johnston, Yu, & Grogan, 2015). Despite the remarkable success of ICB therapy, response rates remain limited with a great fraction of patients being non-responders or acquiring resistances, leaving room for alternative approaches and combination therapy.

Of note, other cancer immunotherapies are gaining attention as a result of their unexpected efficacy in preliminary studies and clinical trials. Oncolytic viruses have largely proven their potential promoting tumor-specific ICD that, in turn, stimulates successful antitumor immune responses. Up to date, the oncolytic virus T-VEC has been approved by the FDA (Food and Department Administration) for the treatment of advanced melanoma (Perez et al., 2018). Adoptive cell transfer is another type of immunotherapy and consists of *ex-vivo* expansion of tumor-reactive T cells that are then transferred back to the patient. This includes chimeric antigenic receptor (CAR)-

T cell therapy that employs engineered T cells expressing a tumor antigen-specific CAR, thus redirecting effector T cells responses towards a defined target cell. This approach is mostly limited to the treatment of hematological malignancies for the moment, since the low infiltration of CAR-T cells in solid tumors reduces the clinical efficacy in these cases (Miliotou & Papadopoulou, 2018).

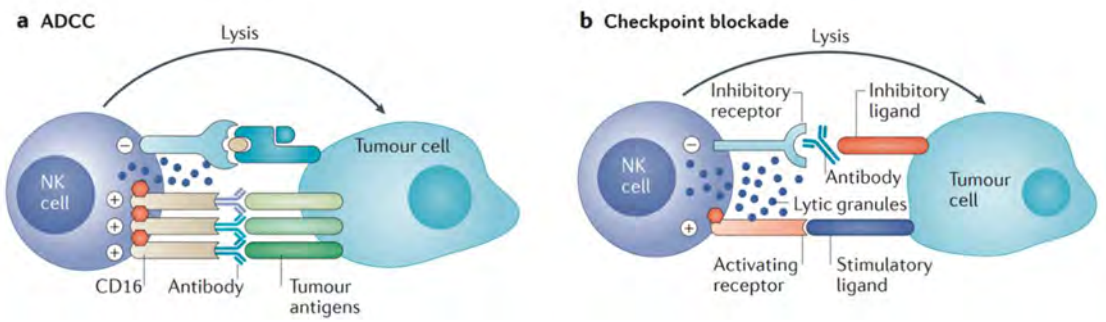

Figure 6. Representative mechanisms of action exerted by therapeutic monoclonal antibodies. a. Engagement of specific antigens on the surface of tumor cells expose the Fc region of mAbs allowing the recognition by the CD16 receptor of NK cells. This provides an activation signal that triggers NK cell-mediated lysis of the tumor cell. **b.** Disruption of checkpoint receptor-ligand interaction by mAbs turns off the inhibition imposed by tumor cells to effector immune subsets, thus allowing the activation of antitumor responses. Modified from Morvan & Lanier, 2016.

Altogether, the encouraging results obtained with immunotherapy in cancer management once more bring to light the superior potential of the immune system in tumor clearance compared to other approaches. Nonetheless, further research in the field of cancer immunotherapy is still necessary in order to improve response rates in patients and overcome the clinical and molecular barriers that limit the efficacy of immunotherapy.

Chronic lymphocytic leukemia

Chronic lymphocytic leukemia (CLL) belongs to the subgroup of hematological cancers and it is the most common adult leukemia in Western countries, accounting for about one third of all the newly diagnosed cases of leukemia (4.7 per 100,000) (Bray et al., 2018). CLL is considered a disease of the elderly, since the median age at diagnosis ranges from 70 to 72 years, and it is more prevalent in men than women (2:1) (Hallek, Shanafelt, & Eichhorst, 2018).

CLL is a lymphoproliferative malignancy characterized by a progressive accumulation of small mature-appearing clonal B cells that typically express CD19, CD5 and CD23, among other surface markers. Leukemia cells normally appear in the blood, bone marrow, lymph nodes and spleen. CLL diagnosis is performed in full blood by immunophenotyping, consisting in the detection of the expression levels of an array of surface markers that determine the presence of clonal subsets (Table

2) (Hallek, Cheson, et al., 2018). Some of these expression markers, mainly ZAP-70 (Wiestner et al., 2003) and CD38 (Ibrahim et al., 2001), are prognostic factors that provide an insight into the progression and clinical outcome of the patient as well. The initial diagnosis of CLL is confirmed in patients with sustained clonal B cells counts ≥ 5,000 per µL for at least three months. Lower presence of clonal B cells corresponds to small lymphocytic lymphoma (SLL), generally considered a low-grade neoplastic manifestation previous to CLL in which tumor cells mainly accumulate in the lymph nodes (Tees & Flinn, 2017).

Table 2. Expression markers analysed in the immunophenotypic diagnosis of CLL.

	Normal B lymphocytes	***CLL cells***
*sIg**	High	Low
CD5	No	High
CD19	High	High
CD23	No	High
CD79b	High	Low
FMC7	High	Low
CD20	High	Low
CD22	High	Low
CD103	No	No
CD200	No	Very high
CD25	Low	Low
CD11c	Low	Low
CD10	No	No
CD43	No	Very high
ROR1	No	High
CD38	High	Variable
ZAP-70	Low	Variable

*sIg: surface immunoglobulin.

Additionally to diagnosis, two different clinical staging systems, developed by Rai (Rai et al., 1975) and Binet (Binet et al., 1981), are routinely employed to classify CLL based on a series of characteristics derived from standard laboratory tests and physical examination (Table 3). These systems provide a prognostic index that reflect the progression of the tumor and the estimated survival of the patient.

Table 3. CLL staging based on Rai and Binet systems.

Rai Staging System

Stage	Clinical criteria	Risk	Average survival (years)
0	Lymphocytosis.	Low	>12
I	Lymphocytosis and enlarged lymph nodes.	Intermediate	8
II	Lymphocytosis and enlarged spleen (and maybe an enlarged liver). Lymph nodes may or may not be enlarged.	Intermediate	6
III	Lymphocytosis and anemia. Lymph nodes, spleen and liver may or may not be enlarged.	High	<2
IV	Lymphocytosis and thrombocytopenia. Enlarged lymph nodes, spleen or liver. Anemia may or may not appear.	High	<2

Binet Staging System

Stage	Clinical criteria		Average survival (years)
A	No anemia or thrombocytopenia.	<3 areas of lymphoid tissue are enlarged	No reduction of life expectancy
B	No anemia or thrombocytopenia.	>3 areas of lymphoid tissue are enlarged	7
C	Anemia and/or thrombocytopenia are present.	Any number of lymphoid tissue areas may be enlarged.	2

There are two different forms of CLL based on their clinical behaviour. This heterogeneity is associated to the degree of somatic hypermutation in the immunoglobulin heavy-chain variable region gene (IGHV), which reflects the differentiation stage of the B cell of origin (Figure 7). A subset of patients carry unmutated IGHV, which correlates with a rapid progression of the malignancy, therefore requiring treatment. In this case, CLL arises from immature B cells that have not undergone differentiation in germinal centres, that is, a pre-germinal subtype of CLL. On the contrary, CLL cells with mutated IGHV come from a post-germinal centre stage and these patients

typically course an indolent and asymptomatic disease, which is normally associated to better prognosis (Fabbri & Dalla-Favera, 2016).

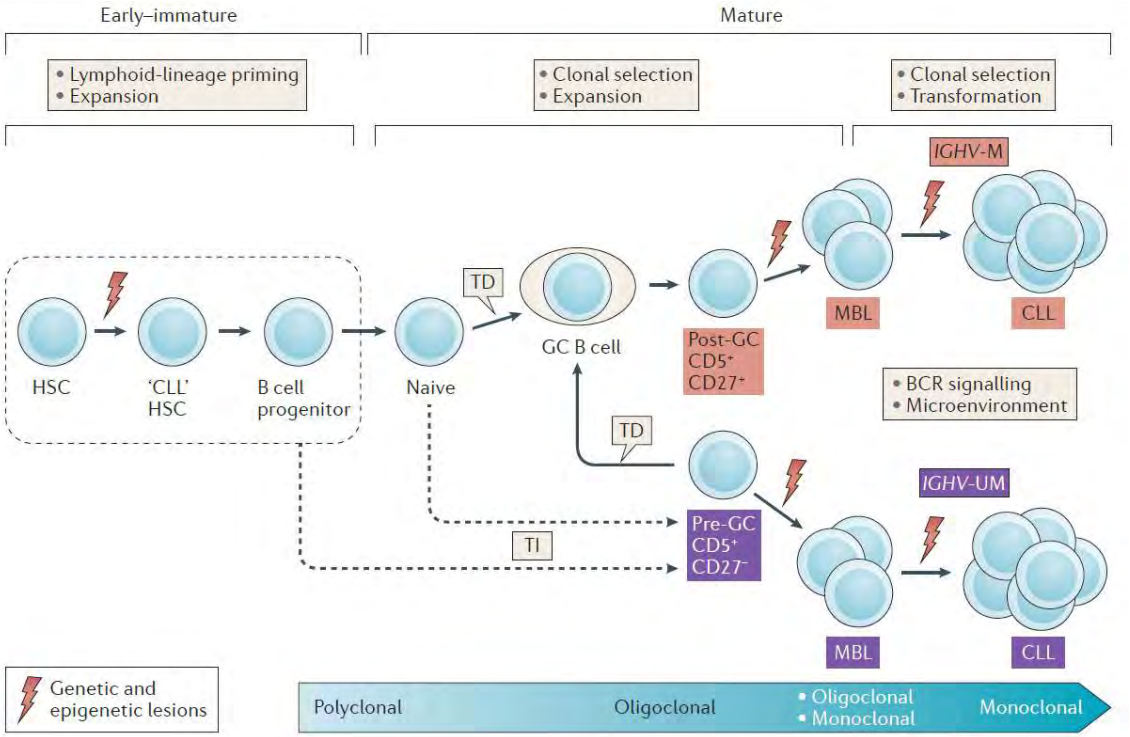

Figure 7. The cellular origin of CLL. Hematopoietic stem cells (HSCs), through accumulation of DNA damage, can transform into a CLL progenitor stem cell (CLL HSCs). At this stage, the B cell progenitor can differentiate into two different fates. Naive B cells are exposed to T-cell dependent (TD) antigen stimulation in the germinal centers and, together with their acquisition of genetic and epigenetic lesions, these cells derive to IGHV-mutated (-M) CLL. On the other hand, T-cell independent antigen exposure promotes differentiation to a pre-germinal IGHV-unmutated (-UM) CLL. In both cases, prior to CLL establishment, the population of B cells is firstly composed by oligoclonal and monoclonal subsets, which is considered a pre-CLL state known as monoclonal B cell lymphocytosis (MBL). Accumulation of genetic instability combined with environmental stimuli end up giving rise to monoclonal CLL. Obtained from Fabbri & Dalla-Favera, 2016.

The variability in the clinical course, outcome and response to therapy of patients with CLL is also dependent on a whole set of genetic aberrations. Deletion of chromosome 13q14 [del(13q)] is the most frequent chromosomal alteration, present in more than 50% of patients with CLL, and is associated to favourable outcome. The frequency of deletion of chromosome 17p13 [del(17p)] or *TP53* mutations is relative low (7% and 10%, respectively) in untreated patients, but these alterations are associated with resistance to chemoimmunotherapy and short survival (Buccheri et al., 2018). Deletion of chromosome 11q22-23 [del(11q)] (20%), with the corresponding loss of *ATM*, is also linked to poor therapeutic response and adverse outcome (Kipps et al., 2017). Other less frequent

alterations are trisomy of the chromosome 12 or the translocation t(11;14)(q13;q32), among others. Likewise, whole genome and exome sequencing studies unravelled recurrent mutations in CLL cells that provide survival advantages, affecting central nodes of signaling pathways such as *NOTCH1*, *SF3B1*, *POT1* or *MYD88* (Maleki et al., 2019; Puente et al., 2011; Quesada et al., 2011; Ramsay et al., 2013; Wang et al., 2014). Transcriptional profiling and epigenomic analyses also revealed large intratumor variability and uncovered distinct profiles associated to clinical subtypes, altogether underlining the molecular and clinical complexity of CLL (Ferreira et al., 2014; Kulis et al., 2012; Queiros et al., 2015).

Early studies unveiled that CLL cells are resistant to apoptosis, hence their prolonged survival and accumulation throughout the body. They count with a defective apoptotic machinery characterized by a dysregulation of distinct apoptotic mediators, such as death-associated protein kinase 1 (DAPK1) (Raval et al., 2007) or myeloid cell leukemia 1 (MCL1) (Hussain et al., 2007). Along these lines, CLL cells display high levels of the antiapoptotic protein B-cell lymphoma 2 (BCL2), which plays a crucial role in their resistance to apoptosis-inducing agents (Packham & Stevenson, 2005; Robertson, Plunkett, McConnell, Keating, & McDonnell, 1996). In addition, there is a constant interplay between leukemia cells and their microenvironment, which provides prosurvival and migratory signals to tumor cells. As a consequence, CLL cells travel into lymph nodes, where they form *proliferation centres*. Here, tumor cells get in contact with non-malignant stromal cells and nurselike cells, establishing an interaction network that mostly involves adhesion molecules (e.g. integrin CD49d or L-selectin), chemokines (e.g. tumour necrosis factor (TNF) ligand superfamily member 13B (TNFRSF13C, best known as BAFF) or CC chemokine receptor type 7 (CCR7)) and various soluble factors (e.g. wingless-type MMTV integration site family, member 5A (WNT5a)) (Burger, 2011; Ten Hacken & Burger, 2016). T cells present in the proliferation centres also contribute to B cell survival and proliferation via CD40 ligation, antigen presentation and production of cytokines such as interleukin (IL)-4 or IL-6.

B cell receptor signaling in CLL

B cell receptor (BCR) signaling is essential for B cell survival and mediates the response to antigen stimulation. The BCR complex consists of a transmembrane immunoglobulin (Ig) that binds the antigen and a signaling heterodimer composed by Igα and Igβ (also known as CD79A and CD79B, respectively). Downstream signaling is carried out by a cascade of linked phosphorylations that initiates with the activation of the proximal kinases LYN and SYK and eventually activates effector signaling pathways, including NF-κB, ERK or PI3K/AKT (Figure 8).

Sustained BCR signaling is a hallmark of CLL and has been described as a key event in the leukemogenesis, not only in CLL, but also in other B-cell malignancies, although it is triggered by different mechanisms depending on the tumor. CLL cells exhibit constitutive BCR signaling principally due to reactivity to autoantigens (Burger & Chiorazzi, 2013; Rosen, Murray, Evaldsson, & Rosenquist, 2010). Nonetheless, B-cell activation can be achieved via two other strategies in CLL cells: recognition of microbial antigens derived from infections (Binder et al., 2003; Hoogeboom et al., 2013; Lanemo Myhrinder et al., 2008) and autoreactivity via homotypic interactions between different BCR complexes (Duhren-von Minden et al., 2012). Unlike other malignancies, such as diffuse large B cell lymphoma (DLBCL), only a small percentage of CLL cases exhibit activating mutations in components of the pathway (Burger & Wiestner, 2018). This aberrant stimulation can translate into enhanced proliferation, most commonly observed in the unmutated IGHV subtype, or B cell anergy, predominantly associated to mutated IGHV, which correlates with the clinical behaviour of each subgroup of patients (Packham et al., 2014). In any case, CLL cells extended survival and impaired apoptosis is dependent on an active BCR signaling, which has opened a therapeutic window for novel small-molecule inhibitors targeting components of the pathway.

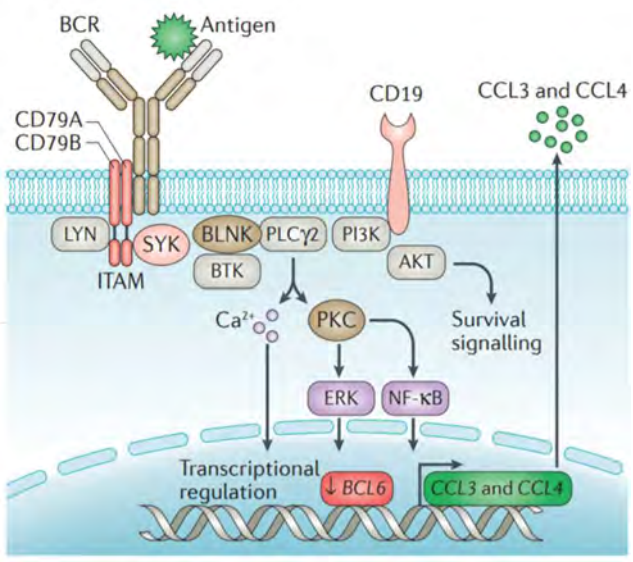

Figure 8. B cell receptor signaling pathway. Antigen stimulation via the BCR complex elicit the activation of the kinases LYN and SYK that initiates a phosphorylation cascade mediated by a set of kinases including BTK, BLNK or PLCγ2. Downstream signaling involves calcium (Ca^{2+}) mobilization and ultimately regulates gene transcription via recruitment of transcription factors from effector signaling pathways such as NF-κB and ERK. Modified from Burger & Wiestner, 2018.

Therapeutic approaches in CLL

Patients with CLL bearing an indolent disease are periodically monitored but not subjected to treatment. However, the majority of patients with CLL eventually require therapeutic intervention

owing to progression of the tumor to an active state and/or development of symptoms. Despite the intense research regarding treatment, CLL still remains an incurable disease. Nowadays, management of patients with CLL comprises a wide range of treatment regimens, which have expanded towards more individualized and targeted treatments. Response rates to treatment remain highly variable as a result of intrinsic or acquired resistances and drug toxicity. Cytogenetic lesions, such as del(17p) or *NOTCH1* mutations, are key drivers of therapy resistance and correlate with poor responses to treatment.

The first line of treatment for patients with CLL applied to date consists of a chemoimmunotherapy regimen that combines fludarabine and cyclophosphamide, two conventional chemotherapeutic agents, with rituximab, an anti-CD20 monoclonal antibody. This is commonly known as the FCR regimen. This therapy approach achieves complete remissions in a significant fraction of newly-diagnosed patients, with better response in low-risk CLL, but its efficacy diminishes in relapsed or refractory patients (Keating et al., 2005; Wierda et al., 2005). Lymphocytopenia is a common adverse effect produced by FCR treatment, resulting in immunosuppression and subsequent infections, and treatment-related secondary cancers have been reported in a small percentage of patients exposed to FCR (Burger & O'Brien, 2018). This drug toxicity represents an important drawback, especially in the case of elderly patients or patients with comorbidities, who require alternative low-intensity treatments.

Over the past 5 years, CLL treatment has expanded towards the development of molecularly targeted therapies that disrupt leukemia cell homeostasis. The reliance of leukemia cells on BCR signaling marked this pathway as a potential therapeutic target in CLL, hence instigating the development of novel agents that inhibit central BCR-related kinases. In line with this, ibrutinib, an irreversible BTK inhibitor, achieved astonishing response rates in clinical trials and it is currently approved for first-line and relapse/refractory CLL treatment (Burger & O'Brien, 2018; Herman et al., 2011). Of note, ibrutinib showed higher efficacy in older patients compared to conventional therapy, highlighting the clinical benefits of targeted therapies (Woyach et al., 2018). Leukemia cells exhibit enhanced PI3K activity due to aberrant BCR signaling. Selective inhibition of PI3K p110δ isoform (PI3Kδ), an isoform primarily expressed in hematopoietic cells, by idelalisib led to improved clinical outcome in relapse/refractory patients (Brown et al., 2014; Herman et al., 2010). Further, idelalisib is approved for patients with resistance to first-line and BTK inhibitor treatment. Following this lead, second-generation BTK and PI3K inhibitors are being clinically tested, like acalabrutinib, a BTK inhibitor that has better selectivity than ibrutinib (Barf et al., 2017), or umbralisib, a novel PI3Kδ inhibitor with a milder toxicity profile than that of idelalisib (Burris et al., 2018). Along similar lines, the distinctive high levels of BCL2 in CLL has given a chance to molecules such as venetoclax, a

BCL2 antagonist, which shows durable clinical activity and is well tolerated alone and in combination with rituximab (Seymour et al., 2017). Despite the exceptional clinical results exerted in CLL, these novel agents have been reported to cause diverse side effects (e.g. infections, neutropenia, pneumonia, etc.), being especially severe the toxicity profile upon idelalisib treatment. Additionally, a substantial portion of patients with CLL subjected to treatment with targeted therapies eventually relapse owing to acquired resistances mediated by histologic transformation or molecular mechanisms, such as mutations in *BTK* and *PLCG2* observed in patients treated with ibrutinib (Ahn et al., 2017; Burger et al., 2016; Walliser et al., 2016) or a recently uncovered point mutation in *BLC2* in patients with refractory CLL after treatment with venetoclax (Blombery et al., 2019). Consequently, CLL still remains an incurable disease, underscoring the need for new therapeutic approaches with reduced toxicity and better response rates independent of the cytogenetic profile of the patient.

OBJECTIVES

Despite the intense research on cancer treatment, management of patients with cancer remains a challenge nowadays. The need for novel therapeutic strategies has prompted the development of two distinct sets of treatments with encouraging clinical results. These treatments mainly focus on the targeted elimination of the tumor or the activation of antitumor immune responses. In the Thesis herein, we aimed to unveil the therapeutic potential of distinct compounds in cancer, evaluating their specificity and direct effect on tumor survival as well as the impact on the antitumor function of the immune system, primarily focusing on NK cells.

The specific objectives proposed in this work were the following:

1. To study the antileukemic activity of analogs of mithramycin A in CLL and evaluate the function of NK cells and T lymphocytes exposed to these compounds.
2. To explore the role of B cell activation on NK cell dysfunction in B-cell malignancies and define the potential therapeutic target causing this immunosuppression.
3. To determine the immunotherapeutic activity of antimitotic drugs in cancer by analyzing their effect on tumor immunogenicity and NK cell interaction with malignant cells.

MATERIALS AND METHODS

Reagents and other materials

Cytochalasin D, nocodazole, docetaxel and salubrinal were purchased from Santa Cruz Biotechnology. Cyclosporine A (CsA) was obtained from Sigma-Aldrich. Mithramycin A (MTA) and its analogue EC-7072 were kindly supplied by EntreChem S.L. Ibrutinib, idelalisib, venetoclax, fluradabine, Z-VAD-fmk and GSK2606414 (PERK inhibitor) were obtained from Selleckchem. The pharmacological inhibitors LY294002 (PI3K inhibitor), KU55933 (ATM inhibitor), GM6001 and BB94 (broad-spectrum MMP inhibitors) and LY2109761 (TGF-β receptor inhibitor) were purchased from Santa Cruz Biotechnology. Stock solutions of these reagents were prepared in dimethyl sulfoxide (DMSO, Sigma-Aldrich) and stored at -80ºC. DMSO was used as control (vehicle) in the corresponding experiments.

Recombinant human (rh) TNF-α, IL-4, IL-6, IL-15, TGF-β and BAFF were purchased from Peprotech. Soluble multimeric CD40 ligand (CD40L) was obtained from Adipogen. rhIL-2 was supplied by ORF Genetics. For shRNA experiments, pSuper ATMi and control pSuper-basic were obtained from Addgene. Lipofectamine LTX was purchased from Invitrogen.

Goat $F(ab')_2$ anti-human IgM and goat $F(ab')_2$ anti-human IgD antibodies were purchased from Southern Biotech. Goat anti-human IgM (μ-chain specific) antibody was obtained from Sigm-Aldrich. IL-2 receptor alpha (IL-2α, CD25; Clone: 5334) blocking antibody was procured by R&D Systems. TGF-β1 blocking antibody (Clone: 19D8) was supplied by Biolegend. PE-conjugated anti-human CD107a antibody (Clone: H4A3) was obtained from BD Biosciences, as well as protein transport inhibitors BD GolgiStop™ and BD GolgiPlug™. HRP (horseradish peroxidase)-conjugated anti-rabbit and anti-mouse secondary antibodies employed in western blotting were purchased from Jackson Immunoresearch Laboratories. The rest of antibodies employed in this work are listed in Tables 5-8 and Tables 10-11.

Additionally, the following dyes were used: carboxyfluorescein diacetate succinimidyl ester (CFSE, Sigma-Aldrich), Hoechst 33342 (Life Technologies), 7-aminoactinomycin D (7-AAD, Invitrogen), propidium iodide (PI, Immunostep), calcein-acetoxymethyl ester (Calcein-AM, Invitrogen) and 3,3'-dihexyloxacarbocyanine iodide ($DiOC_6(3)$; Sigma-Aldrich). FITC-conjugated Annexin V was purchased from Biolegend.

In this work, other reagents employed were sodium pyruvate (HyClone), L-glutamine (Lonza), penicillin-streptomycin mixture (Lonza), Insulin-Transferrin-Selenium (ITS, Gibco), Cytofix/Cytoperm™ solution (BD Biosciences), HRP substrate (Immobilon Millipore), Histopaque®-1077, hydrocortisone, PKH26 reference microbeads, phorbol myristate acetate (PMA), ionomycin, fetal bovine serum (FBS) and bovine serum albumin (BSA) (all from Sigma-Aldrich).

Two different flow cytometers were used to carry out this work: BD FACSCanto™ II (Becton Dickinson) and CytoFLEX S (Beckman Coulter).

Patients with CLL and healthy donors

Blood samples from untreated patients with CLL (n = 112) analyzed in this work were provided by Dr. Ana P. González Rodríguez and Dr. Ángel R. Payer from Hospital Universitario Central de Oviedo (HUCA), Oviedo, and by Dr. Esther González García from Hospital de Cabueñes, Gijón. CLL was diagnosed according to standard clinical and laboratory criteria as established by the World Health Organization (WHO): presence of more that 5000/µL B lymphocytes in the peripheral blood for at least three months. Written informed consent was obtained from all the patients following the Declaration of Helsinki and samples were collected with approval from the local ethics committee (Comité de Ética de la Investigación del Principado de Asturias).

Buffy-coats from healthy donors (n = 56) employed herein were provided by the Centro Comunitario de Sangre y Tejidos del Principado de Asturias.

Cell biology methods

Peripheral blood mononuclear cells (PBMCs)

PBMCs were isolated by Ficoll gradient centrifugation from blood samples obtained from healthy donors and patients with CLL. In brief, samples were layered on top of Histopaque®-1077 and centrifuged at 900 x *g* for 22 minutes at room temperature (RT). Isolated PBMCs were used fresh or cryopreserved in FBS containing 10% DMSO until use. FBS was previously inactivated at 55ºC for 30 minutes.

For some experiments, leukemia cells were isolated by using EasySep™ Direct Human B-CLL Cell Isolation Kit (Stemcell Technologies), T cells were purified by using Pan T Cell Isolation Kit (Miltenyi Biotec) and NK cells were purified by employing MojoSort™ Human NK Cell Isolation Kit (Biolegend). Manufacturers' instructions were followed for each isolation kit and purity of isolated subsets (90~98%) was determined by flow cytometry.

PBMCs and isolated immune subsets from patients with CLL and healthy donors were cultured in Roswell Park Memorial Institute (RPMI) 1640 (Lonza) supplemented with 10% heat-inactivated FBS, 1 mM sodium pyruvate, 2 mM L-glutamine, 100 U/mL penicillin and 10 µg/mL streptomycin at 37ºC and 5% CO_2.

Cells and cell culture conditions

Cell lines employed in this work are provided in Table 4 and were obtained from the American Type Culture Collection (ATCC) unless otherwise indicated. Culture medium was supplemented with 10% heat-inactivated FBS, 1 mM sodium pyruvate, 2 mM L-glutamine, 100 U/mL penicillin and 10 μg/mL streptomycin and cells were maintained at 37ºC and 5% CO_2. NKL cells, kindly furnished by Dr. Eduardo Martínez (Universidad Complutense de Madrid), were cultured in the presence of 50 U/mL IL-2 and 20% FBS. HK-2 cells were further supplemented with 36 ng/mL hydrocortisone (Sigma-Aldrich) and 1X ITS. OP9 cells were cultured in Alpha Minimum Essential Medium (α-MEM, Lonza) supplemented with 20% FBS. Primary fibroblasts obtained from healthy donors were kindly provided by Dr. Isabel Quirós (Universidad de Oviedo) and cultured in supplemented Dulbecco's Modified Eagle Medium (DMEM, Lonza).

Table 4. Cell lines employed in this work.

Cell line	***Origin***	***Species***	***Culture medium***
CA46	Burkitt's lymphoma	Human	RPMI
GRANTA-519	Mantle cell lymphoma		DMEM
HCT-116	Colorectal carcinoma		DMEM
HepG2	Hepatocellular carcinoma		DMEM
HK-2	Kidney		RPMI
JVM2	Mantle cell lymphoma		RPMI
K-562	Chronic myelogenous leukemia		RPMI
MEC-1	Chronic lymphocytic leukemia		RPMI
NKL	NK cell lymphoblastic leukemia/lymphoma		RPMI
OP9	Bone marrow-derived embryonic stem cells	Mouse	α-MEM
Raji	Burkitt's lymphoma	Human	RPMI
Ramos	Burkitt's lymphoma		RPMI
U266	Plasma cell myeloma		RPMI
Z-138	Mantle cell lymphoma		RPMI

Co-culture assays

In this work, two different co-culture experimental settings were performed.

- K-562, HCT-116 and HepG2 cells were seeded in 12-well plates and exposed to cytochalasin D (0.6 µg/mL), nocodazole (100 nM) or docetaxel (3 nM) for 48 hours to generate hyperploid cells. Right after, cells were washed and co-cultured with isolated NK cells in a 1:5 ratio (tumor cell: NK cell) for 48 hours. Surface expression levels of NK cell activating receptors were then evaluated on NK cells by flow cytometry (see *Cytometric detection of surface proteins*; Table 7). NK cells were isolated from healthy donors and cultured in the presence of 100 ng/mL IL-2 for 5 days previous to the co-culture.
- OP9 cells were seeded in 24-well plates and incubated for 24 hours at 37ºC and 5% CO_2. Culture medium was then replaced by fresh complete RPMI with or without 2 x 10^6/mL PBMCs from patients with CLL (estimated 1:1 ratio) were added to the cell culture for 3 days. EC-7072 (200 nM) or DMSO (control) was added to the co-culture for the last 24 hours and leukemia cell viability was assessed by flow cytometry (see *Detection of apoptosis*).

Conditioned media assays

MEC-1, Raji and Z-138 cell lines and PBMCs from patients with CLL and healthy donors were employed to generate conditioned media. Cells were seeded at a density of 2 x 10^6/mL in 12-well plates and treated with 10 µg/mL $F(ab')_2$ anti-human IgM or IgD antibodies for 48 hours. Cell cultures were then centrifuged (250 x *g*, 5 minutes) and supernatants were collected. PBMCs from patients with CLL or healthy donors were cultured in conditioned media for 48 hours and surface expression of NK cell activating receptors (NKG2D, DNAM-1 and NKp46 – see *Cytometric detection of surface proteins*; Table 7) was then analyzed in NK cells and $CD8^+$ T cells by flow cytometry.

Transwell assays

For *in vitro* transwell assays, anti-human IgM (µ-chain specific) antibody was firstly coated on the surface of 12-well culture plates. For that purpose, 500 µL/well of 1X phosphate buffered saline (PBS) containing 10 µg/mL anti-IgM antibody were incubated at 4ºC, overnight. Following incubation, antibody excess was washed away with 1X PBS. Next, 2 x 10^6 PBMCs from healthy donors/well were seeded at the bottom, in contact with the coated antibody, and 10^6 PBMCs were placed in the transwell insert (0.4 µm, Corning). Cells were incubated for 48 hours at 37ºC and 5% CO_2. Surface expression of NK cell activating receptors NKG2D and DNAM-1 (see *Cytometric detection of surface proteins*; Table 7) was then evaluated in NK cells and $CD8^+$ T cells present in both sections of the transwell by flow cytometric detection.

Proliferation assay

To evaluate the proliferation rate of distinct immune subsets, a CFSE-based assay was performed. Briefly, cells were stained with 1 µM CFSE for 30 minutes at 37ºC in the dark. 1 volume of cold (4ºC) culture medium was added to stop the staining, followed by incubation for 5 minutes at 4ºC. Cells were washed twice with pre-warmed (37ºC) culture medium to remove dye excess and subsequently cultured in complete RPMI. Proliferation was determined based on dye dilution, which is a consequence of each cell division, in a flow cytometer.

Cell cycle analysis

Hyperploid K-562, HCT-116 and HepG2 cells were generated by exposure to cytochalasin D (0.6 µg/mL), nocodazole (100 nM) or docetaxel (3 nM) for 48 hours. To determine their DNA content, cells were incubated with 100 µg/mL RNase A for 15 minutes at RT, followed by staining with 50 µg/mL PI for 15 minutes at 4ºC in the dark. Nuclear content was analyzed by flow cytometry, identifying as hyperploid cells those with > 4n.

Additionally, Hoechst 33342, a dye that penetrates live cells, was employed to evaluate the surface expression levels of NK cell activating ligands on cell subpopulations with distinct DNA contents. After surface protein staining (see *Cytometric detection of surface proteins*; Table 7), cells were dyed with 10 µg/mL Hoechst 33342 for 45 minutes at 37ºC. Cell ploidy and its associated surface staining was analyzed in a flow cytometer.

Assessment of NK cell activity

CD107a degranulation assay

To evaluate NK cell activation and degranulation in the context of anti-BCR-mediated B-cell activation, PBMCs from healthy donors were exposed to 10 µg/mL $F(ab')_2$ anti-human IgM or IgD antibodies for 48 hours. Following treatment, PBMCs were cultured alone or co-cultured with K-562 cells at a 10:1 effector:target (E:T) ratio in 96-well plates for 4 hours at 37ºC in the presence of anti-human CD107a antibody. Conditions were always set in duplicate. After 1 hour of incubation, a monensin solution (BD GolgiStop™) was added to the cell culture at the recommended concentration. After the incubation period, PBMCs were stained for immune subset identification (see *Immune cell subset identification*) and results were analyzed by flow cytometry. For further details on this protocol, please refer to (Lorenzo-Herrero, Sordo-Bahamonde, Gonzalez, & Lopez-Soto, 2019a).

Cytotoxicity assays

- Flow cytometry-based cytotoxicity

NK cell-mediated lysis of drug-induced hyperploid cells was evaluated by flow cytometry as described (Lorenzo-Herrero, Sordo-Bahamonde, Gonzalez, & Lopez-Soto, 2019b). For that purpose, DMSO-treated (control) and hyperploid K-562, HCT-116 and HepG2 cells were dyed with CFSE (see *Proliferation assay*) and co-cultured with isolated NK cells or NKL cells at different E:T ratios (2:1, 10:1 and 20:1) for 4 hours at 37ºC. Right afterwards, 10 µg/mL 7-AAD was added to the culture for 10 minutes at RT to discriminate dead cells and data was analyzed in a flow cytometer. Target cells were also cultured alone as a negative control to determine spontaneous lysis. Conditions were set in triplicate. Specific lysis was calculated following the next formula:

$$Specific\ lysis\ (\%) = \frac{(\%7AAD\ positive\ target\ cells\ in\ coculture - \%7AAD\ positive\ target\ cells\ in\ spontaneous\ lysis)}{(100 - 7AAD\ positive\ target\ cells\ in\ spontaneous\ lysis)} x100$$

For some experiments, effector NKL cells were pre-incubated with NK cell receptor blocking antibodies or control IgG (Table 5) for 1 hour at 37ºC.

Table 5. Blocking antibodies employed in this work.

Molecule blocked	*Clone*	*Manufacturer*
NKG2D	1D11	Santa Cruz Biotechnology
DNAM-1	DX11	BD
NKp30	P30-15	Biolegend
Control IgG	n.a.	Santa Cruz Biotechnology

n.a. not applicable. This antibody is polyclonal.

- Calcein AM-based cytotoxicity

NK cell cytotoxic capacity upon anti-BCR-mediated B-cell stimulation was analyzed by calcein-AM fluorometric detection as previously reported. PBMCs from healthy donors were treated with 10 µg/mL $F(ab')_2$ anti-human IgM or IgD antibodies for 48 hours. K-562 cells were stained with 10 µM calcein-AM for 30 minutes at 37ºC, followed by two washing steps with pre-warmed (37ºC) culture medium to remove dye excess. Next, IgM-, IgD-treated or control PBMCs were co-cultured with dyed K-562 cells at three different E:T ratios (10:1, 25:1 and 50:1) in RPMI supplemented with 1% FBS in a 96-well plate for 4 hours at 37ºC. Additionally, K-562 cells were cultured alone to assess spontaneous and maximal target cell lysis. The latter was achieved by treatment with 1% Triton X-100 for 30 minutes at 37ºC. Following incubation, co-cultures were centrifuged (250 x *g*, 5 minutes) and 100 µL supernatant was transferred to a

brand-new 96-well plate. Fluorescence was measured at 485 nm excitation and 530 nm emission wavelengths in a Varioskan™ Lux Multimode microplate reader. Conditions were set in triplicate. Culture medium background signal was also determined and subtracted from all the readings. Specific lysis calculations were made according to the following formula:

$$Specific\ lysis\ (\%) = \frac{(mean\ fluorescence\ in\ coculture - mean\ fluorescence\ in\ spontaneous\ lysis)}{(mean\ fluorescence\ in\ maximal\ lysis - mean\ fluorescence\ in\ spontaneous\ lysis)} x100$$

For ADCC (antibody-dependent cell-mediated cytotoxicity) experiments, Raji cells were used as target cells. Cells were dyed with Calcein-AM and subsequently incubated with or without 10 µg/mL rituximab for 30 minutes at 37ºC, previous to the co-culture.

Flow cytometry

Immune cell subset identification

To determine immune populations, the antibodies listed in Table 6 were employed. The subsets of immune cells were identified as follows: T cells were defined as $CD3^+CD56^-$, CD8+ T cells as $CD3^+CD56^-CD8^+$ and $CD4^+$ T cells as $CD3^+CD56^-CD4^+$; NK cells were identified as $CD3^-CD56^+$ and healthy B cells as $CD19^+$. Leukemia cells were defined as $CD19^+$ since the percentage of healthy B cells ($CD19^+CD5^-$) detected in PMBCs from patients with CLL was inferior to 2% (data not shown). Cells were stained for 20 minutes at RT in the dark and washed with 1X PBS at 250 x *g* for 5 minutes. Data was analyzed in a flow cytometer.

Table 6. Antibodies used for identification of immune subsets.

Protein detected	*Fluorophore*	*Clone*	*Manufacturer*
CD56	APC	C5.9	Cytognos
CD3	APC	33-2A3	Immunostep
CD3	FITC	UCHT-1	Cytognos
CD3	CFBlue	33-2A3	Immunostep
CD8	APC	143-44	Immunostep
CD8	APC-C750	143-44	Immunostep
CD4	PerCP	HP2/6	Immunostep
CD5	APC/Cy7	L17F12	Biolegend
CD19	APC	A3-B1	Immunostep
CD19	CF-Blue	A3-B1	Immunostep

Cytometric detection of surface proteins

Antibodies listed in Table 7 were used to detect surface expression levels of distinct proteins by flow cytometry. Staining was performed following the manufacturer's indications. In short, cells were stained with primary antibodies for 45 minutes at 4ºC followed by centrifugation with 1X PBS (250 x *g*, 5 minutes). Secondary anti-IgG antibodies were subsequently incubated for 45 minutes at 4ºC in the dark. For staining with fluorophore-conjugated antibodies, cells were incubated for 20 minutes at RT in the dark. After a final washing step with 1X PBS, mean fluorescence intensity (MFI) was determined by flow cytometry.

Absolute cell number quantification

To evaluate absolute cell numbers, an equal volume of PKH26 reference microbeads was added to each sample after staining for immune subset identification (see *Immune cell subset identification*). Microbeads (5 x 10^3/tube) were acquired in a flow cytometer and absolute numbers of each immune population within the sample were calculated. Normalized percentage values were determined considering the control (DMSO)-treated cells as 100%.

Detection of apoptosis

Cell viability and apoptosis were evaluated by double-staining with the mitochondrial inner transmembrane potential ($\Delta\Psi_m$)-sensitive dye $DiOC_6(3)$ and the exclusion dye PI, allowing identification of apoptotic [$DiOC_6(3)^{low}$ PI^-] and dead [PI^+] cells (Lissa et al., 2014; Sica, Maiuri, Kroemer, & Galluzzi, 2016). In brief, cells were resuspended in pre-warmed (37ºC) culture medium containing 20 nM $DiOC_6(3)$ and incubated for 30 minutes at 37ºC. Then, 1 µg/mL PI was added to each sample and cells were further incubated for 10 minutes at RT. Data were analyzed by flow cytometry considering $DiOC_6(3)^+$ PI^- cells as viable.

In some experiments, apoptosis was evaluated by double-staining with Annexin V, a protein that selectively binds surface phosphatidylserine, and PI. These method allows the identification of apoptotic [Annexin V^+ PI^-] and dead [PI^+] cells as well. Thus, cells were incubated in Annexin V binding buffer (0.01 M HEPES/NaOH (pH 7.4), 0.14 M NaCl, 2.5 M $CaCl_2$) containing 5 µg/mL Annexin V-FITC for 15 minutes at RT. After washing with 1X PBS (250 x *g*, 5 minutes), PI (1 µg/mL) was subsequently incubated for 10 minutes at RT. Cells were analyzed by flow cytometry considering Annexin V^- PI^- cells as viable. Where indicated, 7-AAD (10 µg/mL) was used instead of PI to discriminate dead cells.

Table 7. Fluorophore-conjugated, primary and secondary antibodies employed for cell surface staining.

Fluorophore-conjugated antibodies

Protein detected	Fluorophore	Clone	Manufacturer	Dilution
CD79A (Igα)	PE	HM47	Biolegend	1:20
CD79B (Igβ)	PE	CB3-1	Biolegend	1:20
IgM	PE	G20-127	BD Biosciences	1:4
NKG2D (CD314)	PE	REA797	Miltenyi	1:200
DNAM-1 (CD226)	PE	11A8	Biolegend	1:200
NKp30 (CD337)	PE	AF29-4D12	Miltenyi	1:50
	APC	P30-15	Biolegend	1:50
NKp44 (CD336)	PE	2.29	Miltenyi	1:50
	APC	P44-8	Biolegend	1:50
NKp46 (CD335)	PE	9E2	Biolegend	1:50
	Pacific Blue	E92	Biolegend	1:20
CD16	FITC	3G8	Immunostep	1:50
CD28	FITC	CD28.2	Biolegend	1:20
CD69	FITC	FN50	Immunostep	1:20

Primary antibodies

Protein detected	Origin	Clone	Manufacturer	Dilution
MICA	Mouse	159227	R&D Systems	1:1000
MICB	Mouse	236511	R&D Systems	1:1000
ULBP1	Mouse	170818	R&D Systems	1:200
ULBP2	Mouse	165903	R&D Systems	1:200
ULBP3	Mouse	166510	R&D Systems	1:200
PVR (CD155)	Mouse	SKIL4	Biolegend	1:5000
Nectin-2 (CD112)	Mouse	TX31	Biolegend	1:5000
B7-H6	Mouse	875001	R&D Systems	1:200
HLA-I	Mouse	W6/32	Universidad Complutense de Madrid	1:2000
Calreticulin	Rabbit	n.a.	Santa Cruz Biotechnology	1:50

Secondary antibodies

Protein detected	Fluorophore	Clone	Manufacturer	Dilution
Mouse IgG	PE	n.a.	Southern Biotech	1:1000
Rabbit IgG	FITC	n.a.	Southern Biotech	1:1000

n.a. not applicable. These antibodies are polyclonal.

Data corresponding to cell viability were normalized to the untreated control as a percentage. Only samples from patients with CLL or healthy donors with at least 50% of viable cells ($DiOC_6(3)^+$; Annexin V^-) in the control (DMSO) condition were employed in this work.

Intracellular flow cytometry

To quantify the intracellular levels of IFN-γ, IL-2 and perforin, PBMCs from healthy donors or patients with CLL were incubated in the presence of 50 ng/mL PMA and 1 µg/mL ionomycin for 4 hours. After 1 hour of incubation, a brefeldin A solution (BD GolgiPlug™) was added to the cell culture at the recommended concentration. Following the 4 hour incubation, cells were stained with subset specific antibodies (see *Immune cell subset identification*). Next, cells were fixed and permeabilized with Cytofix/Cytoperm™ solution for 20 minutes at 4ºC, according to the manufacturer's instructions. Two washing steps with 1X Wash buffer were performed (250 x *g*, 5 minutes). Finally, cells were incubated with intracellular flow cytometry-specific antibodies (Table 8) for 30 minutes at 4ºC and MFI was measured by flow cytometry.

In some experiments, PBMCs were co-cultured with drug-induced hyperploid cells during the incubation period and the differential levels of intracellular cytokines (IFN-γ and IL-2) were analyzed.

Table 8. Antibodies used for intracellular flow cytometry.

Protein detected	*Fluorophore*	*Clone*	*Manufacturer*
IL-2	PE	MQ1-17H12	BD Biosciences
IFN-γ	PE	4S.B3	Biolegend
Perforin	PerCP/Cy5.5	B-D48	Biolegend

Molecular Biology Methods

Caspase-3 activity assay

Intracellular levels of activated caspase-3 were measured by using CaspGLOW™ Fluorescein Active Caspase-3 Staining Kit (Invitrogen). In brief, EC-7072 (200 nM)- or DMSO-treated PBMCs

from patients with CLL were incubated with FITC-DEVD-fmk for 30 minutes at 37ºC following immune subset staining (see *Immune cell subset identification*). Fluorescence corresponding to leukemia cells was next analyzed by flow cytometry. For some experiments, cells were pretreated for 2 hours with the indicated doses of the broad-spectrum caspase inhibitor Z-VAD-fmk.

RNA-seq analysis

Isolated leukemia cells from 8 patients with CLL were incubated with 200 nM EC-7072 or DMSO for 6 hours. Total RNA from isolated CLL cells was extracted using RNeasy Mini-Kit (Qiagen). RNA integrity and concentration were determined using an Agilent-2100 Bioanalyzer (Agilent Genomics) and high-quality RNA samples were further processed. RNA-seq libraries were prepared using TruSeq-Stranded mRNA LT Sample Prep Kit (Illumina) and checked for quality using a DNA 1000 chip on a 2100 Bioanalyzer. Each library was sequenced on a HiSeq 4000 (Illumina) to generate ~20 million uniquely-mapping reads per sample. Generated FASTQ files were first evaluated using FastQC for quality control checks (http://www.bioinformatics.babraham.ac.uk/projects/fastqc/). No problems or biases were identified associated to library preparation or sequencing. Transcript abundance was directly quantified with Salmon (Patro, Duggal, Love, Irizarry, & Kingsford, 2017), employing the human transcriptome version GRCh38 (Ensembl) as reference. Transcript-level quantifications were aggregated for gene-level differential analysis with DESeq2 (Love, Huber, & Anders, 2014), applying a multifactor design for paired samples. Finally, gene set enrichment analysis was carried out with PathfindR (https://www.biorxiv.org/content/10.1101/272450v1). Further gene analysis and representations were performed excluding genes with mean expression lower than 25 in control (DMSO) and EC-7072 conditions. RNA-seq data have been deposited in the Gene Expression Omnibus database (GEO; https://www.ncbi.nlm.nih.gov/geo/) under accession number GSE123777.

qPCR analysis

Real-time PCR was used in the current work to analyze the expression of genes in two different settings.

- The expression level of *ATM* in K-562 cells transfected with pSuper.ATM or control vector was analyzed by qPCR. For that purpose, total RNA was purified using High Pure RNA Isolation Kit (Roche) and purity and concentration were evaluated on a NanoDrop 2000 (ThermoFisher Scientific). 1 µg total RNA were used for cDNA synthesis using High-Capacity cDNA Reverse Transcription Kit (Applied Biosystems). Quantitative RT-PCR was performed using 4 µL cDNA (1:5 dilution) and SYBR Green PCR Master Mix (Applied Biosystems) in a final volume of 20 µL.

- Validation of target genes significantly dysregulated in CLL cells exposed to EC-7072 was performed by qPCR. Isolated leukemia cells from patients with CLL were incubated with EC-7072 (200 nM) or DMSO for 6 hours. Total RNA was extracted using RNeasy Mini Kit and purity and concentration were evaluated on a NanoDrop 2000. 2 µg total RNA were used for cDNA synthesis using High-Capacity cDNA Reverse Transcription Kit. Quantitative RT-PCR was performed using 2 µL cDNA (1:5 dilution) and SYBR Green PCR Master Mix in a final volume of 10 µL.

Amplifications were run according to the manufacturer's recommendations in a 7300 Real-Time PCR System (Applied Biosystems). Each sample was analyzed in triplicate and gene expression levels were normalized to the expression of a reference gene (*GAPDH* or *B2M*). Calculations were made applying the $2^{-\Delta(\Delta Ct)}$ formula, as previously reported (Livak & Schmittgen, 2001). Primers used for each gene detection are provided in Table 9.

Table 9. Primers employed for qPCR analyses.

Gene	***Forward sequence (5' → 3')***	***Reverse sequence (5' → 3')***
CD79B	CCAGGCTGGCGTTGTCTCCTG	GGTACCGGTCCTCCGATCTGGC
SYK	TGCACTATCGCATCGACAAAG	CATTTCCCTGTGTGCCGATTT
LYN	ACCAGGGAGGAGCCCATTTA	CTTCCGCTCGATGTATGCCA
PIK3CD	ACTCTGCCATTGTCTAAGCCACCT	TCACAGCAGGTTCCCAAAGGTGAT
PLCG2	GCCTGTCCCTTTGTAGAAGTGG	GGCCATTATCATTCACAACCG
BCL2	CTGCACCTGACGCCCTTCACC	CACATGACCCCACCGAACTCAAAGA
BCL2L11	GGCCCCTACCTCCCTACA	GGGGTTTGTGTTGATTTGTCA
BID	CGCACCTACGTGAGGAGCTTAGCC	TGACCACATCGAGCTTTAGCCAGTCA
BCL2L1	GATCCCCATGGCAGCAGTAAAGCAAG	CCCCATCCCGGAAGAGTTCATTCACT
NOXA	CAGAGCTGGAAGTCGAGTGT	AGGAGTCCCCTCATGCAAGT
CARD11	TTGTGGGAGAATGTGGAGTGT	TGCCCCTTGGTATGTAGAATG
B2M	TGCTGTCTCCATGTTTGATGTATCT	TCTCTGCTCCCCACCTCTAAGT
ATM	TGGCTACAGATTGCAACCCAA	TGGTGTACGTTCCCCATGTC
GAPDH	CGGAGTCAACGGATTTGGTC	AATCATATTGGAACATGTAAACCATGTAGT

Phosphoflow

Protein phosphorylation levels were evaluated by phosphoflow. Briefly, isolated leukemia cells from patients with CLL were treated with 200 nM EC-7072 or DMSO (control) for 8 or 12 hours. In some experiments, BCR-signaling was activated with goat $F(ab')_2$ anti-human IgM antibody (10

μg/mL) for 45 minutes, CD40L (100 ng/mL) or IL-6 (40 ng/mL) for 15 minutes. Right afterwards, cells were fixed with 1.8% paraformaldehyde for 10 minutes at RT and washed with 1X PBS (250 x *g*, 5 minutes). Cells were then permeabilized with 90% ice-cold methanol for 25 minutes at 4ºC. Subsequently, two washing steps were performed with PBS/1% BSA (250 x *g*, 5 minutes). Cells were incubated with specific phospho-antibodies (Table 10) for 30 minutes at RT and, after a final washing step with PBS/1% BSA, MFI was analyzed in a flow cytometer.

Table 10. Antibodies used for phosphoflow assays.

Protein detected	Fluorophore	Residue	Clone	Manufacturer
*p-SYK**	PE	Y352	1503310	Biolegend
p-BTK	PE	Y223	A16128B	Biolegend
p-PLCγ2	PE	Y759	K86-689.37	BD Bioscience
p-ERK1/2	PE	Y202/Y204	6B8B69	Biolegend
p-AKT	PE	S473	M89-61	BD Bioscience
p-p65 NF-κB	PE	S529	K10-895.12.50	BD Bioscience
p-STAT3	PE	Y705	4/P-STAT3	BD Bioscience
p-H2AX	PE	S139	2F3	Biolegend

*This antibody also detects phosphorylated ZAP70 at Y319. As previously reported, phosphorylation of ZAP70 is highly inefficient in CLL and, therefore, signal detected by this antibody can be mostly attributed to SYK phosphorylation at Y352 (29467184, 17038529).

shRNA transfection

K-562 and HCT-116 cells were seeded in 12-well plates and cultured for 24 hours. Transfection was carried out with lipofectamine LTX. Briefly, 300 ng pSuper ATMi, 300 ng control pSuper-basic or 0.75 μL lipofectamine LTX were incubated in 50 μL culture medium for 5 minutes at RT. Next, each plasmid was mixed with lipofectamine solution (1:1 ratio) and further incubated for 20 minutes at RT. DNA-lipofectamine complexes-containing solution was added to the cell cultures in DMEM or RPMI (depending on the cell line) without antibiotics. Following overnight incubation, plasmid excess was removed through washing with 1X PBS and fresh pre-warmed culture medium was added to the culture. After 48 hours, cells were treated with cytochalasin D (0.6 μg/mL) for 48 hours and MICA expression levels were analyzed by flow cytometry (see *Cytometric detection of surface proteins*).

Western blotting

K-562 and HCT-116 cells were treated with cytochalasin D (0.6 µg/mL) and/or GSK2606414 (1 µM) for 48 hours. Total protein extracts were obtained by whole cell lysis in radio-immunoprecipitate assay (RIPA) buffer [100 mM Tris (pH 7.4), 150 mM NaCl, 0.1% SDS, 1% Triton X-100, 10 mM EDTA, 1% sodium deoxycholate] containing 1 mM sodium fluoride (NaF), 1 mM sodium orthovanadate (Na_3VO_4), 1 mM β-Glycerol phosphate, 1 mM AEBSF (Thermo Scientific), protease inhibitor Complete EDTA-free and phosSTOP (Roche). The soluble protein fraction was separated by centrifugation at 15000 x *g* for 5 minutes at 4ºC and protein concentration was measured using Pierce BCA Protein Assay Kit (Thermo Scientific). Following heat denaturation, 15 µg of total protein were resolved on a 10% SDS-PAGE gel and transferred to polyvinylidene difluoride (PVDF) membranes (Sigma) for 90 minutes at 50 V in a MiniProtean II tank (Bio-Rad) employing transfer buffer (10 mM CAPS, 4 mM NaOH, 20% methanol). Membranes were dyed with Ponceau to ensure that similar protein amounts were present throughout the samples. Membranes were blocked with 3% non-fat dry milk in TBST buffer (50 mM Tris pH 7.4, 150 mM NaCl, 0.05% Tween-20) for 1 hour at RT and incubated overnight with primary antibodies (Table 11) at 4ºC. Afterwards, membranes were washed with TBST buffer for 45 minutes and HRP-conjugated secondary antibodies were incubated in 1,5% non-fat dry milk in TBST buffer (1:10000 dilution) for 1 hour at RT. After a final washing step with TBST buffer, an HRP substrate solution was added to the membranes and signals were detected by chemoluminiscence.

Table 11. Antibodies used for western blot assays.

Protein detected	*Clone*	*Manufacturer*	*Dilution*
eIf2α	Poly6067	Biolegend	1:500
p-eIf2α (Ser51)	D9G8	Cell Signaling	1:1000
α-actin	AC-74	Sigma	1:5000

Statistical analysis

Statistics and data analysis

Statistical tests were performed using SPSS Statistics 23.0 (SPSS Inc). Shapiro-Wilk test was applied to determine sample distribution. Independent samples Student's t-test or Mann-Whitney U test were employed to compare mean samples between groups. Paired samples Student's t-test or Wilcoxon signed-rank test were applied to compare paired samples. p values < 0.05 were considered significant. Flow cytometry data analysis was performed with BD FACSDiva software (BD

Bioscience) and CytExpert software (Beckman Coulter). Graphs were prepared using GraphPad Prism 6.0 software (GraphPad Software Inc.).

Combination index calculations

Synergy, addition or antagonism of drug combinations were evaluated using CalcuSyn Version 2.0 software (Biosoft), which allows the calculation of the combination index (CI) based on the algorithm reported by Chou and Talalay (Chou, 2010). As previously described, CI values < 0.8 represent synergistic effect, values between 0.8-1.2 indicate additive effect and values > 1.2 represent an antagonistic effect (Bijnsdorp, Giovannetti, & Peters, 2011; Chou, 2010). CI values for non-fixed ratio combinations from independent experiments, employing IC_{50}, IC_{25} and IC_{10} concentrations for each compound, were generated and plotted.

RESULTS

1. The mithralog EC-7072 induces chronic lymphocytic leukemia cell death by targeting the B cell receptor signaling pathway

EC-7072 is highly effective against primary leukemia cells from patients with CLL independently from cytogenetic aberrations and IGHV *mutational status*

EC-7072 (also known as MTM-SK) is an analog of MTA, so-called mithralog, generated by targeted inactivation of a ketoreductase implicated in the biosynthesis of MTA and produced by *Streptomyces argillaceus* (Figure 1.1) (Remsing et al., 2003).

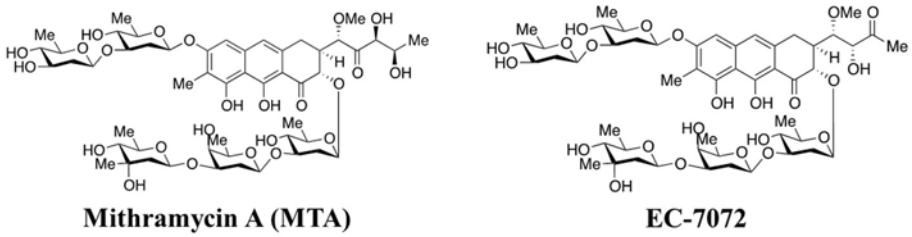

Figure 1.1. Chemical structure of MTA and its analog EC-7072.

To evaluate the *in vitro* therapeutic potential of EC-7072 in CLL, PBMCs isolated from patients with CLL were incubated with the compound and viability and leukemia cell numbers were determined by flow cytometry. Treatment with increasing concentrations of EC-7072 significantly decreased leukemia cell numbers and viability in a dose-dependent manner (Figure 1.2A-B). Viability was affected in a time-dependent fashion as well (Figure 2.2C). This antileukemic activity exerted by the mithralog was comparable to that of MTA (Supplementary Figure 1.1). However, opposed to the strong toxicity associated to MTA, EC-7072 did not significantly affect the viability of non-tumoral primary human fibroblasts and HK-2 cells, an immortalized cell line derived from normal adult human kidney (Supplementary Figure 1.2A-B). Nonetheless, EC-7072 reduced the viability of normal B cells from healthy donors, suggesting that the compound is highly cytotoxic against B cells (Figure 1.2D). Concomitantly, EC-7072 significantly diminished the surviving cell fraction of a panel of tumor cell lines derived from B-cell malignancies (Supplementary Figure 1.2C).

Then, we analyzed the impact of chromosomal and molecular genetic aberrations that are markers of patient prognosis and therapy response in CLL in the cytotoxic effect of EC-7072. No differences in the activity of EC-7072 were observed among patients carrying diverse cytogenetic alterations typically associated to high-risk CLL, such as del(17p) or del(11q) (Figure 1.3A), nor the mutational status of IGHV significantly affected the sensitivity to the mithralog (Figure 1.3B). These data

suggest that the antileukemic activity of EC-7072 is independent of the cytogenetic profile of CLL cells.

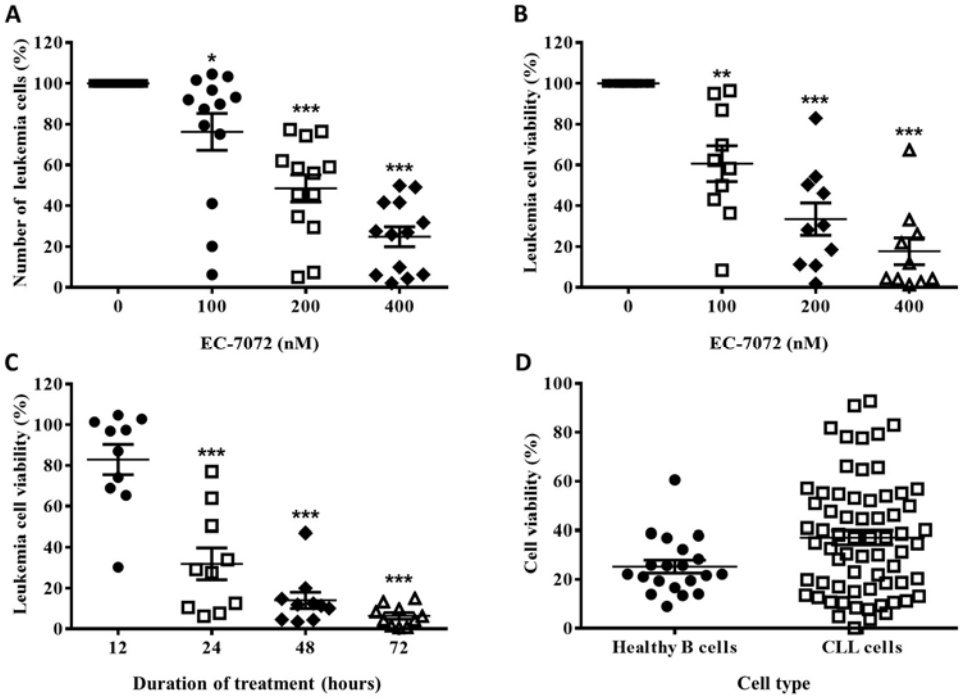

Figure 1.2. EC-7072 has a cytotoxic effect on primary leukemia cells from patients with CLL. PBMCs from patients with CLL (n = 10-13) were incubated with increasing concentrations of EC-7072 (0-400 nM) for 24 hours. **A.** Numbers of leukemia cells were evaluated by flow cytometry. The graph represents the number of cells normalized to their respective control (DMSO) condition for each individual patient. **B.** Viability of leukemia cells was determined by cytofluorometric assessment of $DiOC_6(3)$/PI staining. **C.** PBMCs from patients with CLL (n = 10) were incubated with or without EC-7072 (200 nM) for 12 to 72 hours. Viability of leukemia cells was determined by $DiOC_6(3)$/PI staining. **D.** PBMCs from patients with CLL (n = 63) or healthy donors (n = 20) were incubated with or without EC-7072 (200 nM) for 24 hours and viability of leukemia cells and healthy B cells was evaluated by $DiOC_6(3)$/PI staining. Graphs depict the percentage of viable [$DiOC_6(3)^+$] cells normalized to their respective control (DMSO) condition for each individual patient. (Mean ± SEM; *p < 0.05; **p < 0.01; ***p < 0.001, Student's *t*-test).

EC-7072 does not markedly alter the homeostasis of healthy immune cells from patients with CLL

We next assessed the effect of the compound toward healthy immune subsets, T lymphocytes and NK cells, that are constantly exposed to leukemia cells in the peripheral blood of patients with CLL. Treatment of PBMCs from patients with CLL with increasing doses of EC-7072 exerted minor effects on T cell numbers (Figure 1.4A) and viability (Figure 1.4C and Supplementary Figure 1.3), finding no differences in $CD4^+$ and $CD8^+$ T cell subgroup numbers (Supplementary Figure 1.4). NK cells were slightly altered by exposure to 200 nM EC-7072 for 24 hours, a concentration of the mithralog that dramatically induced CLL cell death (Figure 1.4B-C and Supplementary Figure 1.3).

High doses (400 nM) of the compound were significantly less toxic against NK cells than leukemia cells as well (Figure 1.4B-C). Thus, we performed all subsequent experiments with 200 nM EC-7072, unless otherwise indicated.

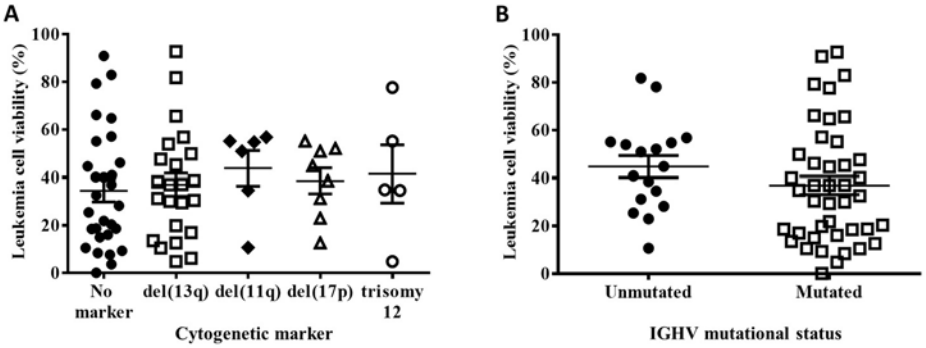

Figure 1.3. The antileukemic effect of EC-7072 is independent of cytogenetic alterations associated to CLL. PBMCs from patients with CLL were treated with 200 nM EC-7072 for 24 hours and CLL cell viability was assessed by flow cytometry. **A.** Cytogenetic profile was obtained for each patient (n = 62). **B.** Mutational status of IGHV was determined for each patient (n = 59). Graphs depict the percentage of viable [$DiOC_6(3)^+$] cells normalized to their respective control (DMSO) condition for each individual patient. (Mean ± SEM; Student's *t*-test).

The production of the antitumor effector molecules IFN-γ and perforin by T cells and NK cells was not significantly altered upon treatment with EC-7072 (Figure 1.5A). Therefore, to test whether the immune cells present in the microenvironment of peripheral CLL cells mediated the leukemia cell death induced by this compound, isolated leukemia cells from patients with CLL were exposed to EC-7072. The antileukemic effect of EC-7072 on PBMCs was mimicked when isolated leukemia cells were employed (Figure 1.5B), bringing to light that the cytotoxic activity of the compound is independent of the activity of immune effector cells.

EC-7072 induces caspase-dependent apoptosis in primary CLL cells that is not counteracted by microenvironmental supportive stimuli.

The initial experiments performed with $DiOC_6(3)$/PI revealed a compromised leukemia cell plasma membrane integrity and mitochondrial transmembrane potential, both apoptosis-related parameters, as a consequence of EC-7072 treatment. Complementary experiments with Annexin V/PI showed that EC-7072 significantly induces CLL cell apoptosis (Figure 1.6A). Contrarily, no significant apoptosis was detected in T cells isolated from patients with CLL incubated with EC-7072, further supporting the selectivity of EC-7072 against B cells in comparison to other immune subsets (Supplementary Figure 1.5). Treatment of CLL cells with EC-7072 promoted a dose-dependent increase of the intracellular levels of active caspase-3 (Figure 1.6B-C). In parallel,

exposure to 200 nM EC-7072 increased the phosphorylation levels of histone H2AX (Figure 1.6D), which has been reported to constitute a cellular response triggered by caspase activation during apoptosis (Rogakou, Nieves-Neira, Boon, Pommier, & Bonner, 2000).

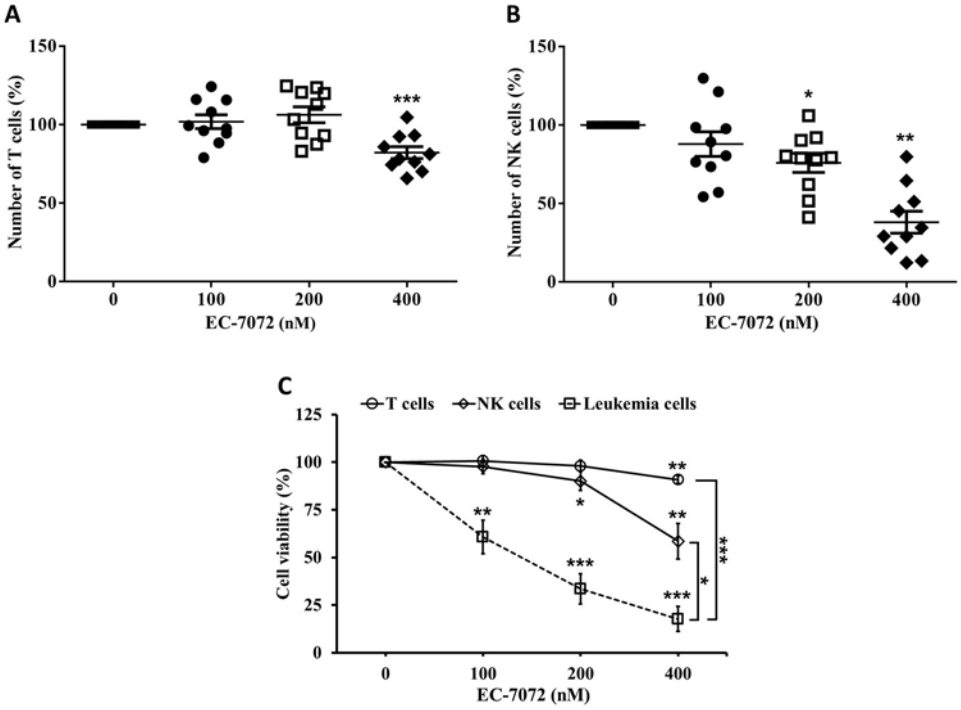

Figure 1.4. EC-7072 shows reduced toxicity against healthy immune subset in patients with CLL. PBMCs from patients with CLL were incubated with increasing concentrations of EC-7072 (0-400 nM) for 24 hours. Numbers of T cells (**A**) and NK cells (**B**) were evaluated by flow cytometry (n = 10). Graphs show the number of cells normalized to their respective control (DMSO) condition for each individual patient. **C.** Viability of immune cell subsets was determined by cytofluorometric assessment of $DiOC_6(3)$/PI staining (n = 6-10). The graph represent the percentage of viable [$DiOC_6(3)^+$] cells normalized to their respective control (DMSO) condition. (Mean ± SEM; *p < 0.05; **p < 0.01; ***p < 0.001, Student's *t*-test).

Cotreatment with increasing doses of the broad-spectrum caspase inhibitor Z-VAD-fmk completely abrogated the death of CLL cells induced by the mithralog (Figure 1.6E), unraveling that EC-7072-induced cell death is achieved via a caspase-dependent pathway. As expected, the protective effect of Z-VAD-fmk correlated with a reduction of active caspase-3 levels on leukemia cells (Figure 1.6F).

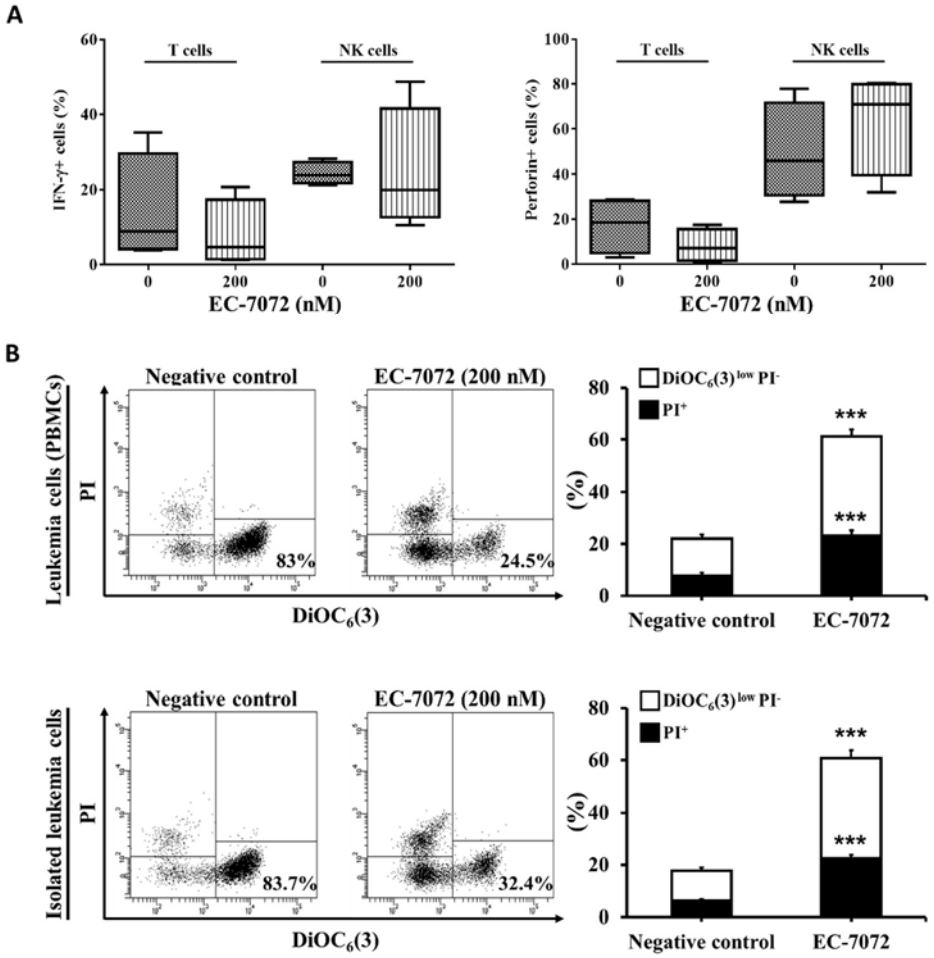

Figure 1.5. EC-7072 exerts a direct effect on CLL cells independent of healthy immune cells. A. PBMCs from patients with CLL (n = 4) exposed to 200 nM EC-7072 for 24 hours were stimulated with PMA/ionomycin and IFN-γ and perforin levels were assessed by intracellular flow cytometry. Graphs represent the percentage of IFN-γ^+ and perforin$^+$, respectively. **B.** Viability of leukemia cells treated with EC-7072 (200 nM, 24 hours) was determined in the presence and absence of other immune cell subsets (n = 24). Dot plots correspond to a representative experiment and percentage of viable cells in included for each condition. Bars represent the percentages of apoptotic [$DiOC_6(3)^{low}$ PI^-] and dead [PI^+] cells (mean ± SEM; ***p < 0.001, Student's *t*-test).

CLL cells display a strong dependence on prosurvival and growth signals provided by the microenvironment (Burger & Wiestner, 2018; ten Hacken & Burger, 2014). Thus, we explored whether exposure to an array of microenvironmental-derived cytokines associated to enhanced CLL survival and drug resistance could overcome the cytotoxicity produced by EC-7072 in CLL cells. As shown in Figure 1.7A-E, none of the soluble factors employed (CD40L, BAFF, TNF-α, IL-6 or IL-4) significantly affected the leukemia cell death brought about by the mithralog. Besides, coculture of PBMCs with the stromal cell line OP9, which mimic a protective microenvironmental niche, did not improve CLL cell survival upon EC-7072 exposure (Figure 1.7F). Hence, EC-7072-mediated CLL cell depletion is not prevented by microenvironmental stimulatory signals.

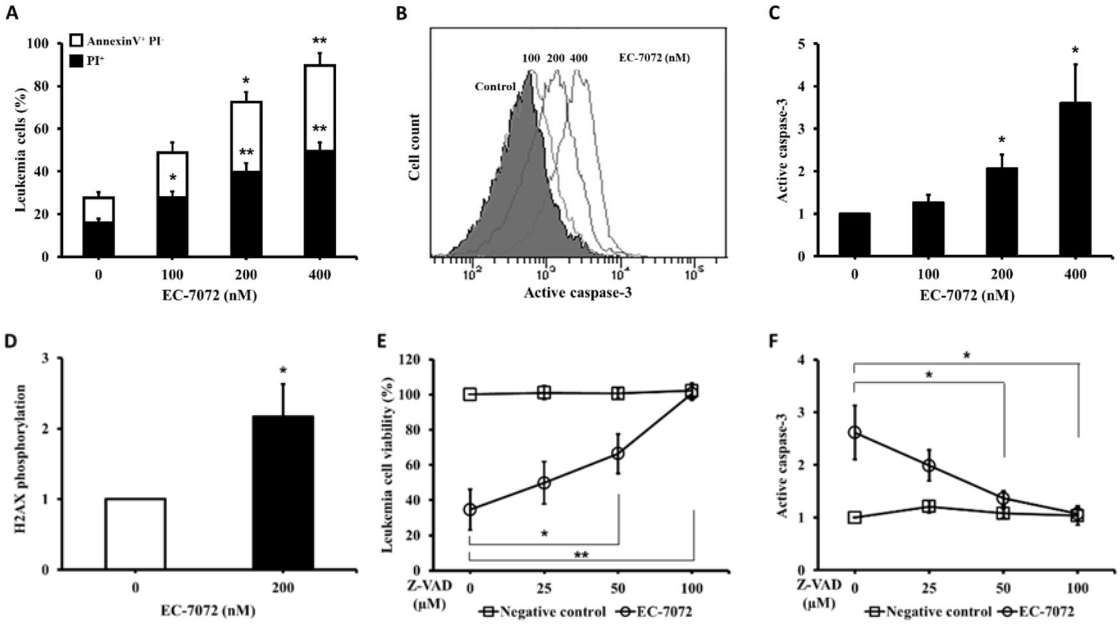

Figure 1.6. EC-7072 triggers caspase-dependent apoptosis in CLL cells. PBMCs from patients with CLL were incubated with 200 nM EC-7072 for 24 hours. **A.** Apoptosis of CLL cells was analyzed by double staining with Annexin V/PI. Bars represent the percentages of apoptotic [Annexin V^+ PI^-] and dead [PI^+] cells. **B-C.** Levels of active caspase-3 were assessed by flow cytometry. The histogram corresponds to a representative experiment and bars depict the normalized MFI of active caspase-3. **D.** Phosphorylation of histone H2AX was determined by phosphoflow. The graph shows the normalized MFI. **E-F.** PBMCs from patients with CLL were treated with EC-7072 (200 nM) and/or increasing doses of Z-VAD. Viability and active caspase-3 were studied in CLL cells. Graphs depict the normalized percentages of viable cells (**E**) and the normalized levels of active caspase-3 (**F**). (Mean ± SEM; *p < 0.05; **p < 0.01, Student's *t*-test).

EC-7072 modulates the transcriptome of primary CLL cells

To elucidate the mechanisms underlying the antileukemic effect of EC-7072, the transcriptional profile of primary leukemia cells from patients with CLL exposed to EC-7072 was studied. RNA-seq analysis identified 2531 differentially expressed genes in EC-7072-treated compared with control (DMSO) leukemia cells, unveiling a dramatic impact on the transcriptome of CLL cells mediated by EC-7072 (Figure 1.8A). Functional profiling of these transcripts revealed that EC-7072 modulates the expression of key mediators of signaling pathways that are crucial for CLL cell homeostasis and survival. In agreement, a broad downregulation of genes required for functional BCR signaling, such as members of the BCR complex (*CD79B*), BCR proximal-related kinases (*SYK*, *LYN*, *PIK3CD*) and downstream signaling effectors (*PLCG2*, *CARD11*) was found in EC-7072 treated CLL cells, which was subsequently validated by qPCR (Figure 1.8B and Supplementary Figure 1.6A).

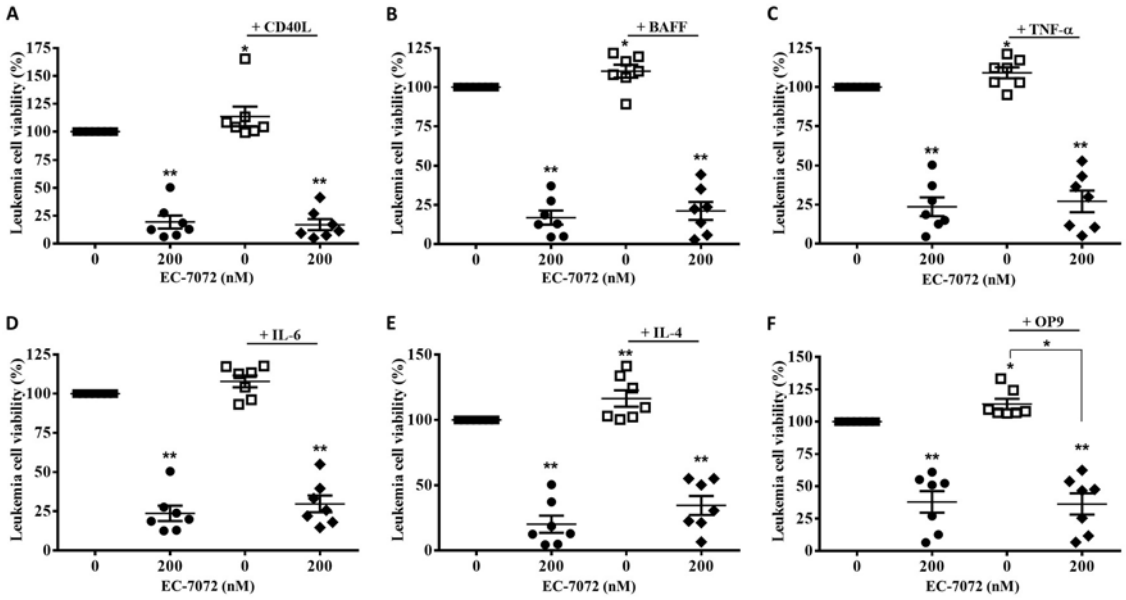

Figure 1.7. Microenvironmental stimuli typically associated to CLL survival do not abrogate the antileukemic effect of EC-7072. PBMCs from patients with CLL (n = 7) were incubated with 200 nM EC-7072 in combination with 100 ng/mL CD40L (**A**), 50 ng/ml BAFF (**B**), 40 ng/mL TNF-α (**C**), 40 ng/mL IL-6 (**D**) or 40 ng/mL IL-4 (**E**) for 24 hours. **F.** PBMCs from patients with CLL (n = 7) were incubated with OP9 cells for 72 hours and EC-7072 (200 nM) was added to the coculture for the last 24 hours. Leukemia cell viability was assessed by cytofluorimetric analysis. Graphs depict the mean percentage of viable [$DiOC_6(3)^+$] cells normalized to their respective control (DMSO) condition for each individual patient. Dark lines represent mean ± SEM. (*p < 0.05; **p < 0.01, Student's *t*-test).

Accordingly, KEGG pathway analysis of the protein-coding genes differentially expressed in treated CLL cells revealed an enrichment of multiple cascades engaged by the BCR-dependent signaling, such as NF-kB, JAK/STAT, PI3K/AKT and MAPK pathways (Figure 1.8C). Dysregulation of these signaling networks can lead to modulation of the expression of molecules that control apoptosis, a process that also scored among the most-enriched pathways in CLL cells exposed to EC-7072 (Figure 1.8C-D). Despite the mithralog did not trigger detectable cell death under these experimental settings (6 hours, 200 nM EC-7072) (data not shown), a reprogramming of the expression profile of genes that govern apoptosis was identified (Supplementary Figure 1.6B). Among this, the expression of the apoptotic regulator *BCL2* was significantly downregulated in primary CLL cells after incubation with EC-7072 (Supplementary Figure 1.6C). In contrast, *BCL2* expression was not modulated by the compound in T cells isolated from patients with CLL, thereby reinforcing the ability of EC-7072 to selectively induce leukemia cell apoptosis without significantly affecting other immune cell subsets (Supplementary Figure 1.6D).

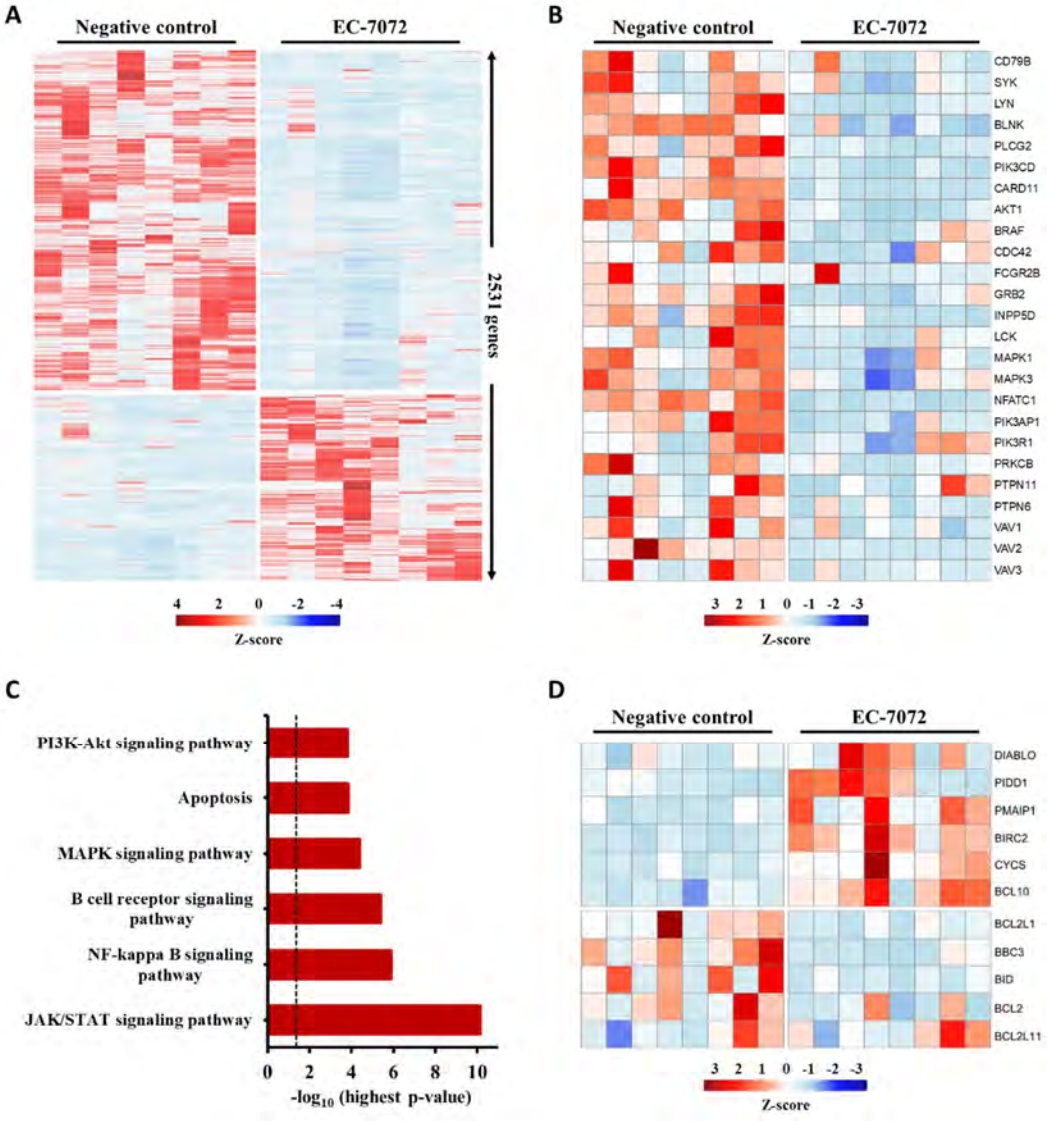

Figure 1.8. EC-7072 modulates the transcriptome of CLL cells. RNA-seq analysis was performed on total RNA extracted from isolated leukemia cells from patients with CLL (n = 8) treated with 200 nM EC-7072 for 6 hours. **A.** Heat map representation of the group of genes with significantly different expression between negative control (DMSO) and EC-7072-treated samples. The color scale represents the per-gene Z-score. Genes were selected based on adjusted p-value < 0.05, log2 (fold change) < -1 or > 1. **B.** Heat map representation corresponding to representative genes from BCR signaling that are significantly dysregulated by EC-7072 in CLL cells. The color scale represents the per-gene Z-score. **C.** Selected relevant pathways for CLL cell homeostasis significantly modulated by EC-7072 obtained through KEGG pathway analysis. Bars represent the -log10 of the highest p-value obtained from the iterative pathway analysis (dashed line corresponds to p-value = 0.05). **D.** Heat map representation of expression of genes related to apoptosis regulation that are significantly dysregulated by EC-7072 in CLL cells. The color scale represents the per-gene Z-score.

EC-7072 inhibits tonic BCR pathway by suppressing the expression and phosphorylation of key signaling nodes

The intense reprogramming of BCR signaling components at different levels of the pathway triggered by EC-7072 suggests that this compound might induce CLL cell apoptosis via inhibition of the BCR cascade. In agreement with the transcriptomic studies, EC-7072 significantly downregulated CD79B and IgM CLL cell surface expression, while the levels of CD79A remained the same after treatment, all of which are integrating parts of the BCR complex (Figure 1.9).

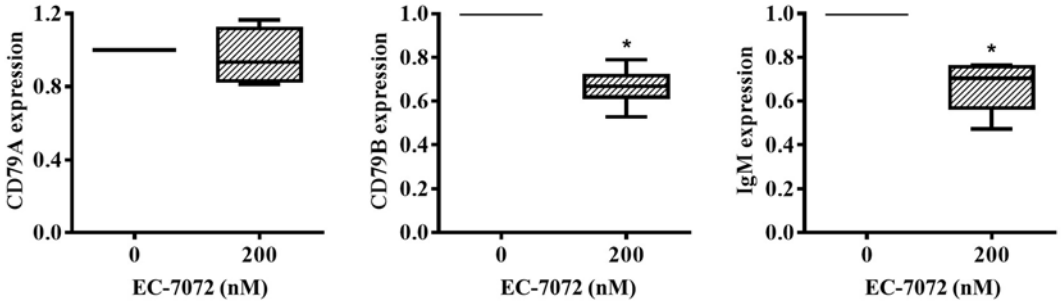

Figure 1.9. The BCR complex is negatively affected by EC-7072 in CLL cells. Surface expression of CD79A, CD79B and IgM was assessed in leukemia cells from patients with CLL (n = 5-6) incubated with 200 nM EC-7072 for 8 hours. Boxes represent the normalized MFI (*p < 0.05, Student's *t*-test).

Further, we evaluated the phosphorylation of BCR signaling nodes by phosphospecific flow cytometry. As previously reported, basal phosphorylation levels of components of the BCR cascade were highly heterogeneous among patients with CLL (Myklebust et al., 2017). Nevertheless, incubation with EC-7072 resulted in a generalized reduction of the levels of p-SYK, p-BTK and p-PLCγ2 in isolated leukemia cells (Figure 1.10A-B), a treatment that does not result in detectable CLL cell death (data not shown). In agreement, EC-7072-exposed CLL cells showed a significant downregulation in the phosphorylation levels of the downstream effector kinase ERK1/2 and the transcription factors p65 NF-κB and STAT3 (Figure 1.10C-D), which correlates with RNAseq analysis. No marked changes were detected in the phosphorylation of AKT, implying that the antileukemic cytotoxicity of EC-707 is not likely to involve modulation of AKT signaling (Figure 1.10C-D). It is worth mentioning that stimulation with CD40L or IL-6 strongly increased the phosphorylation levels of p65 NF-κB and STAT3 respectively, providing evidence that the phosphoflow analyses performed in this work were reliable and robust (Supplementary Figure 1.7). In summary, these data suggest that EC-7072 impairs tonic BCR signaling in primary CLL cells at different levels of the cascade.

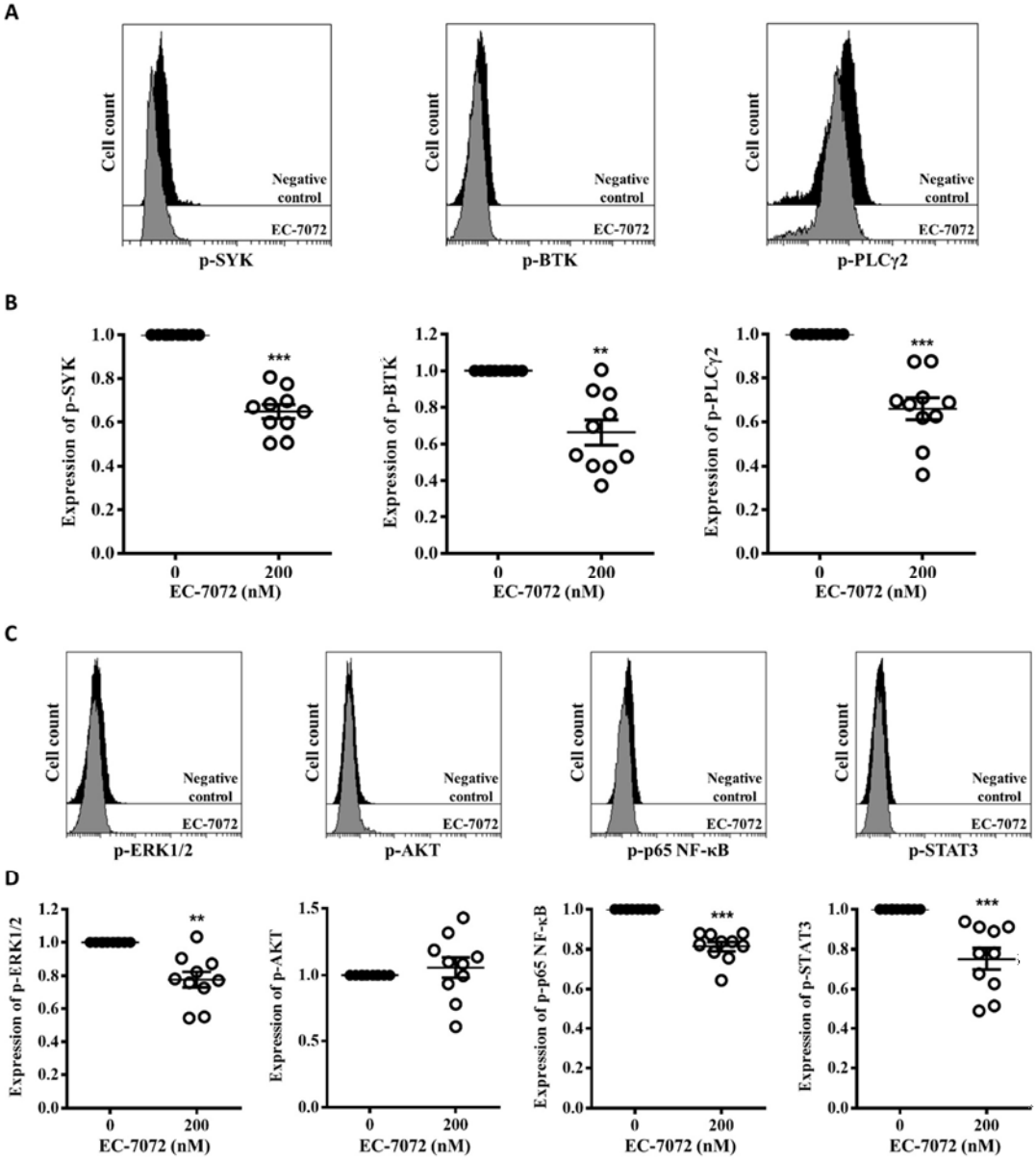

Figure 1.10. BCR signaling is downregulated by EC-7072 in CLL cells at different levels. Phosphorylation levels for BCR proximal kinases (**A-B**) and downstream effectors (**C-D**) were evaluated by phosphoflow in isolated leukemia cells from patients with CLL (n = 10) exposed to EC-7072 (200 nM) for 8 hours. Histograms depict the MFI from a representative patient. Graphs show the normalized MFI from each individual patient and dark lines correspond to mean ± SEM (**p < 0.01; ***p < 0.001, Student's *t*-test).

Activation of the BCR partially abrogates EC-7072-induced cell death of primary CLL cells

Given that BCR signaling is attenuated in CLL cells by EC-7072, we next asked whether this suppressive effect was responsible for the CLL cell death registered upon exposure to the mithralog. For that purpose, EC-7072-treated isolated leukemia cells from patients with CLL were stimulated with anti-IgM antibodies and viability and phosphorylation of BCR nodes were evaluated. As shown

in Figure 1.11, BCR over-stimulation with anti-IgM antibodies significantly enhanced leukemia cell survival in the presence of EC-7072.

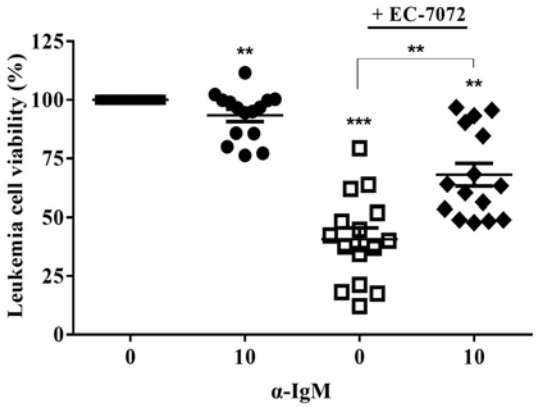

Figure 2.11. Activation of BCR signaling partially restores CLL viability in the presence of EC-7072. Viability was assessed in leukemia cells from patients with CLL after incubation with EC-7072 (200 nM) and/or anti-IgM antibodies (10 µg/ml) for 24 hours. The graph represents the percentage of viable [$DiOC_6(3)^+$] cells normalized to their control (DMSO) condition for each individual experiment (mean ± SEM; **p < 0.01; ***p < 0.001, Student's *t*-test).

As expected, BCR engagement highly increased the basal phosphorylation of key mediators of the pathway (Figure 1.12). Accordingly, the levels of phosphorylated SYK and PLCγ2 in CLL cells treated with EC-7072 were induced upon BCR crosslinking compared to unstimulated CLL cells exposed to the mithralog (Figure 1.12A-B). Similar results were observed in p-ERK1/2, p-AKT, p-p65 NF-κB and p-STAT3 (Figure 1.12C-D). Furthermore, the expression of *BCL2* was restored to basal levels in stimulated CLL cells treated with the mithralog (Supplementary Figure 1.8). Overall, these results support the crucial role of BCR signaling modulation in the antileukemic activity of EC-7072.

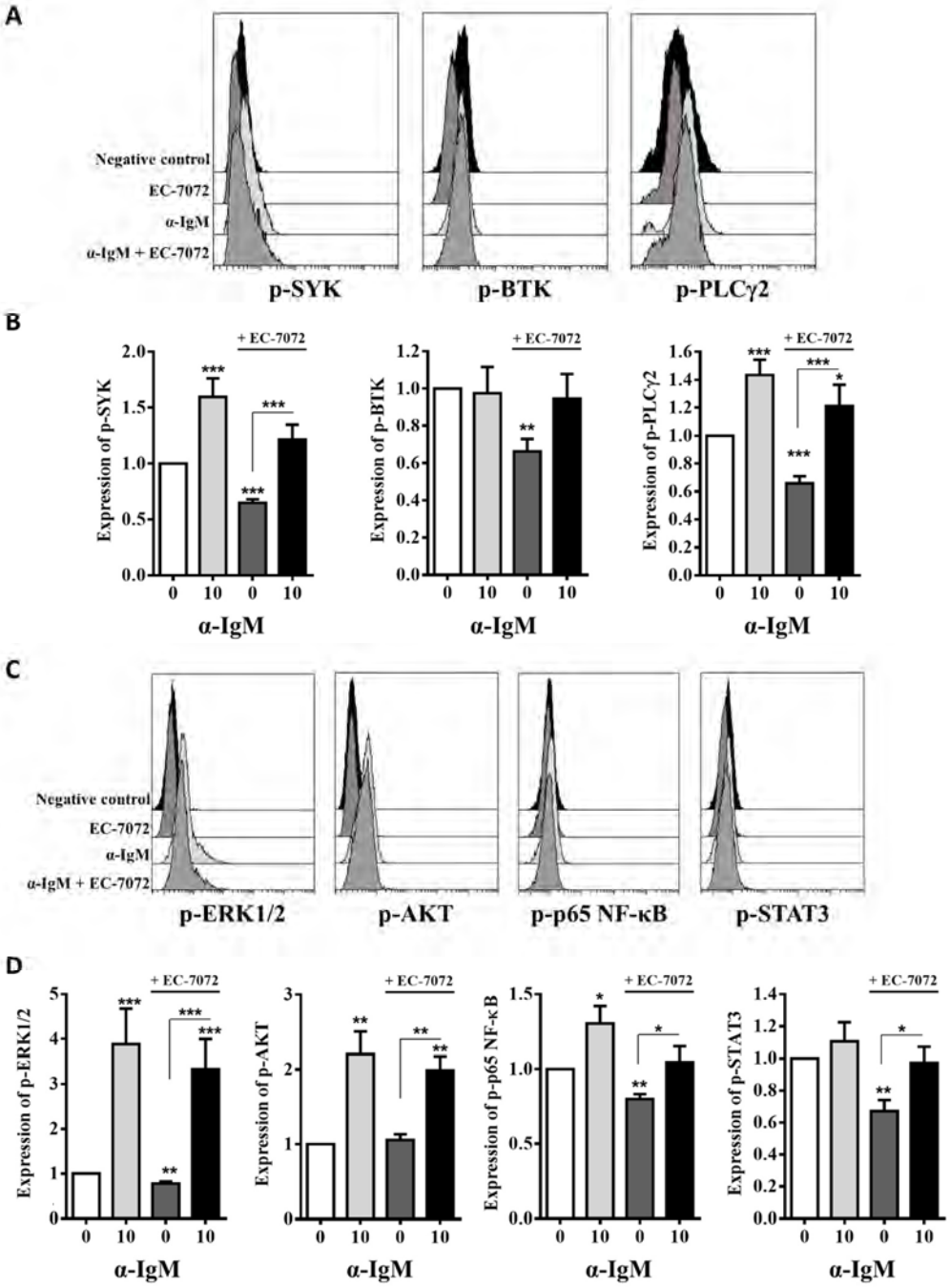

Figure 1.12. BCR crosslinking attenuates the downregulation of key mediators exerted by EC-7072 in CLL cells. Isolated leukemia cells from patients with CLL (n = 6-10) were treated with EC-7072 (200 nM) and/or anti-IgM antibodies (10 μg/ml) for 8 hours and phosphorylation levels of BCR proximal kinases (**A-B**) and downstream mediators (**C-D**) were determined by phosphoflow. Histograms depict the MFI from a representative patient. Bars correspond to the normalized MFI from each individual patient (mean ± SEM; *p < 0.05; **p < 0.01; ***p < 0.001, Student's *t*-test).

EC-7072 displays a cytotoxic activity against primary CLL cells analogous and additive with that of therapies routinely used in CLL

Several components of the BCR signaling pathways that are affected by EC-7072, such as BTK, stand out as targets of recent therapeutic approaches for CLL. Thus, we analyzed whether the antileukemic efficacy of EC-7072 is comparable to that of therapies currently approved for patients with CLL. For that purpose, PBMCs from patients with CLL were incubated with increasing concentrations of EC-7072, fludarabine (a nucleoside analog), ibrutinib (a BTK inhibitor), idelalisib (a PI3Kδ inhibitor) or venetoclax (a BCL2 antagonist), at previously-described doses (Anderson et al., 2016; Herman et al., 2011; Herman et al., 2010), and leukemia cell viability was assessed by flow cytometric detection. EC-7072 exerted similar cytotoxicity against CLL cells than ibrutinib and venetoclax, while it proved more efficient in eliminating CLL cells that fludarabine or idelalisib (Supplementary Figure 1.9). To determine the effect of combining EC-7072 with the tested drugs, the CI of each combination was calculated. PBMCs were treated with non-fixed ratio combinations employing IC_{10}, IC_{25} and IC_{50} doses. CI values unraveled that combination of EC-7072 with ibrutinib or venetoclax achieved a general additive efficacy. On the contrary, the cytotoxic effect of idelalisib or fludarabine is synergistic with that of EC-7072 (Figure 1.13).

The side toxicity produced by the distinct drug combinations on the viability of healthy immune subsets, T cells and NK cells, from patients with CLL was also assessed. Of note, EC-7072 showed significantly less toxicity against T cells and NK cells that ibrutinib and fludarabine under the conditions studied, whereas venetoclax and idelalisib exerted reduced toxicity on these cell subsets, similar to EC-7072 (Supplementary Figure 1.10). Nonetheless, all the combinations produced higher side toxicity on healthy immune cell subsets, mainly NK cells (Supplementary Figure 1.10).

Collectively, these experiments indicate that EC-7072 displays an additive or synergistic antileukemic effect with agents currently approved for CLL therapy, pointing out that the use of this mithralog alone or in combination regimens may represent a novel therapeutic approach for CLL.

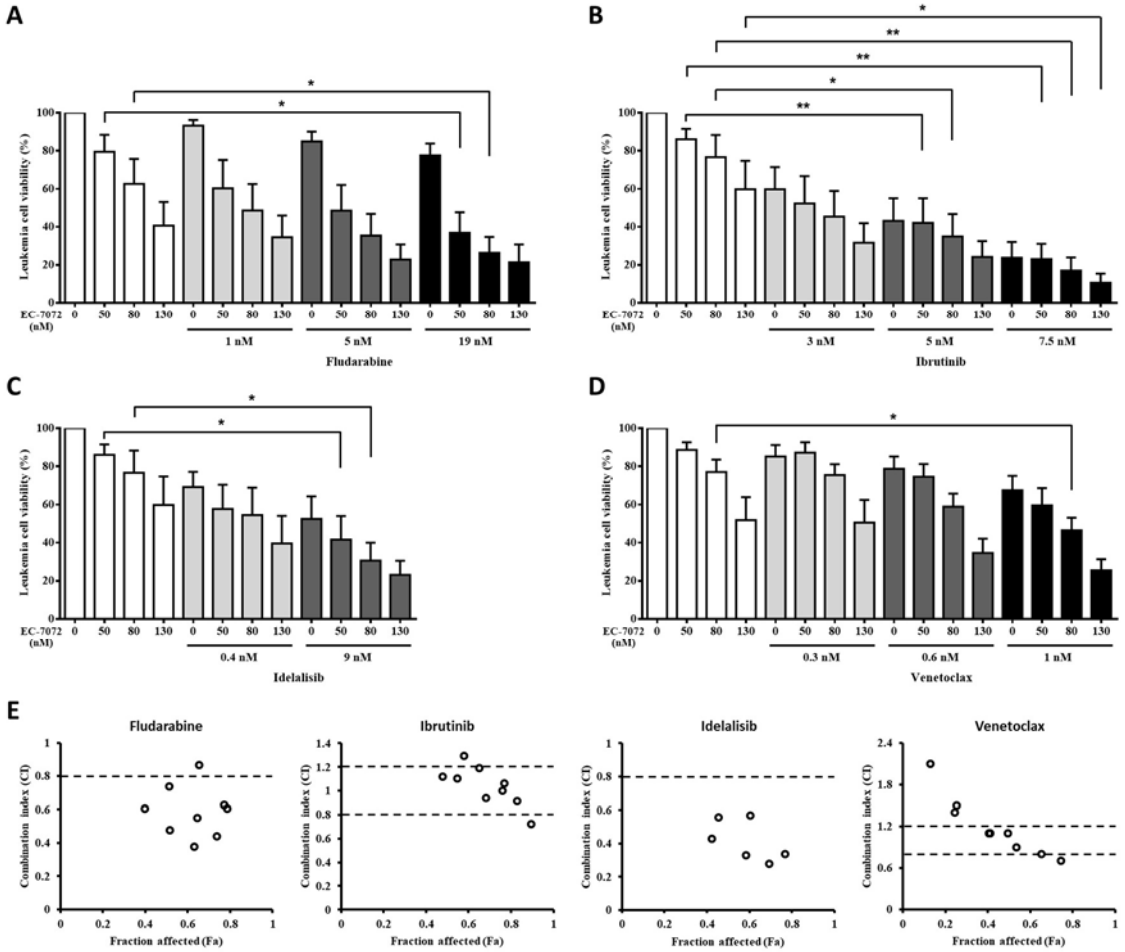

Figure 1.13. EC-7072 exerts additive or synergistic antileukemic effect in combination with therapies currently approved for CLL treatment. PMBCs from patients with CLL were treated with non-fixed ratio combinations of EC-7072 with fludarabine (**A**), ibrutinib (**B**), idelalisib (**C**) or venetoclax (**D**) and viability of CLL cells was evaluated by flow cytometry. Bars represent to the normalized percentage of viable [$DiOC_6(3)^+$] cells (mean ± SEM; *p < 0.05; **p < 0.01, One-way ANOVA). **E.** CI values were calculated by the Chou-Talalay method and plotted. CI values < 0.8 represent synergistic effect, values between 0.8-1.2 indicate additive effect and values > 1.2 represent an antagonistic effect.

Discussion

The antitumor properties of MTA have been extensively described, along with a high toxicity associated to treatment that has limited the clinical use of this antibiotic (L. Green & Donehower, 1984; Torrance, Agrawal, Vogelstein, & Kinzler, 2001). Given the therapeutic potential of MTA in cancer, an array of analogs of the compound, or mithralogs, have been generated over the years to overcome this problem, rendering agents with reduced side effects and/or improved antitumor activity (Baig et al., 2008; Osgood et al., 2016; Remsing et al., 2003). In the present work, we report that the mithralog EC-7072 exerts a robust antileukemic activity in CLL.

EC-7072 exhibited reduced toxicity against healthy cells from different origins compared to MTA, in agreement with several studies demonstrating that EC-7072 is well-tolerated in mice (Malek et al., 2012; Osgood et al., 2016). Both non-malignant and leukemia B cell viability were negatively affected by EC-7072 treatment, indicating that the compound may display selectivity against this immune population. Circulating NK cells and, primarily, T cells were largely unaffected by EC-7072, further supporting this hypothesis. Besides, no changes in the immune production of key antitumor effector molecules (IFN-γ and perforin) were brought about by the mithralog, suggesting that EC-7072 does not aggravate the immune dysfunction frequently observed in patients with CLL. Nonetheless, CLL cells showed similar sensitivity to EC-7072 in the absence of other immune cell subsets, indicating that the compound exerts a direct antileukemic activity.

The molecular events linked to BCR activation are crucial for healthy and leukemia B cell survival and homeostasis. Upon BCR engagement, a phosphorylation cascade of upstream mediators is activated inside the cell, eventually followed by activation of downstream signaling pathways that include NF-κB, JAK/STAT or MAPK (Koehrer & Burger, 2016). These pathways sustain cell viability by, among others, upregulating the expression of antiapoptotic proteins of the BCL2 family (Hata, Engelman, & Faber, 2015). As a consequence, disruption of the BCR pathway often results in leukemia cell death and represents one of the therapeutic strategies employed in the treatment of CLL. Targeted agents inhibiting BCR signaling components exhibit improved efficacy compared to conventional treatments (Woyach, Johnson, & Byrd, 2012). RNA-seq experiments unveiled that EC-7072 profoundly modulates the BCR signaling pathway at multiple levels in leukemia cells from patients with CLL, downregulating the expression of components of the BCR complex (e.g. *CD79B*), upstream mediators (e.g. *SYK*) and downstream effectors (e.g. *PLCG2*) (Figure 1.14). Concomitantly, signaling pathways activated by the BCR cascade were also found altered by EC-7072, suggesting a general dysregulation of BCR signaling in CLL cells upon treatment. In addition, a general reprogramming of genes that govern apoptosis was observed in CLL cells exposed to the

mithralog, in consonance with previous results demonstrating that EC-7072 induces caspase-dependent apoptosis.

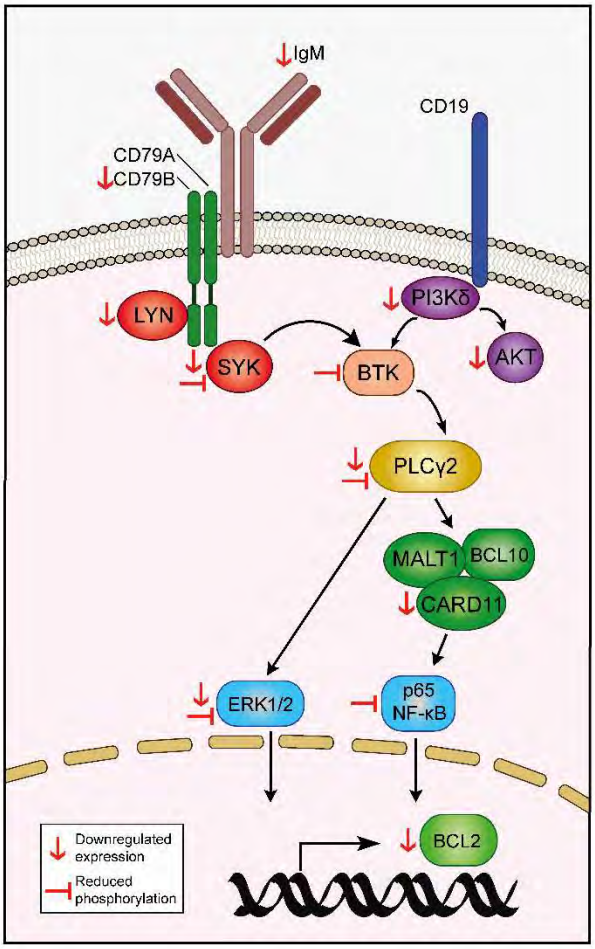

Figure 1.14. Hypothetical model of action of EC-7072 targeting the BCR signaling pathway in CLL cells. Red downwards arrows (↓) represent downregulation of protein (CD79B and IgM) or transcriptional expression in CLL cells upon EC-7072 treatment. Left tack symbols (⊣) represent reduced phosphorylation levels of key components of the BCR cascade detected by phosphoflow analysis in primary CLL cells after exposure to EC-7072.

Concomitantly with the transcriptomic studies, the levels of phosphorylated signaling components of the BCR cascade were decreased in leukemia cells in the presence of EC-7072, suggesting that the compound may disrupt tonic activation of BCR-dependent signaling cascades (Figure 1.14). This is further reinforced by the reduced surface expression of BCR subunits (CD79B and IgM) observed in CLL cells upon EC-7072 treatment. Nonetheless, BCR stimulation was able to partially restore the phosphorylation levels of BCR-related signaling nodes and significantly reverted the apoptotic cell death induced by EC-7072. Altogether, these results support that the cytotoxicity of the compound against CLL cells may involve modulation of the BCR signaling pathway.

Most of the novel therapies for treatment of CLL are targeted agents that inhibit mediators of the BCR signaling pathway. However, a major problem of CLL therapies is the development of therapeutic resistance in high-risk patients, which has prompted the design of combination therapies (Blombery et al., 2019; Seymour et al., 2017). Of note, the antileukemic activity of EC-7072 was independent of the presence of molecular and cytogenetic aberrations typically associated to therapy resistance in patients with CLL and was not affected by microenvironment-derived factors that promote leukemia cell survival (Dreger et al., 2018). Acquired resistance to targeted CLL therapies is frequently driven by mutations in genes encoding BCR signaling mediators. Thus, co-occurring mutations in *BTK* and *PLCG2* have been shown to mediate ibrutinib resistance (Woyach et al., 2014), while a point mutation in *BCL2* has recently been identified in patients with CLL resistant to treatment with venetoclax (Blombery et al., 2019). The dramatic impact of EC-7072 on the transcriptome of CLL cells opens the question of whether the mithralog would be effective in the presence of mutational events affecting components of the BCR signaling pathway that are targets of these novel agents, hence providing rationale for its use in combined CLL therapies. Indeed, we found that EC-7072 displays comparable or higher killing activity on CLL cells than that of fludarabine, ibrutinib, idelalisib and venetoclax. In addition, EC-7072 exhibit synergy when combined with idelalisib and fludarabine, and combination with ibrutinib and venetoclax resulted in an additive effect. Conversely, the mithralog was significantly less toxic to non-malignant immune cells from the same patients than other agents, mainly fludarabine, which frequently causes lymphocytopenia in patients with CLL (Keating et al., 1998).

Overall, our findings provide evidence that the mithralog EC-7072 induces leukemia cell death by modulation the status of BCR signaling in CLL cells. The compound enhances the antileukemic activity of approved therapeutic agents and is effective independent of the IGHV mutational status or cytogenetic alterations, thus arising the question of whether EC-7072 may be a potential novel standalone or combination therapeutic option for patients with CLL and other B-cell malignancies.

2. B cell activation hinders NK cell-mediated antitumor responses by downregulation of NKG2D immunoreceptor

BCR crosslinking dysregulates the surface expression of activating receptors in effector immune populations

B-cell malignancies typically display aberrant BCR signaling activation. This pathway is critical for B cell development and homeostasis and its tonic activation has been linked to pathogenesis and survival of malignant B cells (Niemann & Wiestner, 2013; Rickert, 2013). Nonetheless, the role of B cell activation in other features of these types of cancer, such as the immune suppression reported in NK cells and T lymphocytes, remains to be fully dilucidated.

To evaluate the impact of exacerbated BCR signaling activation on the phenotype of effector immune cells, PBMCs from healthy donors or patients with CLL were incubated with anti-IgM or anti-IgD antibodies, two specific anti-BCR antibodies that activate B cells, and the expression profile of an array of activating immunoreceptors was assessed on NK cells and $CD8^+$ T cells by flow cytometry. BCR crosslinking drastically reduced the expression levels of NKG2D in NK cells (Figure 2.1A) and $CD8^+$ T cells (Supplementary Figure 2.1A), whereas it exerted a modest downregulation of DNAM-1 in these immune subsets (Figure 2.1B and Supplementary Figure 2.1B). On the contrary, increased surface expression of NKp46 in NK cells was detected upon B cell activation (Figure 2.1C). No changes were observed in NKp30 and NKp44 expression in NK cells (data not shown). Similar results were obtained in NK cells and $CD8^+$ T cells from patients with CLL after B cell stimulation with anti-IgM or anti-IgD antibodies (Figure 2.1 and Supplementary Figure 2.1). Of note, NKG2D basal levels in NK cells from patients with CLL were significantly lower than the expression observed in NK cells from healthy donors, a hallmark of immunosuppression previously reported in this malignancy (Huergo-Zapico, Acebes-Huerta, Gonzalez-Rodriguez, et al., 2014; Parry et al., 2016) (Supplementary Figure 2.2). Additionally, treatment with anti-IgM or anti-IgD antibodies did not affect the viability of healthy B cells (Supplementary Figure 2.3A) or CLL cells (Supplementary Figure 2.3B), as evidenced by double staining with $DiOC_6(3)$/PI, hence demonstrating that the dysregulation of immune receptors observed on NK cells and $CD8^+$ T cells is not a consequence of triggering B cell apoptosis.

To determine the extent of the immune suppression suffered by these immune subsets due to B cell activation, PBMCs from healthy donors were exposed to anti-IgM and anti-IgD antibodies in the presence of the stimulatory cytokines IL-2 and IL-15. As expected, treatment with IL-2, and IL-15 in a lesser extent, increased the expression of NKG2D in NK cells (Supplementary Figure 2.4A) and similar effect was observed in $CD8^+$ T cells (Supplementary Figure 2.4B). Nonetheless, the

prosurvival signals provided by these cytokines did not counteract the downregulation of NKG2D on these immune subsets upon treatment with anti-BCR antibodies (Supplementary Figure 2.4A-B).

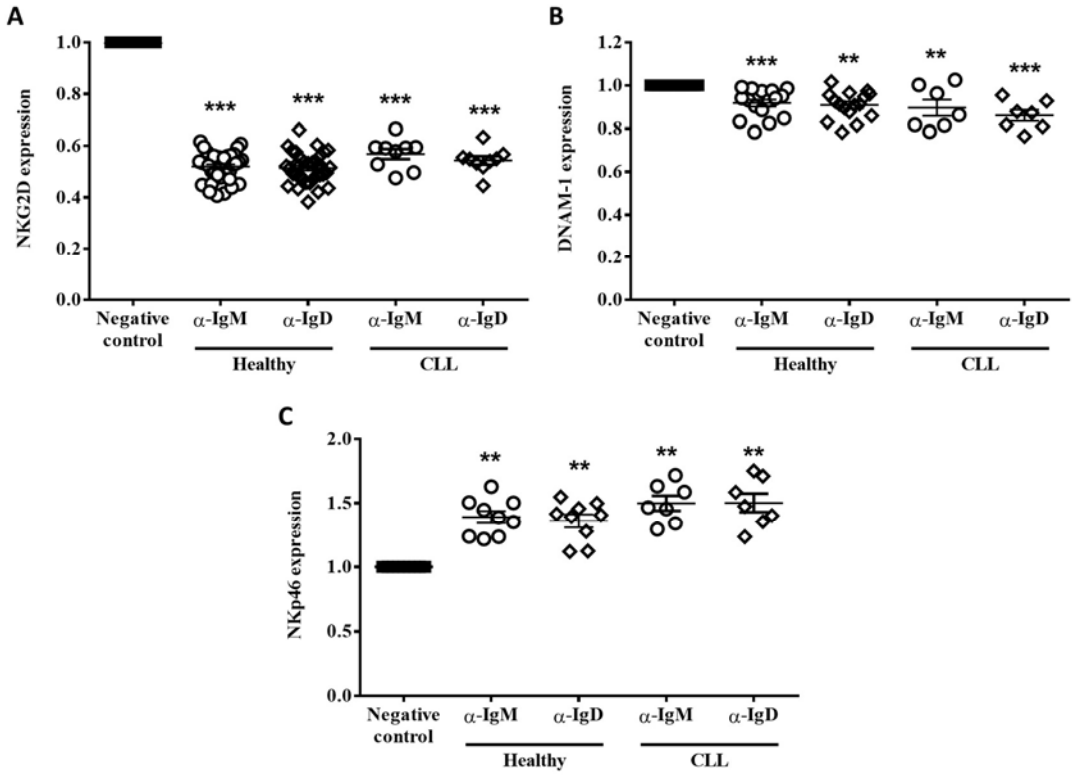

Figure 2.1. BCR stimulation modulates the immunoreceptor phenotype of NK cells. PMBCs from healthy donors (n = 9-36) or patients with CLL (n = 7-9) were incubated with F(ab')$_2$ anti-IgM (10 µg/mL) or anti-IgD (10 µg/mL) antibodies for 48 hours. Surface expression levels of NKG2D (**A**), DNAM-1 (**B**) and NKp46 (**C**) were assessed in NK cells by flow cytometry. Graphs depict the MFI for each receptor normalized to their respective control condition. (Mean ± SEM; **p < 0.01; ***p < 0.001, Student's t-test).

B cell activation is further enhanced by engagement of co-stimulatory molecules expressed on the cell surface, being CD40 a crucial receptor in the interaction with T helper cells and, thus, in adaptive immunity (Bishop, Haxhinasto, Stunz, & Hostager, 2003). Therefore, we assessed whether CD40 ligation influenced the expression of NKG2D, DNAM-1 and NKp46 in effector immune populations. Treatment of PBMCs from healthy donors with CD40L alone partially decreased the expression of NKG2D and DNAM-1 in NK cells (Figure 2.2A), whereas no effect was detected in the levels of these receptors in NK cells from patients with CLL (Figure 2.2B). No significant changes were observed in NKp46 expression in the conditions studied. Besides, $CD8^+$ T cells suffered a moderate reduction of DNAM-1 levels upon exposure of PBMCs from healthy donors to CD40L (Supplementary Figure 2.5A). Subsequently, the effect of combining CD40L with anti-IgM antibodies on the surface levels of the receptors studied was also evaluated by flow cytometry.

NKG2D was further downregulated in healthy NK cells upon co-stimulation of B cells compared to treatment with anti-IgM antibodies alone, while no differences were found in DNAM-1 and NKp46 receptors (Figure 2.2A). On the other hand, CLL cell co-activation failed to potentiate the decrease of NKG2D expression exerted in NK cells by BCR crosslinking (Figure 2.2B). No cooperative effect on the immunoreceptor expression profile of $CD8^+$ T cells from healthy donors and patients with CLL was registered (Supplementary Figure 2.5A-B).

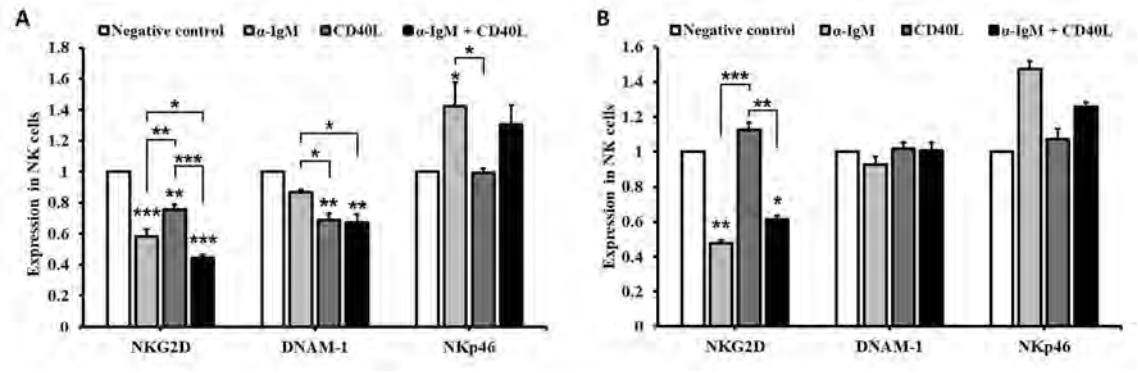

Figure 2.2. Co-stimulation of B cells with CD40 ligand potentiate NKG2D downregulation in NK cells. PMBCs from healthy donors (n = 4-6) (**A**) or patients with CLL (n = 3) (**B**) were incubated with $F(ab')_2$ anti-IgM antibodies (10 µg/mL) and/or CD40L (200 ng/mL) for 48 hours. Surface expression levels of NKG2D, DNAM-1 and NKp46 were determined in NK cells by flow cytometry. Bars show the normalized MFI for each receptor. (Mean ± SEM; *p < 0.05; **p < 0.01; ***p < 0.001, One-way ANOVA).

B cell activation hampers NK cell cytotoxic activity against tumor cells

Since NKG2D, a central activating receptor mediating the cytotoxic function of NK cells, is reduced owing to B cell activation, we assessed whether NK cell antitumor activity is modulated as well. For that purpose, PBMCs from healthy donors incubated with anti-IgM or anti-IgD antibodies were cocultured with K-562 tumor cells and NK cell responses were analyzed. As shown in Figure 2.3A, the cytotoxic activity of NK cells from anti-IgM- or anti-IgD-treated PBMCs was reduced compared to the control condition in the three E:T ratios tested. Concomitantly, BCR crosslinking translated into attenuated activation of NK cells upon coculture with K-562 cells, as evidenced by the decreased levels of the degranulation marker CD107a (Figure 2.3C-D). Noticeably, no differences were detected in the production of IFN-γ by NK cells (Figure 2.3B).

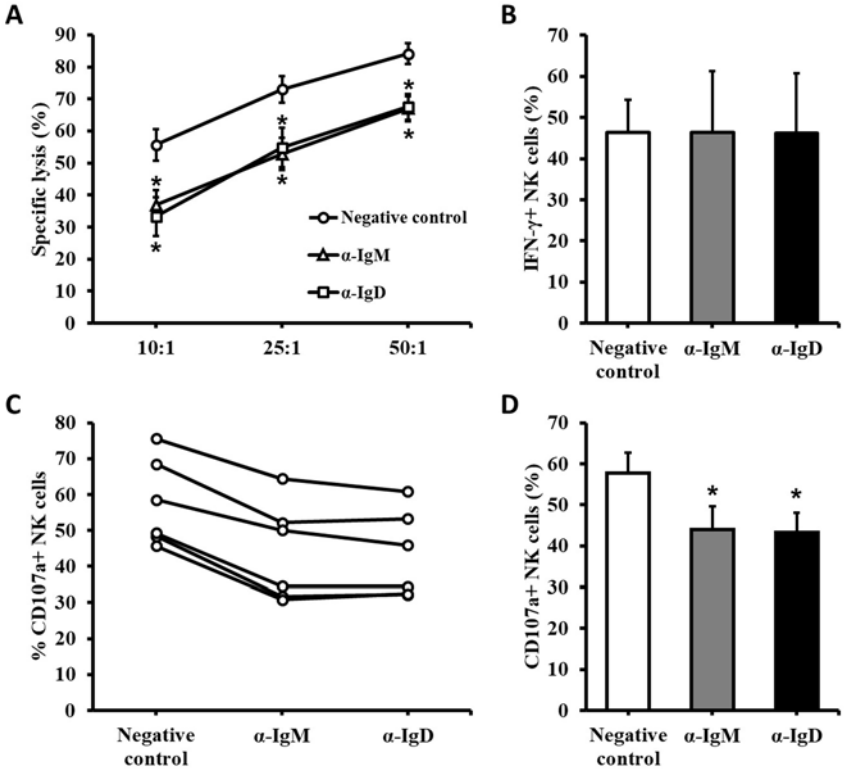

Figure 2.3. NK cell cytotoxic activity is hindered as a consequence of B cell activation. PMBCs from healthy donors were treated with F(ab')$_2$ anti-IgM (10 µg/mL) and/or anti-IgD (10 µg/mL) antibodies for 48 hours. **A.** Calcein-stained K-562 cells were coculture with control or treated PBMCs for 4 hours and specific lysis was analyzed by fluorometric detection. The graph represents the percentage of specific lysis of K-562 cells at E:T ratios 10:1, 25:1 and 50:1. **B.** IFN-γ production was measured in NK cells after exposure to K-562 cells for 4 hours in the presence of PMA/ionomycin. Bars depict the mean percentage of IFN-γ^+ NK cells. **C-D.** Control and treated PBMCs were cocultured with K-562 for 4 hours and CD107a levels were assessed in NK cells by flow cytometry. Lines correspond to individual samples (C). Bars show the mean percentage of CD107a$^+$ NK cells (D). (Mean ± SEM; *$p < 0.05$, Wilcoxon signed-rank test).

NK cells are also able to identify and eliminate target cells via ADCC. Hence, we next studied whether B cell stimulation negatively affects this process. First, we analyzed the expression levels of CD16, the NK cell receptor in charge of recognizing the Fc regions of antibodies bound to cell surface antigens. Treatment of PBMCs from healthy donors with anti-IgM or anti-IgD antibodies resulted in decreased expression levels of CD16 in NK cells (Figure 2.4A). No significant differences in the percentage of CD16$^+$ NK cells were found (data not shown), therefore suggesting that BCR crosslinking exerts a general downregulation of CD16 in the NK cell subset. In line with this, B cell stimulation with anti-IgM and anti-IgD antibodies abrogated the enhanced NK cell-mediated lysis of Raji tumor cells observed in the presence of rituximab (Figure 2.4B).

Altogether, these experiments bring to light that B cell activation via BCR crosslinking results in impaired cytotoxic function of NK cells.

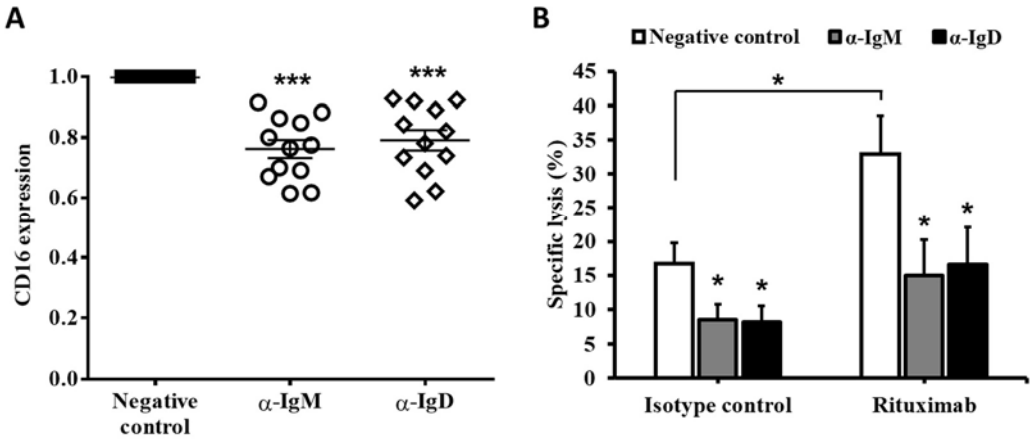

Figure 2.4. B cell stimulation impairs ADCC. PMBCs from healthy donors were treated with F(ab')$_2$ anti-IgM (10 μg/mL) and/or anti-IgD (10 μg/mL) antibodies for 48 hours. **A.** CD16 expression levels were analyzed by flow cytometry. Graph shows the normalized MFI (mean ± SEM; ***$p < 0.001$, Student's t-test). **B.** Raji cell pretreated with rituximab (10 μg/mL) were cocultured with control and stimulated PBMCs for 4 hours and specific lysis was assessed by fluorometric detection. Bars show the mean percentage of specific lysis (mean ± SEM; *$p < 0.05$, Wilcoxon signed-rank test).

NKG2D downregulation is not mediated by direct cell to cell contact upon B cell stimulation

To gain further insight into the BCR crosslinking-mediated NKG2D downregulation in NK cells, we next analyzed whether this effect is induced owing to direct B cell-NK cell contact or via soluble factors produced upon B cell activation. First, PBMCs from healthy donors or patients with CLL were incubated with conditioned media collected from control or anti-BCR antibody-treated PBMCs. The decrease in NKG2D expression levels was comparable in NK cells exposed to treated-PBMC conditioned media in healthy and CLL samples to that previously observed upon direct treatment (Figure 2.5A). Accordingly, DNAM-1 expression was slightly reduced in NK cells from healthy donors, finding no differences in anti-BCR conditioned media-exposed NK cells from CLL (Figure 2.5B). Culture with conditioned media from treated-PBMCs induced the expression of NKp46 in NK cells from both origins (Figure 2.5C). Similar results were detected in NKG2D expression in NK cells from healthy volunteers following incubation with conditioned media obtained from control and anti-BCR-treated cell lines derived from B-cell malignancies (Supplementary Figure 2.6).

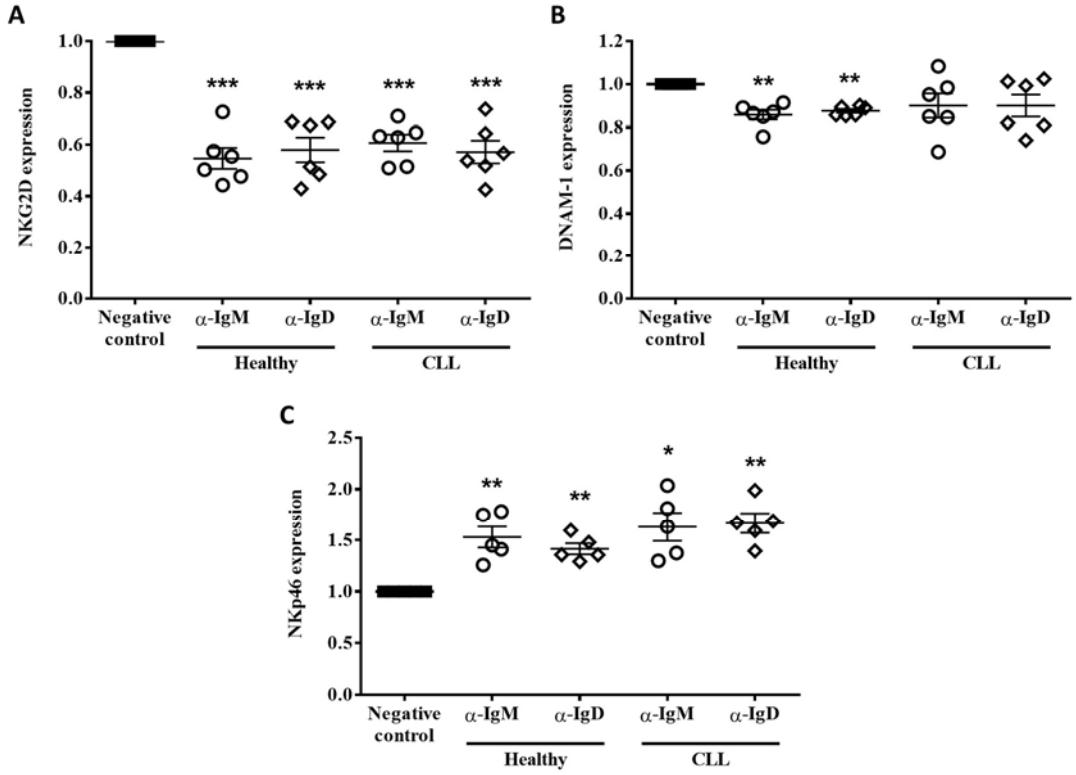

Figure 2.5. Conditioned media from BCR-activated PBMCs modulates the immunoreceptor profile of NK cells. PMBCs from healthy donors (n = 5-6) or patients with CLL (n = 5-6) were incubated with $F(ab')_2$ anti-IgM (10 µg/mL) or anti-IgD (10 µg/mL) antibodies for 48 hours and supernatants were collected. Then, expression of NKG2D (**A**), DNAM-1 (**B**) and NKp46 (**C**) were determined in NK cells from PBMCs cultured with control, anti-IgM or anti-IgD antibody-treated supernatants for 48 hours by flow cytometry. Graphs show the normalized MFI for each receptor. (Mean ± SEM; *p < 0.05; **p < 0.01; ***p < 0.001, Student's t-test).

To further confirm these results, transwell assays were performed employing PBMCs from healthy donors (Figure 2.6A). As expected, NKG2D expression was significantly reduced in NK cells present in the bottom section of the transwell, since these PBMCs are directly exposed to anti-IgM antibodies (Figure 2.6B). Likewise, the NK cell population located in the upper section of the transwell insert suffered a significant downregulation of NKG2D (Figure 2.6B). DNAM-1 was remarkably downmodulated in NK cells in both conditions (Figure 2.6C).

In summary, this experimental evidence support that B cell activation induces NK cell immunosuppression via secretion of yet-unknown soluble factors to the cell culture.

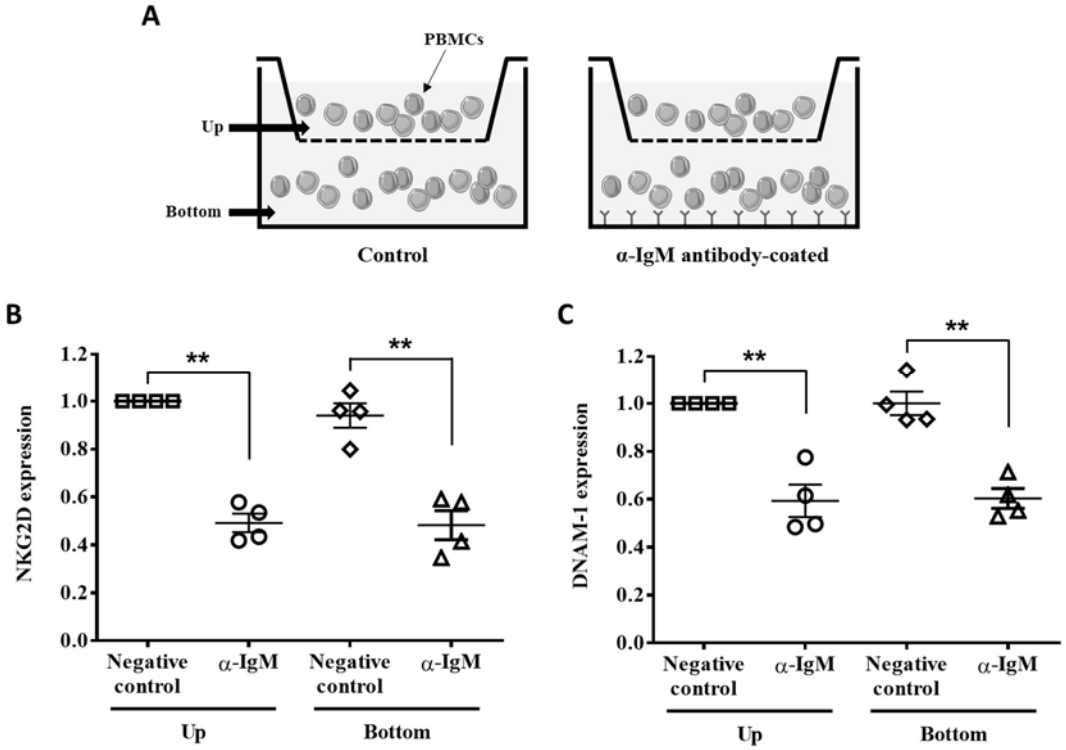

Figure 2.6. NKG2D is downregulated in NK cells upon coculture in transwell inserts with IgM-treated PBMCs. Culture plates were coated with anti-IgM (μ-chain specific) antibodies (10 μg/mL) at 4°C overnight. PBMCs from healthy donors (n = 4) were cultured in contact with the coated antibody or inside transwell inserts (0.4 μm) for 48 hours. **A.** Diagram illustrating the transwell system employed in this work. **B.** NKG2D and **C.** DNAM-1 expressions were analyzed by flow cytometry. Graphs represent the normalized MFI for each receptor. (Mean ± SEM; **p < 0.01, Student's t-test).

NKG2D is not downregulated due to shedding and interaction with NKG2DLs from stimulated B cells.

Shedding of NKG2Ls is a widely-known strategy employed by tumor cells to evade NK cell-mediated killing. Soluble NKG2DLs interact with NKG2D on the cell surface of NK cells and $CD8^+$ T cells, promoting the internalization of the receptor and, hence, limiting NKG2D-mediated tumor recognition (Groh et al., 2002; Lundholm et al., 2014; Song et al., 2006). The cleavage of NKG2DLs is mostly carried out by matrix metalloproteinases (MMPs) (Chitadze et al., 2013; Liu, Atteridge, Wang, Lundgren, & Wu, 2010; Waldhauer et al., 2008). To determine whether this mechanism of NKG2D suppression play a role in our experimental conditions, PBMCs from healthy donors were pretreated with the broad-spectrum MMP inhibitors GM6001 and BB-94 and subsequently stimulated with anti-BCR antibodies. As shown in Figure 2.7, MMP inhibition did not abrogate the downregulation of NKG2D expression in NK cells induced by anti-IgM or anti-IgD antibody treatment. In line with this, no changes in the surface levels of MICA/B and ULBP1-3 in healthy B

cells were detected upon BCR stimulation (data not shown), altogether suggesting that NKG2D is not downregulated in NK cells owing to soluble ligands shed by activated B cells.

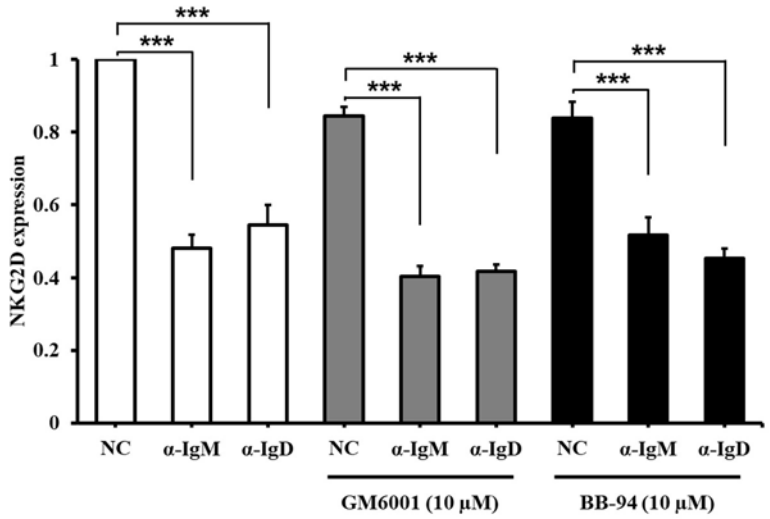

Figure 2.7. MMP inhibition does not revert NKG2D downregulation in NK cells after treatment with anti-BCR antibodies. PBMCs from healthy donors (n = 3) were pretreated with MMP inhibitors GM6001 (10 μM) or BB-94 (10 μM) for 2 hours and anti-IgM or anti-IgD antibodies (10 μg/mL) were added to the culture for 48 hours. NKG2D expression in NK cells was evaluated by flow cytometry. Bars depict the MFI normalized to the negative control condition (NC) (mean ± SEM; ***p < 0.001, One-way ANOVA).

TGF-β is not involved in NKG2D downregulation on NK cells in the presence of BCR-activated B cells.

Given that NKG2D downregulation does not require direct cell-cell interactions, we next tried to unveil the main soluble factor underpinning the immunosuppression observed in NK cells upon B cell activation. Transforming growth factor beta (TGF-β) has been extensively described as a suppressor of NK cell activation that reduces surface expression of NKG2D, without affecting NKp46 expression (Crane et al., 2010; Lee, Lee, Kim, & Heo, 2004; Otegbeye et al., 2018; Wilson et al., 2011). Nonetheless, pretreatment of PBMCs from healthy donors with LY2109761, a TGF-β receptor type I and II inhibitor (Melisi et al., 2008), did not subvert NKG2D downmodulation in the presence of anti-BCR antibodies (Figure 2.8). LY2109761 treatment restored NKG2D expression when combined with TGF-β, providing evidence of the specificity of the assay and demonstrating that TGF-β does not mediate the decrease of NKG2D in NK cells upon anti-BCR crosslinking.

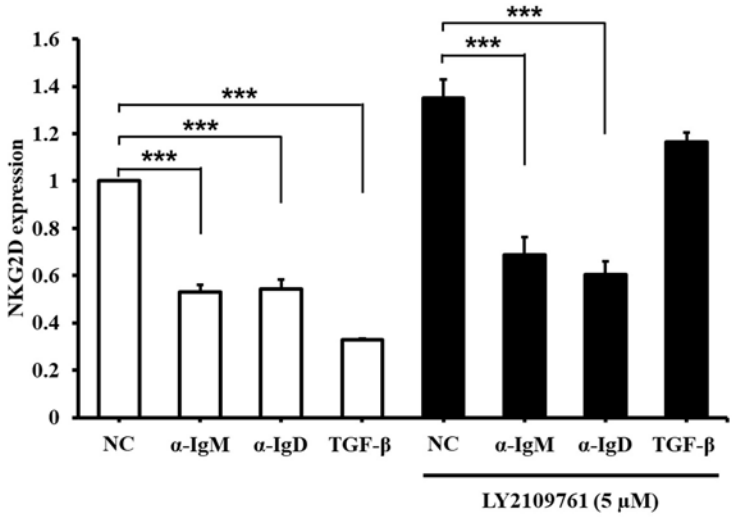

Figure 2.8. MMP inhibition does not revert NKG2D downregulation in NK cells after treatment with anti-BCR antibodies. PBMCs from healthy donors (n = 3) were pretreated with TGF-β receptor inhibitor LY2109761 (5 μM) for 2 hours and anti-IgM or anti-IgD antibodies (10 μg/mL) or TGF-β (10 ng/mL) were added to the culture for 48 hours. NKG2D expression in NK cells was assessed by flow cytometry. The graph shows the MFI normalized to the negative control condition (NC) (mean ± SEM; $p < 0.001$, One-way ANOVA).

Discussion

The BCR stands as a central regulator of B cell maintenance, differentiation and development, defining the cell fate during maturation (Avalos, Meyer-Wentrup, & Ploegh, 2014). Signaling through the BCR has been described as a pivotal driver of tumorigenesis in B-cell malignancies and constitutive BCR activation is a common feature of this type of cancer (Niemann & Wiestner, 2013; Rickert, 2013). Additionally, malignant B-cell transformation frequently compromises the normal function of the immune system and, thus, patients with leukemia or lymphoma typically experience acute immunosuppression. Herein, we provide evidence supporting a link between BCR-mediated B cell activation and attenuation of NK cell-mediated antitumor immune responses.

B cell stimulation via BCR crosslinking with specific antibodies decreased the surface expression levels of the activating receptor NKG2D on NK cells and $CD8^+$ T cells from healthy donors and patients with CLL. Given the relevance of NKG2D in cancer immunosurveillance (Lopez-Soto et al., 2015), these results suggest that the ability of effector immune cells, mainly NK cells, to recognize tumor cells might be impaired in the presence of activated B cells. DNAM-1 expression remained unaffected. Interestingly, a slight increase in NKp46 expression was observed on NK cells upon B cell activation. The differential regulation of NKG2D and NKp46 could correspond to a compensatory mechanism, a process recently reported in T cells regarding immune checkpoint receptor regulation (Huang, Francois, McGray, Miliotto, & Odunsi, 2017; Shayan & Ferris, 2015). Treatment with IL-2 or IL-15 did not counteract NKG2D downregulation on NK cells and $CD8^+$ T cells in healthy donors. These data indicate that the molecular events induced by these cytokines are not likely affected by stimulated B cells and, thus, involved in the dysregulation of NKG2D expression observed in the conditions studied. Co-stimulation of B cells via CD40 further decreased surface NKG2D expression on NK cells from healthy donors, reinforcing the hypothesis that activated B cells indirectly regulate the immune phenotype of NK cells. Concomitant with NKG2D downregulation, NK cell cytotoxicity against tumor cells was hindered in the presence of BCR-stimulated B cells. Furthermore, rituximab-induced NK cell-mediated tumor lysis/ADCC was also attenuated, which correlated with decreased CD16 expression on NK cells. Altogether, these data bring to light that activation of BCR signaling in B cells interferes with the antitumor functions of NK cells, which may constitute an immune evasion strategy in B-cell malignancies.

Conditioned-media and transwell assays demonstrated that activated B cells do not require direct cell to cell contact to negatively affect NKG2D expression on NK cells, hence indicating that this effect might be mediated by a soluble factor released upon BCR crosslinking. MMP inhibition failed to restore NKG2D surface levels on NK cells, dismissing the hypothesis that BCR stimulation favors NKG2DL shedding, a popular strategy employed by tumor cells to induce NKG2D internalization,

which results in decreased receptor presence on the cell surface (Groh et al., 2002; Lundholm et al., 2014; Song et al., 2006). TGF-β is a negative regulator of NKG2D with broad immunosuppressive properties (Crane et al., 2010; Lee et al., 2004; Otegbeye et al., 2018; Wilson et al., 2011). Nonetheless, NKG2D downregulation was not counteracted by TGF-β receptor inhibition. Taking these results into account, we hypothesized that BCR crosslinking may promote the release of as-yet-unknown soluble factors, presumably cytokines, that modulate NKG2D expression and, as a consequence, tumor recognition and elimination by NK cells. Accordingly, disruption of the molecular processes initiated by these soluble factors may represent a novel strategy to boost NK cell-mediated antitumor responses in B-cell malignancies.

3. Drug-induced hyperploidy stimulates antitumor NK cell responses

Generation of hyperploid cells

K-562, HCT-116 and Hep-G2 cells were exposed to three different polyploidy-inducing chemotherapeutic agents (Figure 3.1) and the impact of these compounds on the cell cycle and viability was analyzed by flow cytometry.

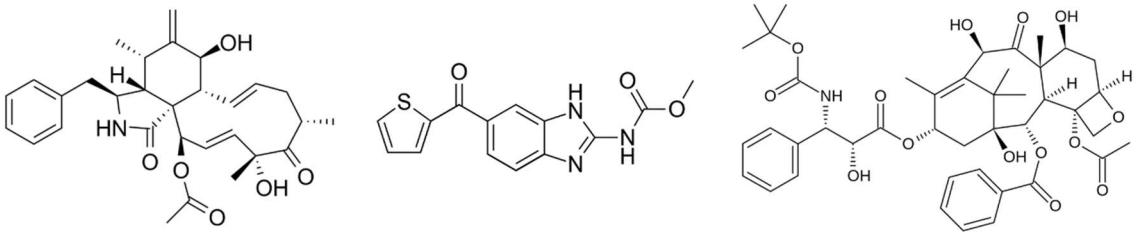

Figure 3.1. Hyperploidy-inducing agents employed in the present work. Cytochalasin D binds to actin filaments, inhibiting microfilament polymerization. Nocodazole and docetaxel interfere with microtubule polymerization. The three compounds are therefore antimitotic agents.

Treatment with cytochalasin D, nocodazole and docetaxel resulted in the accumulation of hyperploid cells with >4n DNA content in all the studied cell lines (Figure 3.2A). Of note, HCT-116 cells exhibited a higher grade of hyperploidy compared to K-562 and Hep-G2 cell lines, as evidenced by the appearance of a 16n karyotype subgroup after drug exposure. Additionally, cytochalasin D induced apoptosis in all the cell lines, whereas nocodazole and docetaxel significantly affected HCT-116 and Hep-G2 cells, but not K-562 (Figure 3.2B). In consonance with a work by Senovilla et al. (2012), an increase in the levels of surface CRT was detected in the tumor cells upon acquisition of hyperploid karyotype (Figure 3.2C).

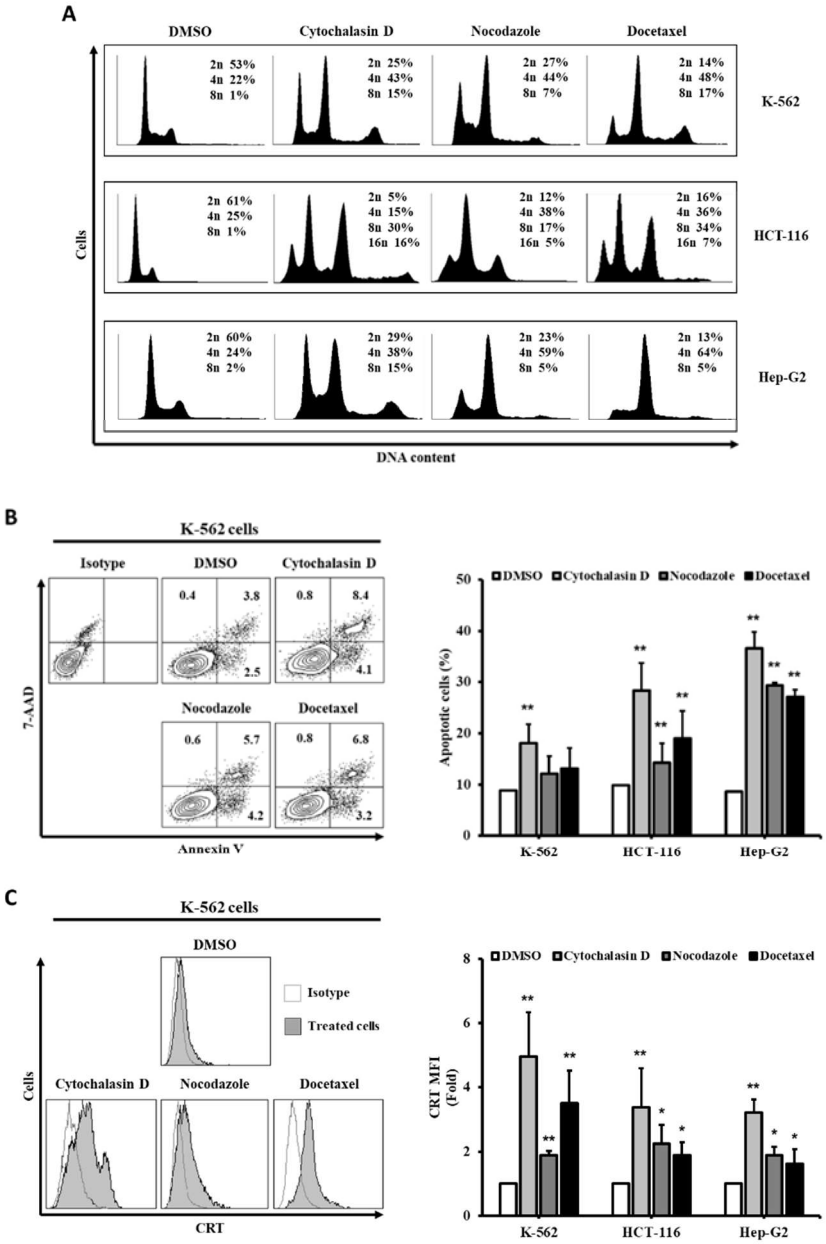

Figure 3.2. Treatment with antimitotic drugs affect DNA ploidy, apoptosis and CRT expression in tumor cells. K-562, HCT-116 and Hep-G2 cells were treated with 0.6 µg/ml cytochalasin D, 100 nM nocodazole or 3 nM docetaxel for 48 hours. **A.** Cells were analyzed for DNA content by flow cytometry. Histograms depict a representative experiment and percentages corresponding to the different DNA contents are indicated for each panel. **B.** Apoptosis was determined by cytofluorometric assessment of Annexin V/7-AAD staining. Dot plots correspond to a representative experiment for K-562 cells. Bars represent the percentage of apoptotic cells [Annexin V^+ 7-AAD^-] for each cell line. **C.** Surface CRT expression was determined by flow cytometry. Histograms show a representative experiment performed with K-562 cells. Bars represent the normalized MFI (fold induction) of surface CRT. At least three independent experiments were performed (mean ± standard error of the mean (SEM); *$p < 0.05$; **$p < 0.01$, Mann-Whitney U test).

Induction of hyperploidy enhances the expression of NKG2D, DNAM-1 and NKp30 ligands in cancer cells

Since acquisition of drug-induced hyperploidy activates adaptive immune responses via ICD (Senovilla et al., 2012), we next evaluated whether this phenotype also affected the crosstalk between NK cells and tumor cells. For that purpose, we first assessed the effect of drug-induced hyperploidy on the tumor expression of an array of human ligands for the NK cell activating receptors NKG2D, DNAM-1 and NKp30. Despite some cell line and drug-specific differences, treatment of K-562, HCT-116 and Hep-G2 with antimitotic agents induced a general upregulation of the surface expression of NKG2D ligands (Figure 3.3A). MICA was mainly upregulated in K-562 and HCT-116 cells (Figure 3.3B), whereas Hep-G2 cells exhibited a stronger upregulation of ULBP1 and ULBP3 ligands (Figure 3.3C,E). Likewise, a significant increase in DNAM-1 ligands PVR and Nectin-2 levels was observed in HCT-116 cells, especially in response to cytochalasin D treatment (Figure 3.4A-B). PVR expression was also enhanced in K-562 cells, while no changes were registered in Hep-G2 cells. B7-H6, an NKp30 ligand, was induced in cytochalasin D-treated HCT-116 and Hep-G2 cells as well (Figure 3.4C). No major effect was observed on the expression of HLA-I molecules, which act as inhibitory ligands, except for cytochalasin D-treated K-562 cells, in which an upregulation of HLA-I expression was detected (Figure 3.4D).

To further evaluate the connection between hyperploidization and induction of NK cell activating ligands, the expression of MICA and ULBP2 in diploid and hyperploid (2n and >4n) subgroups was determined in control and cytochalasin D-treated HCT-116 and K-562 cells. As shown in Figure 3.5, the hyperploid population of tumor cells showed enhanced expression of MICA and ULBP2 compared to their treated diploid counterpart. Of note, exposure of HCT-116 and K-562 to cytochalasin D increased the basal expression of these ligands in the diploid population compared to the control (DMSO) as well, suggesting that antimitotic agents induce NKG2D ligand expression *per se* and acquisition of hyperploidy further potentiates this effect.

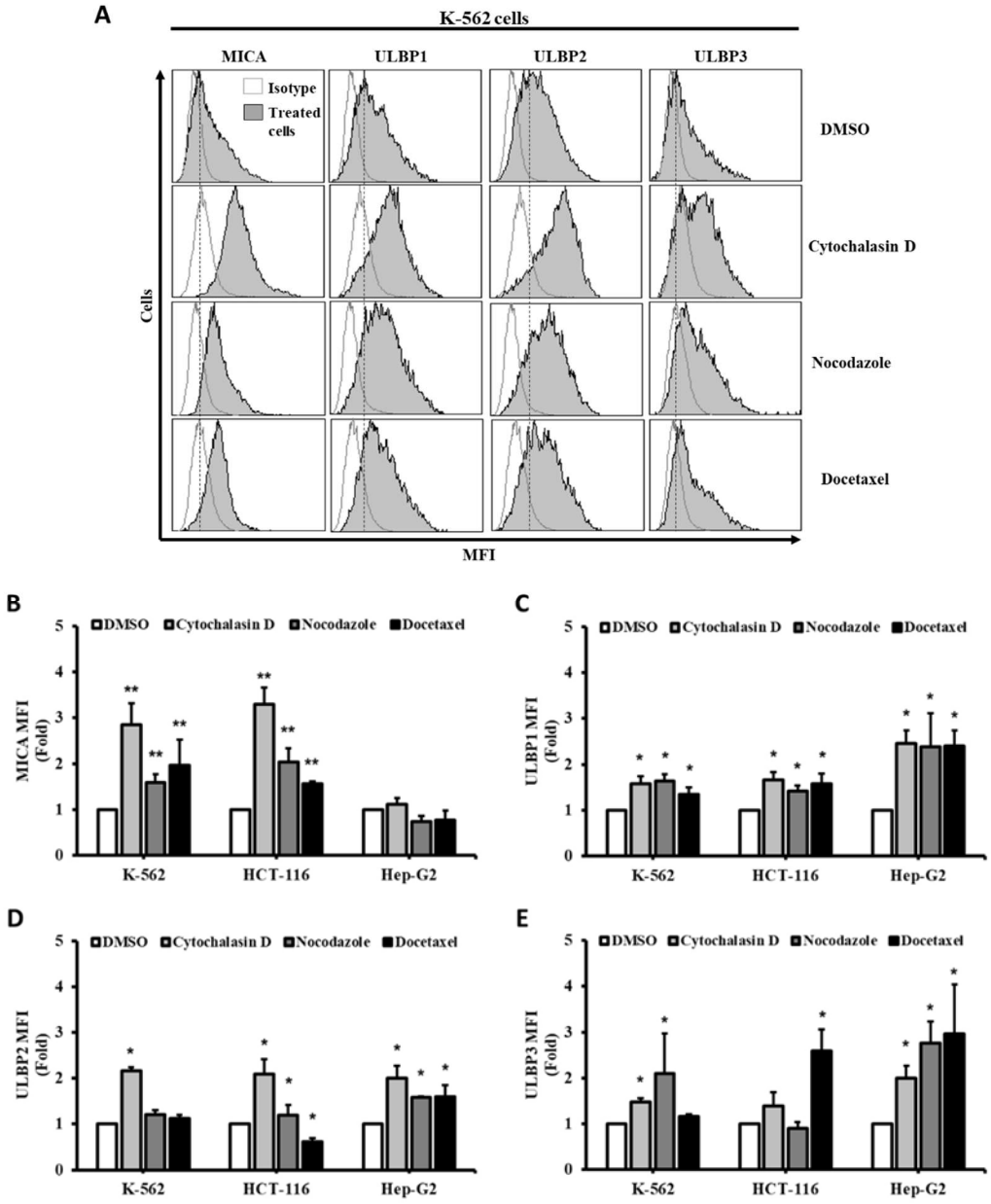

Figure 3.3. Treatment with antimitotic drugs induces NKG2D ligand expression in tumor cells. K-562, HCT-116 and Hep-G2 cells were treated with 0.6 μg/ml cytochalasin D, 100 nM nocodazole or 3 nM docetaxel for 48 hours and surface expression of NKG2D ligands was evaluated by flow cytometry. **A.** Histograms correspond to a representative experiment employing K-562 cells. Graphs show the normalized MFI (fold induction) of MICA (**B**), ULBP1 (**C**), ULBP2 (**D**) and ULBP3 (**E**). At least three independent experiments were performed (mean ± SEM; *$p < 0.05$; **$p < 0.01$, Mann-Whitney U test).

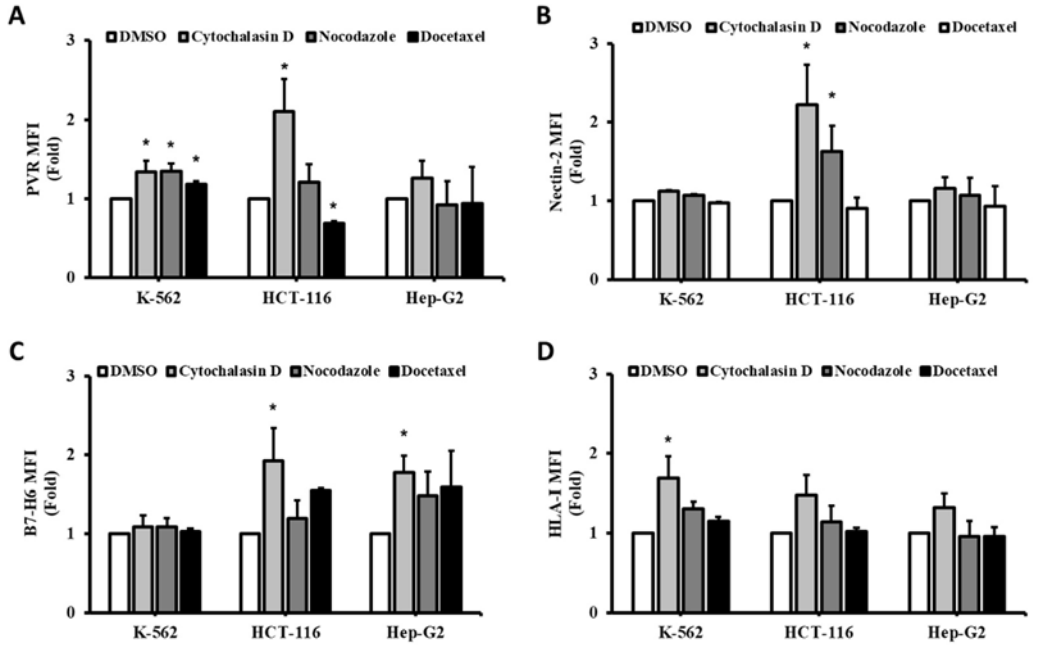

Figure 3.4. Treatment with antimitotic drugs induces DNAM-1 ligand expression in tumor cells. K-562, HCT-116 and Hep-G2 cells were treated with 0.6 μg/ml cytochalasin D, 100 nM nocodazole or 3 nM docetaxel for 48 hours and surface expression of DNAM-1 and NKp30 ligands, as well as HLA-I, was evaluated by flow cytometry. Graphs show the normalized MFI (fold induction) of PVR (**A**), Nectin-2 (**B**), B7-H6 (**C**) and HLA-I (**D**). At least three independent experiments were performed (mean ± SEM; *p < 0.05, Mann-Whitney U test).

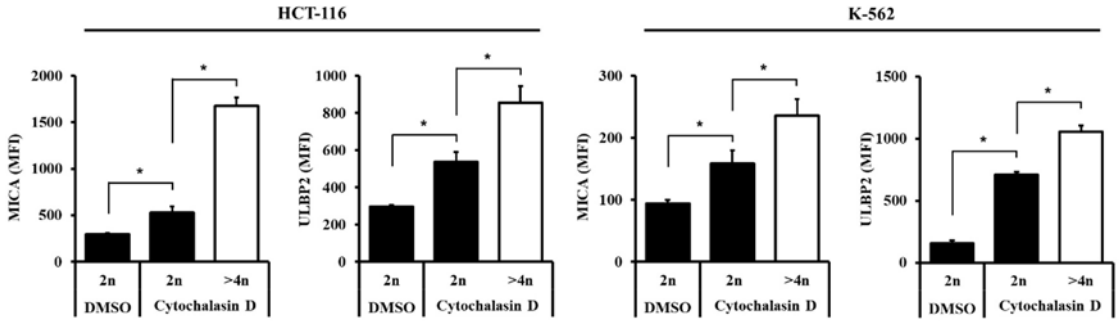

Figure 3.5. Hyperploid cells show enhanced expression of NKG2D ligands. K-562 and HCT-116 cells were treated with 0.6 μg/ml cytochalasin D, 100 nM nocodazole or 3 nM docetaxel for 48 hours. Expression of MICA and ULBP2 was evaluated in different karyotypes by flow cytometry. Graphs represent the MFI. At least three independent experiments were performed (mean ± SEM; *p < 0.05, Mann-Whitney U test).

Hyperploid tumor cells modulate the immune phenotype and induce the cytotoxic activity of NK cells

Given the changes in the immunogenic profile observed in drug-induced hyperploid tumor cells, we next studied whether NK cell activity was modulated by the exposure to hyperploid cancer cells. The expression of IFN-γ was increased in NK cells, $CD8^+$ T cells and NKT cells upon coculture with tumor cells treated with cytochalasin D, detecting no changes when these immune cells were

cocultured with nocodazole- and docetaxel-treated tumor cells (Figure 3.6A). Accordingly, cytochalasin D-exposed tumor cells were more susceptible to NK cell-mediated killing, as demonstrated by *in vitro* cytotoxicity assays (Figure 3.6B). This effect was more robust in Hep-G2 and K-562 cells, in which a significant increase of NK cell-mediated lysis was observed independently of the E:T ratio employed. Treatment with nocodazole and docetaxel sensitized Hep-G2 cells to NK cell-mediated lysis as well (Supplementary Figure 3.1), while no significant differences on K-562 and HCT-116 cells were detected (data not shown).

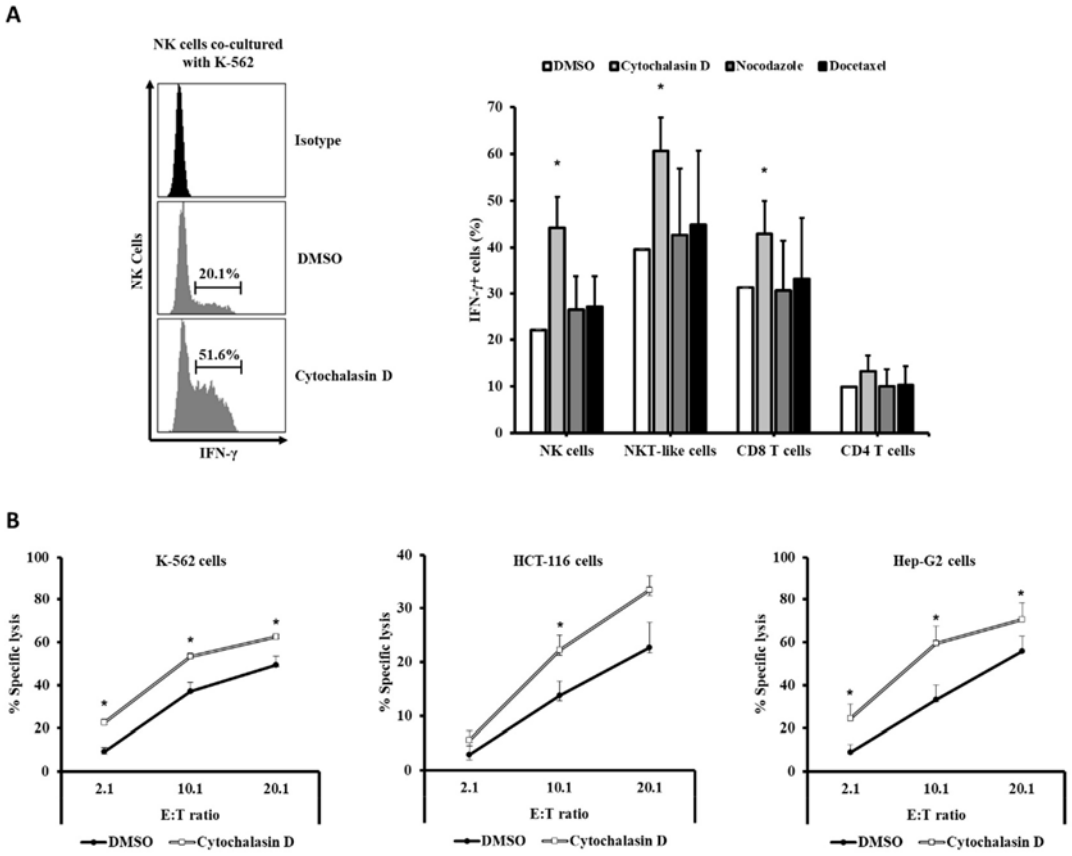

Figure 3.6. Hyperploid tumor cells are more susceptible to NK cell-mediated lysis. K-562, HCT-116 and Hep-G2 cells were treated with 0.6 µg/ml cytochalasin D, 100 nM nocodazole or 3 nM docetaxel for 48 hours. **A.** PBMCs from healthy donors (n = 4) were cocultured with hyperploid and control (DMSO) cells and IFN-γ production was evaluated by intracellular flow cytometry. Histograms show a representative staining for NK cells. Graph corresponds to the percentage of IFN-γ positive cells. **B.** Cytochalasin D-treated cells were cocultured with NKL cell line at three different E:T ratios and cytotoxicity was evaluated by flow cytometry. Graphs represent the percentage of specific lysis. (Mean ± SEM; *p < 0.05, Mann-Whitney U test).

The enhanced NK cell-mediated cytotoxicity detected upon coculture with treated Hep-G2 was abrogated in the presence of NKG2D and DNAM-1 blocking antibodies, but not when NKp30 was blocked (Figure 3.7), suggesting that NK cells rely on NKG2D and DNAM-1, rather than NKp30, signaling for the recognition of hyperploid cancer cells.

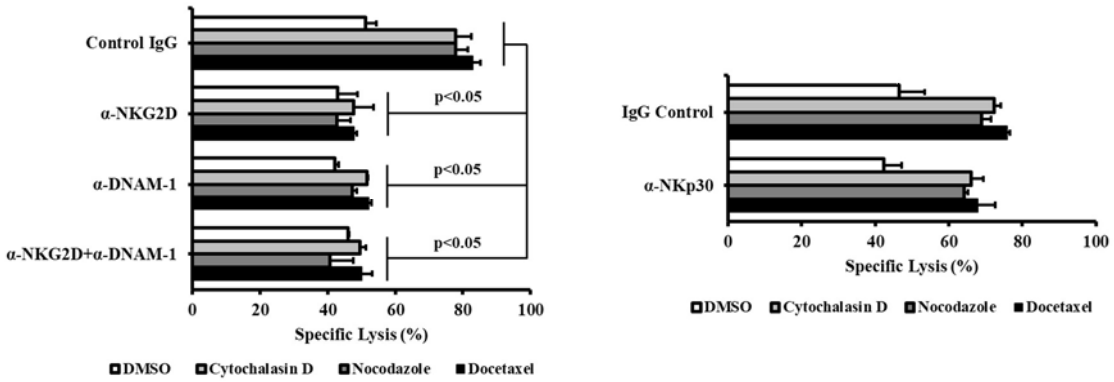

Figure 3.7. NKG2D and DNAM-1 blocking antibodies inhibit the increased NK cell-mediated lysis of hyperploid tumor cells. Hep-G2 cells treated with 0.6 μg/ml cytochalasin D, 100 nM nocodazole or 3 nM docetaxel for 48 hours were coculture with NKL cells preincubated with NKG2D, DNAM-1 or NKp30 blocking antibodies (15 μg/mL). Cytotoxicity was determined by flow cytometry. Graphs represent the percentage of specific lysis. At least three independent experiments were performed. (Mean ± SEM; Mann-Whitney U test).

We also assessed whether the immune phenotype of NK cells was modified by the coculture with treated tumor cells. Exposure to hyperploid cells induced the expression of NKG2D, DNAM-1 and NKp30 in NK cells, especially in the presence of K-562 cells independently of the treatment (Figure 3.8A-D). Cytochalasin D-treated HCT-116 and Hep-G2 exerted a modest modulation of these receptors. No changes were detected in NKp44 and NKp46 (Figure 3.8E-F). CD69, an early activation marker, was also evaluated in these conditions, observing an increase in the levels of the protein in NK cells cocultured with treated-HCT-116 cells (Figure 3.8G). Altogether, these data bring to light that drug-induced hyperploid cells promote NK cell activation, which, in turn, leads to a more efficient elimination of tumor cells.

Drug-induced hyperploidy stimulates NK cell proliferation through the activation of $CD4^+$ T cells

Activation of immune subsets commonly translates into cell proliferation. Hence, we next asked whether drug-induced hyperploid cells have an impact on the proliferation of lymphocyte subsets. Coculture with cytochalasin D- and nocodazole-treated K-562 cells significantly increased the proliferation of NK cells and NKT cells, whereas no effect was observed on $CD4^+$ or $CD8^+$ T cells (Figure 3.9A-B). NK cells exposed to docetaxel-treated tumor cells showed reduced proliferation. Contrastingly, isolated NK cells failed to proliferate in the presence of tumor cells incubated with cytochalasin D and nocodazole, implying that the effect on NK cell proliferation is indirect and depends on a different lymphocytic population (Figure 3.9A,C).

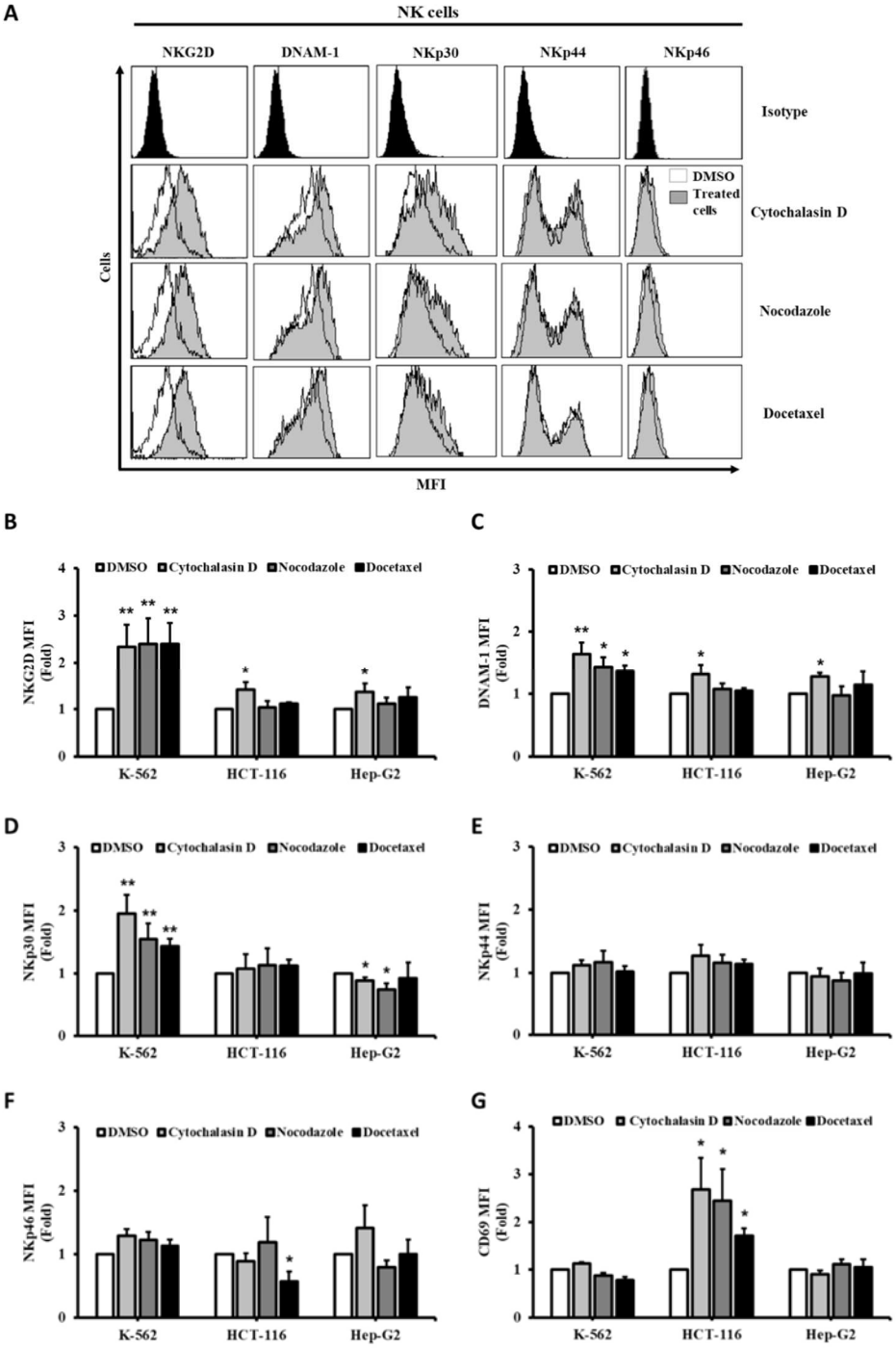

Figure 3.8. Coculture with hyperploid tumor cells modulates the expression of immunoreceptors in NK cells. K-562, HCT-116 and Hep-G2 cells treated with 0.6 µg/ml cytochalasin D, 100 nM nocodazole or 3 nM docetaxel for 48 hours were coculture with isolated NK cells from healthy donors for 48 hours (n = 4). Expression of NKG2D, DNAM-1, NKp30, NKp44, NKp46 and CD69 was analyzed by flow cytometry. **A.** Histograms show the MFI of representative experiment. **B-G.** Graphs represent the normalized MFI. (Mean ± SEM; *p < 0.05; **p < 0.01, Mann-Whitney U test).

Given that IL-2, a cytokine mainly produced by T cells, is crucially involved in the proliferation of NK cells (Caligiuri et al., 1993; Henney, Kuribayashi, Kern, & Gillis, 1981; Trinchieri et al.,

1984), we hypothesized that the effect of hyperploid malignant cells might rely on the production of IL-2 by immune cells. Indeed, coculture with K-562 cells treated with cytochalasin D stimulated the production of IL-2 by $CD4^+$ T cells and, in a lesser extent, by $CD8^+$ T cells and NKT cells (Figure 3.10A). No NK cell production of IL-2 was found (data not shown). Further, treatment with an anti-IL-2 receptor (IL-2Rα) blocking antibody or CsA, an immunosuppressant drug that inhibits IL-2 production by T cells, completely abrogated the NK cell proliferation induced by hyperploid K-562 cells (Figure 3.10B). Collectively, these data indicate that hyperploid cell-promoted proliferation of NK cells is mediated by the production of IL-2 by T cells, mainly $CD4^+$ T cells.

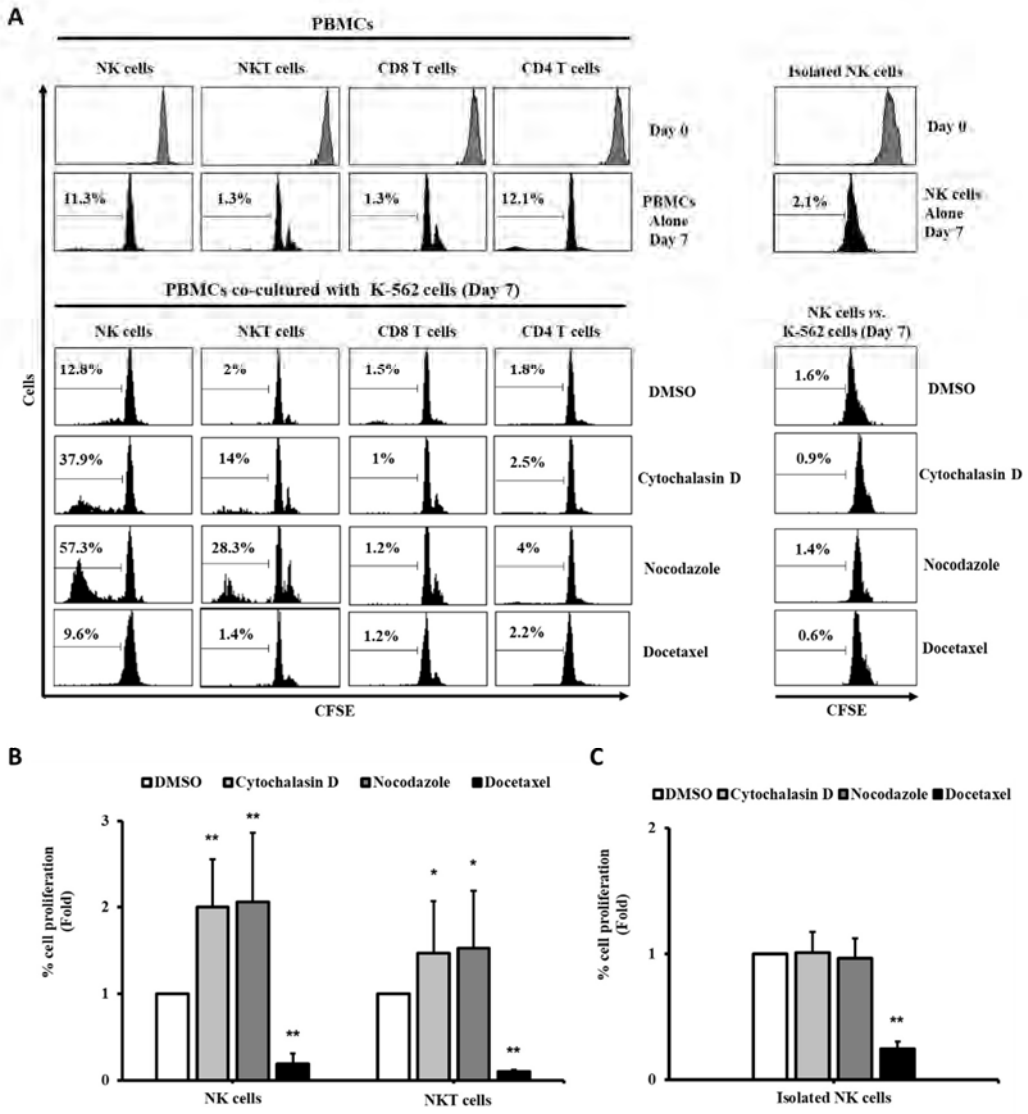

Figure 3.9. Exposure to hyperploid tumor cells induced proliferation of immune subsets. K-562 cells treated with 0.6 µg/ml cytochalasin D, 100 nM nocodazole or 3 nM docetaxel for 48 hours were coculture with CFSE-stained PBMCs (n = 6) or isolated NK cells (n = 4) for 7 days. Proliferation rates were determined by flow cytometry. **A.** Histograms show a representative experiment and percentages corresponding to cell proliferation are indicated for each panel. **B-C.** Graphs represent the normalized percentage of cell proliferation. (Mean ± SEM; *p < 0.05; **p < 0.01, Mann-Whitney U test).

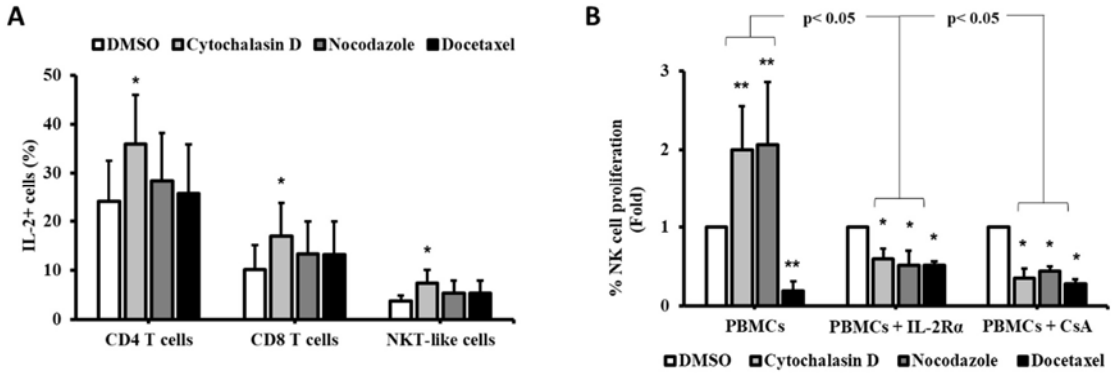

Figure 3.10. IL-2 production by T cells is required for NK cell proliferation upon coculture with hyperploid cells. A. PBMCs from healthy donors (n = 4) were exposed to K-562 cells treated with 0.6 µg/ml cytochalasin D, 100 nM nocodazole or 3 nM docetaxel and IL-2 production was evaluated in immune subsets by intracellular flow cytometry. The graph shows the percentage of IL-2 positive cells. **B.** CFSE-stained PBMCs (n = 4) were incubated with control (DMSO) and treated K-562 cells in the presence or absence of anti-IL-2Rα blocking antibody (15 µg/mL) or CsA (1 µM) and NK cell proliferation was assessed. The graph depicts the normalized percentage of proliferating NK cells (Mean ± SEM; *p < 0.05; **p < 0.01, Mann-Whitney U test).

Stress signaling pathways are involved in the upregulation of MICA in hyperploid tumor cells

We next tried to unveil the molecular mechanisms underpinning the upregulation of MICA in hyperploid tumor cells. It has been reported that hyperploid cells exhibit constitutively elevated levels of ER stress (Kepp et al., 2013; Senovilla et al., 2012). Indeed, an increased amount of phosphorylated eIF2α was observed in HCT-116 cells treated with cytochalasin D compared with control cells. No significant changes were detected in K-562 cells, suggesting that ER stress is not involved in the immunophenotype observed in this cell line as a consequence of the treatment (Figure 3.11).

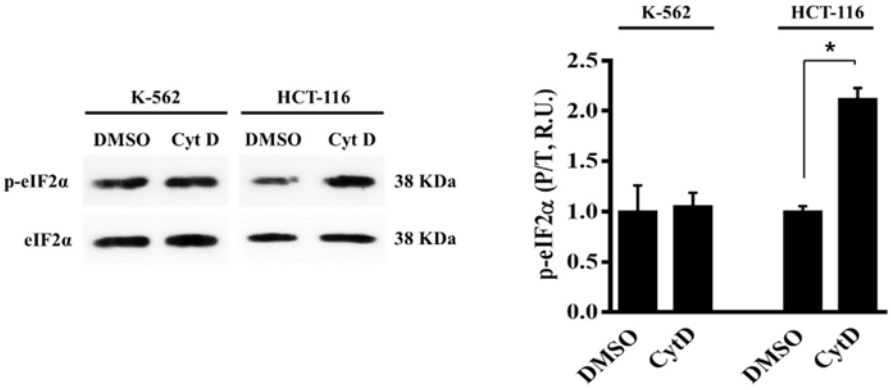

Figure 3.11. Hyperploidy stimulates ER stress in tumor cells. K-562 and HCT-116 cells were incubated with 0.6 µg/ml cytochalasin D (CytD) for 48 hours and protein extracts were obtained (n = 3). Levels of total and phosphorylated eIF2α were determined by western blotting. Bars represent the quantification of p- eIF2α in relative units (R.U.) (mean ± SEM; *p < 0.05, Mann-Whitney U test).

To further evaluate the role of ER stress signaling in the stimulation of MICA in hyperploid cells, HCT-116 cells were treated GSK2606414, a potent and specific PERK inhibitor (Axten et al., 2012), and the expression of MICA evaluated by flow cytometry. As depicted in Figure 3.12A, treatment with GSK2606414 reduced the phosphorylation of eIF2α induced by cytochalasin D, which correlated with an attenuation of the enhanced MICA expression in cytochalasin D-treated HCT-116 (Figure 3.12B). It is worth mentioning that the expression levels of HLA-I did not change after treatment with GSK2606414, supporting the specificity of the effect registered in MICA as a consequence of PERK inhibition (data not shown). In addition, exposure to salubrinal, an inhibitor of eIF2α dephosphorylation and protector of ER stress (Boyce et al., 2005), also mitigated the surface levels of MICA in hyperploid tumor cells (Supplementary Figure 3.2).

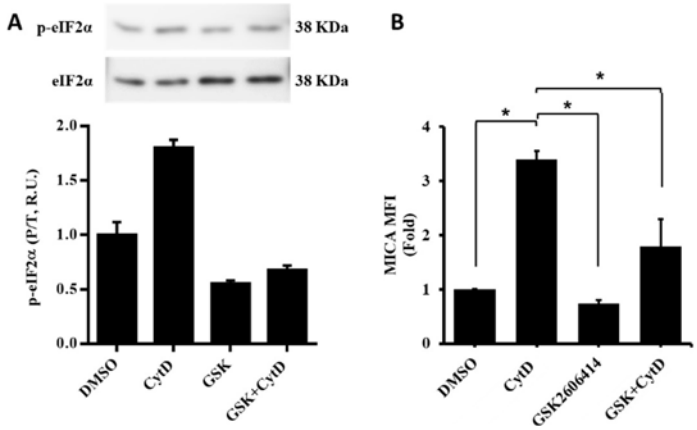

Figure 3.12. ER stress is implicated in the upregulation of MICA in hyperploid tumor cells. HCT-116 cells were exposed to 0.6 μg/ml cytochalasin D (CytD) and or 1 μM GSK2606414 (GSK) for 48 hours. **A.** Levels of total and phosphorylated eIF2α were determined by western blotting (n = 2). Bars represent the quantification of p- eIF2α in relative units (R.U.). **B.** Expression of MICA was evaluated by flow cytometry (n = 3). Graph shows the normalized MFI. (Mean ± SEM; *p < 0.05, Mann-Whitney U test).

Hyperploid cells are characterized by a marked genomic instability, which, in turn, activates the DNA damage response (DDR) (Chow & Poon, 2010), a relevant mechanism reported to upregulate MICA expression by activating PI3K and ATM pathways (Cerboni et al., 2014; Gasser, Orsulic, Brown, & Raulet, 2005). At this respect, treatment of K-562 cells with LY-294002, a PI3K blocker, did not markedly change the induction of MICA (Supplementary Figure 3.3). Nonetheless, ATM inhibition, achieved by exposure to the ATM inhibitor KU55933, completely revoked the induction of MICA on the surface of K-562 hyperploid cancer cells, while there was a partial response observed in HCT-116 cells (Figure 3.13A). Depletion of ATM expression by transfection of K-562 and HCT-116 cells with a plasmid expressing a specific shRNA similarly counteracted the upregulation of MICA upon cytochalasin D treatment (Figure 3.13B). In the same line, pharmacological inhibition of ATM completely reverted the specific NK cell-mediated killing of K-562 cells (Figure 3.13C),

revealing a key role for ATM in the induction of the immunogenicity observed in hyperploid tumor cells. Altogether, these data bring forward the DDR and ER stress, on a certain degree depending on the model studied, as essential players in the stimulation of MICA expression and, subsequently, in the enhanced susceptibility to NK-cell mediated killing of hyperploid cancer cells.

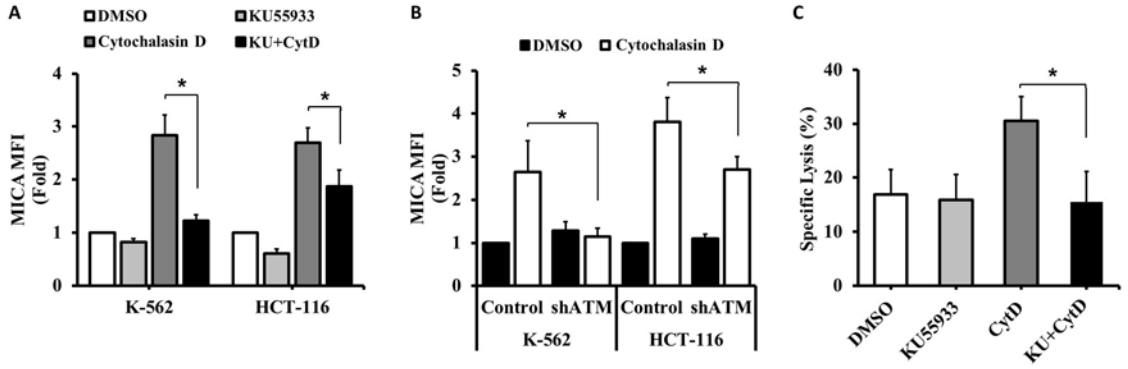

Figure 3.13. ATM partially mediates the upregulation of MICA in hyperploid tumor cells. A. HCT-116 and K-562 cells were pretreated with the ATM inhibitor KU55933 (10 µM) and/or exposed to cytochalasin D (0.6 µg/ml; CytD) for 48 hours (n = 3). Levels of surface MICA were measured by flow cytometry. Bars depict the normalized MFI. **B.** Hyperploidy was induced HCT-116 and K-562 cells transfected with a plasmid containing a shRNA for *ATM* silencing or a control plasmid by cytochalasin D and MICA expression was assessed (n = 3). Bars show the normalized MFI. **C.** K-562 cells were treated with KU55933 and/or cytochalasin D and cocultures with NKL cells (n = 4). Bars depict the percentage of specific lysis for each condition. (Mean ± SEM; *p < 0.05, Mann-Whitney U test).

Discussion

Polyploidization is a characteristic event taking place in the early stages of tumorigenesis that has been observed in many types of cancers (Davoli & de Lange, 2011; Gordon et al., 2012). Apart from cell cycle control mechanisms that ensure genomic integrity, recent work has unraveled an extrinsic control of DNA ploidy exerted by the immune system, which eliminates hyperploid cells through the activation of antitumor T cell responses (Senovilla et al., 2012). Herein, we provide evidence supporting that induction of hyperploidy via antimitotic drugs activates antitumor immune responses mediated by NK cells.

No loss of HLA class I molecule expression was detected in tumor cells after acquisition of drug-induced hyperploidy, suggesting that NK cell inhibitory receptors, such as KIR, are not involved in the NK cell activation observed in the conditions studied. Contrastingly, drug-induced hyperploid malignant cells showed a significant upregulation of the expression of ligands for NK cell activating receptors, particularly for NKG2D and DNAM-1. Cell ploidy studies revealed a strong positive correlation between increased ligand expression (MICA and ULBP2) and DNA content, further supporting a link between cancer polyploidy and enhanced tumor immunogenicity. Exposure to NKG2D- and DNAM-1-blocking antibodies abrogated the incremented hyperploid tumor cell lysis observed *in vitro*, bringing to light the crucial role of these receptors in the NK cell-mediated cytotoxic response against hyperploid cancer cells. Concomitantly, NK cells co-cultured with hyperploid tumor cells suffered an upregulation of NKG2D and DNAM-1. Therefore, additionally to oncogenes, tumor progression and stress and proliferative signals, which are stimuli known to regulate NKG2D ligand expression (Huergo-Zapico, Acebes-Huerta, Lopez-Soto, et al., 2014; Iannello, Thompson, Ardolino, Lowe, & Raulet, 2013; Jung, Hsiung, Pestal, Procyk, & Raulet, 2012; Lopez-Soto et al., 2013; Textor et al., 2011), induction of hyperploidy stands as a novel process involved in the activation of NKG2D-mediated antitumor responses.

Acquisition of hyperploidy is typically related to genomic instability, which, in turn, activates the DDR, a stress-regulated pathway that stimulates NKG2D ligand expression via ATM and ATR protein kinases (Cerboni et al., 2014; Gasser et al., 2005; Soriani et al., 2009). Pharmacological and genetic inhibition of ATM subverted the increase of MICA surface levels in hyperploid cancer cells, indicating that the DDR takes a central part in the upregulation of NKG2D ligand expression upon induction of tumor hyperploidy. Likewise, pharmacological inhibitors targeting ER stress signaling pathways partially attenuated hyperploidy-associated MICA induction in distinct tumor models, implying that ER stress may constitute a complementary mechanism mediating the immune recognition of drug-induced hyperploid cancer cells by NK cells. These data are in line with a recent

study reporting that ER stress elicits the surface exposure of CRT in hyperploid tumor cells, eventually stimulating T cell-mediated immune responses (Kepp et al., 2013; Senovilla et al., 2012).

Herein, we also unveil a cooperative effect between T lymphocytes and NK cells in the immunosurveillance against hyperploid cancer cells. An increase in IL-2 production was detected in T cells, mainly $CD4^+$ T cells, upon co-culture with hyperploid tumor cells, a feature that promoted NK cell proliferation, since absence of T cells abrogated this effect. In line with this, blockade of IL-2, a key cytokine in NK cell activation and proliferation (Henney et al., 1981), completely revoked NK cell proliferation, reinforcing the hypothesis that hyperploidization initiates a coordinated immune response against tumor cells that involves a crosstalk between T cells and NK cells. This is further supported by clinical observations demonstrating that taxanes, a group of hyperploidy-inducing agents that inhibit microtubule polymerization, lead to increased IL-2 levels in serum and enhanced NK cell activity in patients with advanced breast cancer (Tsavaris, Kosmas, Vadiaka, Kanelopoulos, & Boulamatsis, 2002). Further, several works have reported that hyperploid cancer cells activate T cell responses via CRT exposure and subsequent activation of antigen-presenting cells (APCs) (Chaput et al., 2007; Obeid et al., 2007; Senovilla et al., 2012). Hence, hyperploid tumor-derived antigens presented by APCs after phagocytosis likely trigger $CD4^+$ T cell activation. Nonetheless, no proliferation was observed in this immune subset, suggesting a more complex interaction between $CD4^+$ T cells and hyperploid tumor cells that requires further investigation.

It has been largely accepted that the immune system contributes to tumor eradication and the features that allow tumor cell recognition by immune cells are subjected to intense study. Aberrant DNA content is a characteristic that favors cancer immunosurveillance via antigen-specific T cell responses. The work herein complements this observation demonstrating that NK cells may also take part in this response by detecting stress-induced molecules (i.e. NKG2D and DNAM-1 ligands) expressed on the surface of hyperploid cancer cells. Moreover, these data provide rationale for the development of immunotherapeutic strategies modulating tumor cell ploidy as an alternative to conventional treatments currently used for patients with cancer.

GENERAL DISCUSSION

Cancer comprises a highly heterogeneous group of diseases at a molecular and clinical level, being the leading cause of death in a great number of countries. Despite its importance, management of patients with cancer still represents a challenge, mainly due to the variability in tumor biology and interpatient differences in response to treatment, which hinder the development of broad-spectrum therapies. Nonetheless, targeted and immunotherapeutic approaches show superior clinical efficacy to that of conventional cancer regimens, thus being a major focus of interest for basic and clinical cancer research. Several small molecule inhibitors, like ibrutinib and idelalisib, have largely proven their therapeutic value in cancers such as CLL (Burger & O'Brien, 2018). On the other hand, cancer immunotherapy aims to activate antitumor immune responses through different approaches, such as immune checkpoint blockade or ADCC-inducing antibodies (Dougan, Dranoff, & Dougan, 2019; Ribas & Wolchok, 2018).

CLL is a hematologic disease characterized by clonal expansion of malignant B cells that, up to date, remains incurable. Nonetheless, patients suffering this malignancy have greatly benefited from the development of targeted therapies. Initial tests assessing the effectivity of kinase inhibitors selectively targeting BCR-related kinases achieved high response rates and, in some cases, durable remissions in patients with CLL (Burger & O'Brien, 2018; Burger & Wiestner, 2018). Combination regimens with conventional treatments further improved the objective response rates (Chanan-Khan et al., 2016; Seymour et al., 2018; Smith et al., 2017), completely revolutionizing the clinical management of patients with CLL. As an illustration, ibrutinib, an irreversible BTK inhibitor, is currently employed as a treatment for refractory or relapsed patients (O'Brien et al., 2018), whereas venetoclax, a novel BCL2 antagonist, was recently approved for CLL owing to the encouraging results reported by several clinical trials (Coutre et al., 2018; Roberts et al., 2016; Seymour et al., 2018). Herein, we found that EC-7072, an analog of mithramycin A, displays a promising antileukemic activity against primary CLL cells *ex vivo*. The cytotoxicity exerted by the compound was comparable to that of an array of targeted drugs (that include ibrutinib, idelalisib and venetoclax) and the nucleoside analogue fludarabine, conventionally employed in chemotherapy regimens. In addition, EC-7072 improved the killing rates of these drugs against CLL cells upon combined treatment *in vitro*, exhibiting synergy with idelalisib and fludarabine, while an additive effect was observed in the case of combinations with ibrutinib and venetoclax. The viability of circulating healthy immune subsets, NK cells and T lymphocytes, was mostly unaffected by EC-7072 at the concentrations tested. Therefore, the compound does not likely aggravate the immune suppression typically associated to patients with CLL, in contrast to currently-applied treatments, such as fludarabine ("Highlights in chronic lymphocytic leukemia from the 2018 American Society of Clinical Oncology annual meeting," 2018; Keating et al., 1998). Transcriptomic studies unraveled that CLL cells exposed to EC-7072 suffered a dramatic modulation of upstream components of the

BCR pathway (e.g. SYK, PI3K, PLCG2) as well as downstream effectors activated by the BCR cascade (e.g. NF-κB, JAK/STAT). Protein-coding genes controlling apoptosis, such as *BCL2*, were also dysregulated in the presence of EC-7072, supporting previous experiments demonstrating that the compound triggers caspase-dependent apoptosis in CLL cells. Phosphoflow analyses revealed that EC-7072 reduces the phosphorylation levels of BCR-related kinases, reinforcing the hypothesis that selective inhibition of the BCR signaling pathway might be the mechanism underpinning the antileukemic activity of EC-7072 in CLL. Still, the molecular events mediating the cytotoxic properties of EC-7072 against CLL cells deserve future investigation. Intrinsic and acquired resistance to treatment remains as a major handicap in CLL. Mutation of genes encoding BCR signaling components commonly hinders the efficacy of targeted approaches, such is the case of co-occurring mutations in *BTK* and *PLCG2* that are linked to ibrutinib resistance (Woyach et al., 2014). At this respect, the dysregulation of the transcriptome exerted by EC-7072 on CLL cells might represent a therapeutic advantage in patients with CLL carrying mutational events affecting elements of the BCR cascade. Altogether, EC-7072 may be an alternative treatment for patients with CLL alone or in combination regimen owing to its therapeutic potential *in vitro*, thus supporting the high interest of further studying the activity of the mithralog in a clinical setting.

The relevance of the BCR signaling pathway in CLL and other B-cell malignancies has been widely described, prompting the appearance of drugs specifically targeting components of the cascade that have proven their value as novel therapeutic approaches (Burger & Wiestner, 2018). As already mentioned in this work, the BCR pathway is also crucial for the correct function and homeostasis of healthy B cells. Antigen recognition through the BCR complex activates a series of signaling events that propagate via phosphorylation of proximal kinases, eventually leading to the activation of downstream effector pathways that support B cell survival and proliferation. In addition, BCR engagement can induce the production of molecules with immunosuppressive properties. For example, B cells have been reported to secrete IL-10 in response to BCR stimulation in certain autoimmune diseases (Fillatreau, Sweenie, McGeachy, Gray, & Anderton, 2002; Kalampokis, Yoshizaki, & Tedder, 2013), an ability shared by CLL cells (Alhakeem et al., 2018). In this work, we describe a link between BCR activation in B cells and suppression of NK cell-mediate antitumor immune responses, which might partially explain the immune dysfunction observed in patients with B-cell malignancies.

BCR stimulation in B cells significantly reduced the expression levels of NKG2D on NK cells and $CD8^+$ T cells from healthy donors, suggesting that tumor recognition by NK cells and, in a lesser extent, by $CD8^+$ T cells is impaired in the presence of activated B cells. A recent study in samples from patients with CLL reported that NKG2D expression is downregulated in circulating NK cells

and $CD8^+$ T cells from these patients compared to healthy donors (Huergo-Zapico, Acebes-Huerta, Gonzalez-Rodriguez, et al., 2014), which may be related to the constitutive BCR activation typically associated to CLL cells. In line with this, we found that BCR stimulation in CLL cells further reduced NKG2D expression on these effector immune subsets. The antitumor activity of NK cells was hampered upon BCR stimulation, since a decrease in both NK cell-mediated lysis and ADCC of tumor cells was observed. These results suggest that activated B cells may cause NK cell dysfunction, a common feature present in patients with B-cell malignancies (Chiu, Ernst, & Keating, 2018; Huergo-Zapico, Acebes-Huerta, Gonzalez-Rodriguez, et al., 2014). NKG2D downregulation was detected in NK cells cultured in conditioned media from BCR-activated healthy and malignant B cells, indicating that stimulated B cells might release soluble factors which, in turn, are responsible for NK cell suppression. Transwell assays produced similar results, further reinforcing this hypothesis. Two main mechanisms of immune evasion leading to NKG2D downregulation have been described in cancer: 1) shedding of NKG2DLs by the tumor cell, which eventually causes internalization of the receptor (Groh et al., 2002; Lundholm et al., 2014; Song et al., 2006); and 2) secretion of TGF-β (Crane et al., 2010; Lee et al., 2004; Otegbeye et al., 2018), a suppressive cytokine involved in the control of the immune function that can be produced by B cells as well (Bjarnadottir et al., 2016; Klinker & Lundy, 2012). Nonetheless, pharmacological inhibition of MMPs and TGF-β receptors failed to restore NKG2D levels on NK cells, suggesting that NK cell function is negatively affected by a different factor produced upon BCR engagement. Thus, the mechanism underlying the immunosuppressive role of B cell stimulation in NK cell activity deserves deeper investigation. Impairment of the molecular events triggered by yet-unknown factors released by stimulated B cells may constitute a novel immunotherapeutic approach to boost NK cell-mediated antitumor responses in B-cell malignancies.

The immune system plays a crucial role in cancer clearance and NK cells stand out as a first line of defence. Engagement of NK cell activating receptors and subsequent NK cell stimulation leads to tumor cell death via cytotoxicity without prior antigen priming, hence the therapeutic potential of boosting NK cell responses for cancer treatment. It has been extensively described that conditions of cell stress, such as genotoxic stress, frequently upregulate the surface expression of NK cell activating ligands, favoring immune recognition and elimination (C. J. Chan, Smyth, & Martinet, 2014). A study from Senovilla *et al*. demonstrated that DNA ploidy is tightly controlled by the immune system and induction of hyperploidy triggers antitumor T cell responses (Senovilla et al., 2012). Here, we demonstrate that acquisition of hyperploidy via exposure to antimitotic drugs activates NK cell-mediated antitumor immune responses as well.

Treatment with antimitotic drugs significantly increased the expression of an array of NK cell activating ligands on tumor cell lines from different origin. Surface expression levels of MICA and ULBP2 positively correlated with DNA content, suggesting that tumor immunogenicity is partly controlled by cell ploidy. Concomitantly, cytotoxicity experiments brought to light that acquisition of hyperploidy is involved in the activation of cancer immunosurveillance by NK cells, a stimulation essentially mediated by NKG2D and DNAM-1 signaling. Of note, upregulation of NK cell ligands on tumor cells was primarily elicited by ATM and partially by ER stress signaling pathways, in agreement with previous studies describing the importance of these pathways in the immune function (Cerboni et al., 2014; Gasser et al., 2005; Kepp et al., 2013; Senovilla et al., 2012; Soriani et al., 2014). Additionally, exposure to hyperploid tumor cells promoted IL-2 production by T cells, which led to NK cell proliferation. Consequently, hyperploid cancer cells are subjected to a tight immune control that involves a crosstalk between NK cells and T lymphocytes. Altogether, these data bring to light the potential of employing drugs that modulate tumor cell ploidy in cancer immunotherapy. Indeed, previous studies have shown that antimitotic drugs, like taxanes, have immunostimulatory properties (O. T. Chan & Yang, 2000; Hodge et al., 2013). For instance, taxanes enhanced NK cell activity in patients with advanced breast cancer (Tsavaris et al., 2002), suggesting that the therapeutic efficacy of antimitotic drugs may not only come from direct tumor cell elimination via inhibition of cell division, but also from the activation of anticancer immune responses.

Overall, the results presented in this Thesis demonstrate the therapeutic potential of a set of treatments in cancer, analyzing the role of the immune system in their efficacy, and provide rationale for further clinical evaluation of the strategies studied. Patients with cancer generally show immune dysfunction, therefore the interest in restoring the killing capacity of NK cells or increasing tumor immunogenicity to promote cancer clearance. Nonetheless, the effectivity of activating immune responses is limited, mostly owing to evasion mechanisms developed by tumor cells. On the other hand, targeted treatments achieve promising response rates in patients, minimizing the side toxicity owing to their specificity, though acquired resistance lowers their efficacy. We propose that combination of immunotherapeutic strategies with approaches directly targeting the tumor may overcome their limitations and improve the management of patients with cancer.

CONCLUSIONS

1. The mithralog EC-7072 induces caspase-3-dependent apoptosis on leukemia cells from patients with CLL *in vitro*, without markedly affecting circulating NK cells and T lymphocytes.
2. EC-7072 modulates the activation status of BCR signaling pathway in CLL cells and reduces the phosphorylation levels of key mediators of this pathway.
3. Activation of the BCR partially counteracts the antileukemic activity of EC-7072, whereas microenvironment-derived factors fail to restore CLL cell viability.
4. Combination of EC-7072 with ibrutinib, idelalisib, venetoclax or fludarabine results in cooperative killing of leukemia cells from patients with CLL.
5. BCR crosslinking in healthy B cells and CLL cells results in NKG2D downregulation on NK cells and $CD8^+$ T cells from healthy donors and patients with CLL.
6. NK cell-mediated killing of tumor cells and ADCC activity are hampered in the presence of BCR-activated B cells.
7. No direct cell to cell contact is required to induce NKG2D downregulation on NK cells and $CD8^+$ T cells upon BCR crosslinking in B cells.
8. Hyperploidy-inducing drugs promote an upregulation of ligands for NK cell activating receptor on cancer cell lines, rendering them more susceptible to NK cell-mediated elimination.
9. Co-culture with hyperploid tumor cells induces the expression of NKG2D, DNAM-1 and NKp30 receptors, as well as IFN-γ production, in NK cells.
10. IL-2 production by T cells is increased in the presence of hyperploid tumor cells, which promotes NK cell proliferation.
11. MICA upregulation in hyperploid tumor cells is primarily mediated by ATM protein kinase and, in certain cancer cell lines, by endoplasmic reticulum stress signaling pathways.

CONCLUSIONES

1. El mitrálogo EC-7072 induce una apoptosis dependiente de caspasa 3 en células leucémicas de pacientes con leucemia linfática crónica (LLC) *in vitro*, sin afectar marcadamente a linfocitos T y células NK circulantes.
2. EC-7072 modula el estado de activación de la vía de señalización de BCR en células leucémicas de pacientes con LLC y disminuye los niveles de fosforilación de mediadores clave de dicha ruta.
3. La activación del BCR contrarresta parcialmente la actividad antileucémica de EC-7072, mientras que el tratamiento con factores del microambiente tumoral no restaura la viabilidad de las células leucémicas.
4. La combinación de EC-7072 con ibrutinib, idelalisib, venetoclax o fludarabina resulta en un aumento en la capacidad citotóxica de dichos compuestos frente a células leucémicas de pacientes con LLC.
5. La estimulación de linfocitos B sanos y células leucémicas mediante la activación del BCR produce una disminución de la expresión de NKG2D en células NK y linfocitos T $CD8^+$ de donantes sanos y pacientes con LLC.
6. La eliminación de células tumorales mediada por células NK así como la citotoxicidad mediada por anticuerpo se encuentran impedidas en presencia de linfocitos B activados.
7. La reducción de la expresión de NKG2D en células NK y linfocitos T $CD8^+$ debida a la activación del BCR en linfocitos B no requiere contacto celular.
8. Los fármacos que inducen hiperploidía promueven un incremento en la expresión de ligandos activadores de células NK en líneas celulares tumorales, lo que incrementa la susceptibilidad de estas células a ser eliminadas por células NK.
9. El co-cultivo con células tumorales hiperploides induce la expresión de NKG2D, DNAM-1 y NKp30, así como la producción de IFN-γ, en células NK.
10. La producción de IL-2 se incrementa en los linfocitos T en presencia de células tumorales hiperploides, estimulando así la proliferación de las células NK.
11. La regulación positiva de MICA en células tumorales hiperploides es mediada principalmente por la proteína quinasa ATM y, en ciertos modelos celulares, por vías de señalización de estrés de retículo endoplasmático.

BIBLIOGRAPHY

Ahn, I. E., Underbayev, C., Albitar, A., Herman, S. E., Tian, X., Maric, I., . . . Wiestner, A. (2017). Clonal evolution leading to ibrutinib resistance in chronic lymphocytic leukemia. *Blood, 129*(11), 1469-1479. doi: 10.1182/blood-2016-06-719294

Alhakeem, S. S., McKenna, M. K., Oben, K. Z., Noothi, S. K., Rivas, J. R., Hildebrandt, G. C., . . . Bondada, S. (2018). Chronic Lymphocytic Leukemia-Derived IL-10 Suppresses Antitumor Immunity. *J Immunol, 200*(12), 4180-4189. doi: 10.4049/jimmunol.1800241

Anderson, M. A., Deng, J., Seymour, J. F., Tam, C., Kim, S. Y., Fein, J., . . . Roberts, A. W. (2016). The BCL2 selective inhibitor venetoclax induces rapid onset apoptosis of CLL cells in patients via a TP53-independent mechanism. *Blood, 127*(25), 3215-3224. doi: 10.1182/blood-2016-01-688796

Andre, P., Denis, C., Soulas, C., Bourbon-Caillet, C., Lopez, J., Arnoux, T., . . . Vivier, E. (2018). Anti-NKG2A mAb Is a Checkpoint Inhibitor that Promotes Anti-tumor Immunity by Unleashing Both T and NK Cells. *Cell, 175*(7), 1731-1743 e1713. doi: 10.1016/j.cell.2018.10.014

Andrews, L. P., Marciscano, A. E., Drake, C. G., & Vignali, D. A. (2017). LAG3 (CD223) as a cancer immunotherapy target. *Immunol Rev, 276*(1), 80-96. doi: 10.1111/imr.12519

Avalos, A. M., Meyer-Wentrup, F., & Ploegh, H. L. (2014). B-cell receptor signaling in lymphoid malignancies and autoimmunity. *Adv Immunol, 123*, 1-49. doi: 10.1016/B978-0-12-800266-7.00004-2

Axten, J. M., Medina, J. R., Feng, Y., Shu, A., Romeril, S. P., Grant, S. W., . . . Gampe, R. T. (2012). Discovery of 7-methyl-5-(1-{[3-(trifluoromethyl)phenyl]acetyl}-2,3-dihydro-1H-indol-5-yl)-7H-p yrrolo[2,3-d]pyrimidin-4-amine (GSK2606414), a potent and selective first-in-class inhibitor of protein kinase R (PKR)-like endoplasmic reticulum kinase (PERK). *J Med Chem, 55*(16), 7193-7207. doi: 10.1021/jm300713s

Baig, I., Perez, M., Brana, A. F., Gomathinayagam, R., Damodaran, C., Salas, J. A., . . . Rohr, J. (2008). Mithramycin analogues generated by combinatorial biosynthesis show improved bioactivity. *J Nat Prod, 71*(2), 199-207. doi: 10.1021/np0705763

Barf, T., Covey, T., Izumi, R., van de Kar, B., Gulrajani, M., van Lith, B., . . . Kaptein, A. (2017). Acalabrutinib (ACP-196): A Covalent Bruton Tyrosine Kinase Inhibitor with a Differentiated Selectivity and In Vivo Potency Profile. *J Pharmacol Exp Ther, 363*(2), 240-252. doi: 10.1124/jpet.117.242909

Barnum, K. J., & O'Connell, M. J. (2014). Cell cycle regulation by checkpoints. *Methods Mol Biol, 1170*, 29-40. doi: 10.1007/978-1-4939-0888-2_2

Baychelier, F., Sennepin, A., Ermonval, M., Dorgham, K., Debre, P., & Vieillard, V. (2013). Identification of a cellular ligand for the natural cytotoxicity receptor NKp44. *Blood, 122*(17), 2935-2942. doi: 10.1182/blood-2013-03-489054

Bijnsdorp, I. V., Giovannetti, E., & Peters, G. J. (2011). Analysis of drug interactions. *Methods Mol Biol, 731*, 421-434. doi: 10.1007/978-1-61779-080-5_34

Binder, C. J., Horkko, S., Dewan, A., Chang, M. K., Kieu, E. P., Goodyear, C. S., . . . Silverman, G. J. (2003). Pneumococcal vaccination decreases atherosclerotic lesion formation: molecular mimicry between Streptococcus pneumoniae and oxidized LDL. *Nat Med, 9*(6), 736-743. doi: 10.1038/nm876

Binet, J. L., Auquier, A., Dighiero, G., Chastang, C., Piguet, H., Goasguen, J., . . . Gremy, F. (1981). A new prognostic classification of chronic lymphocytic leukemia derived from a multivariate survival analysis. *Cancer, 48*(1), 198-206.

Bishop, G. A., Haxhinasto, S. A., Stunz, L. L., & Hostager, B. S. (2003). Antigen-specific B-lymphocyte activation. *Crit Rev Immunol, 23*(3), 149-197.

Bjarnadottir, K., Benkhoucha, M., Merkler, D., Weber, M. S., Payne, N. L., Bernard, C. C. A., . . . Lalive, P. H. (2016). B cell-derived transforming growth factor-beta1 expression limits the induction phase of autoimmune neuroinflammation. *Sci Rep, 6*, 34594. doi: 10.1038/srep34594

Blombery, P., Anderson, M. A., Gong, J. N., Thijssen, R., Birkinshaw, R. W., Thompson, E. R., . . . Roberts, A. W. (2019). Acquisition of the Recurrent Gly101Val Mutation in BCL2 Confers Resistance to Venetoclax in Patients with Progressive Chronic Lymphocytic Leukemia. *Cancer Discov, 9*(3), 342-353. doi: 10.1158/2159-8290.CD-18-1119

Borrego, F., Masilamani, M., Marusina, A. I., Tang, X., & Coligan, J. E. (2006). The CD94/NKG2 family of receptors: from molecules and cells to clinical relevance. *Immunol Res, 35*(3), 263-278. doi: 10.1385/IR:35:3:263

Boyce, M., Bryant, K. F., Jousse, C., Long, K., Harding, H. P., Scheuner, D., . . . Yuan, J. (2005). A selective inhibitor of eIF2alpha dephosphorylation protects cells from ER stress. *Science, 307*(5711), 935-939. doi: 10.1126/science.1101902

Brandt, C. S., Baratin, M., Yi, E. C., Kennedy, J., Gao, Z., Fox, B., . . . Levin, S. D. (2009). The B7 family member B7-H6 is a tumor cell ligand for the activating natural killer cell receptor NKp30 in humans. *J Exp Med, 206*(7), 1495-1503. doi: 10.1084/jem.20090681

Bray, F., Ferlay, J., Soerjomataram, I., Siegel, R. L., Torre, L. A., & Jemal, A. (2018). Global cancer statistics 2018: GLOBOCAN estimates of incidence and mortality worldwide for 36 cancers in 185 countries. *CA Cancer J Clin, 68*(6), 394-424. doi: 10.3322/caac.21492

Brown, J. R., Byrd, J. C., Coutre, S. E., Benson, D. M., Flinn, I. W., Wagner-Johnston, N. D., . . . Furman, R. R. (2014). Idelalisib, an inhibitor of phosphatidylinositol 3-kinase p110delta, for relapsed/refractory chronic lymphocytic leukemia. *Blood, 123*(22), 3390-3397. doi: 10.1182/blood-2013-11-535047

Buccheri, V., Barreto, W. G., Fogliatto, L. M., Capra, M., Marchiani, M., & Rocha, V. (2018). Prognostic and therapeutic stratification in CLL: focus on 17p deletion and p53 mutation. *Ann Hematol, 97*(12), 2269-2278. doi: 10.1007/s00277-018-3503-6

Burger, J. A. (2011). Nurture versus nature: the microenvironment in chronic lymphocytic leukemia. *Hematology Am Soc Hematol Educ Program, 2011*, 96-103. doi: 10.1182/asheducation-2011.1.96

Burger, J. A., & Chiorazzi, N. (2013). B cell receptor signaling in chronic lymphocytic leukemia. *Trends Immunol, 34*(12), 592-601. doi: 10.1016/j.it.2013.07.002

Burger, J. A., Landau, D. A., Taylor-Weiner, A., Bozic, I., Zhang, H., Sarosiek, K., . . . Wu, C. J. (2016). Clonal evolution in patients with chronic lymphocytic leukaemia developing resistance to BTK inhibition. *Nat Commun, 7*, 11589. doi: 10.1038/ncomms11589

Burger, J. A., & O'Brien, S. (2018). Evolution of CLL treatment - from chemoimmunotherapy to targeted and individualized therapy. *Nat Rev Clin Oncol, 15*(8), 510-527. doi: 10.1038/s41571-018-0037-8

Burger, J. A., & Wiestner, A. (2018). Targeting B cell receptor signalling in cancer: preclinical and clinical advances. *Nat Rev Cancer, 18*(3), 148-167. doi: 10.1038/nrc.2017.121

Burris, H. A., 3rd, Flinn, I. W., Patel, M. R., Fenske, T. S., Deng, C., Brander, D. M., . . . O'Connor, O. A. (2018). Umbralisib, a novel PI3Kdelta and casein kinase-1epsilon inhibitor, in relapsed or refractory chronic lymphocytic leukaemia and lymphoma: an open-label, phase 1, dose-

escalation, first-in-human study. *Lancet Oncol, 19*(4), 486-496. doi: 10.1016/S1470-2045(18)30082-2

Caligiuri, M. A., Murray, C., Robertson, M. J., Wang, E., Cochran, K., Cameron, C., . . . et al. (1993). Selective modulation of human natural killer cells in vivo after prolonged infusion of low dose recombinant interleukin 2. *J Clin Invest, 91*(1), 123-132. doi: 10.1172/JCI116161

Cerboni, C., Fionda, C., Soriani, A., Zingoni, A., Doria, M., Cippitelli, M., & Santoni, A. (2014). The DNA Damage Response: A Common Pathway in the Regulation of NKG2D and DNAM-1 Ligand Expression in Normal, Infected, and Cancer Cells. *Front Immunol, 4*, 508. doi: 10.3389/fimmu.2013.00508

Coutre, S., Choi, M., Furman, R. R., Eradat, H., Heffner, L., Jones, J. A., . . . Davids, M. S. (2018). Venetoclax for patients with chronic lymphocytic leukemia who progressed during or after idelalisib therapy. *Blood, 131*(15), 1704-1711. doi: 10.1182/blood-2017-06-788133

Crane, C. A., Han, S. J., Barry, J. J., Ahn, B. J., Lanier, L. L., & Parsa, A. T. (2010). TGF-beta downregulates the activating receptor NKG2D on NK cells and CD8+ T cells in glioma patients. *Neuro Oncol, 12*(1), 7-13. doi: 10.1093/neuonc/nop009

Chan, C. J., Smyth, M. J., & Martinet, L. (2014). Molecular mechanisms of natural killer cell activation in response to cellular stress. *Cell Death Differ, 21*(1), 5-14. doi: 10.1038/cdd.2013.26

Chan, O. T., & Yang, L. X. (2000). The immunological effects of taxanes. *Cancer Immunol Immunother, 49*(4-5), 181-185.

Chanan-Khan, A., Cramer, P., Demirkan, F., Fraser, G., Silva, R. S., Grosicki, S., . . . investigators, H. (2016). Ibrutinib combined with bendamustine and rituximab compared with placebo, bendamustine, and rituximab for previously treated chronic lymphocytic leukaemia or small lymphocytic lymphoma (HELIOS): a randomised, double-blind, phase 3 study. *Lancet Oncol, 17*(2), 200-211. doi: 10.1016/S1470-2045(15)00465-9

Chaput, N., De Botton, S., Obeid, M., Apetoh, L., Ghiringhelli, F., Panaretakis, T., . . . Kroemer, G. (2007). Molecular determinants of immunogenic cell death: surface exposure of calreticulin makes the difference. *J Mol Med (Berl), 85*(10), 1069-1076. doi: 10.1007/s00109-007-0214-1

Chitadze, G., Lettau, M., Bhat, J., Wesch, D., Steinle, A., Furst, D., . . . Kabelitz, D. (2013). Shedding of endogenous MHC class I-related chain molecules A and B from different human tumor entities: heterogeneous involvement of the "a disintegrin and metalloproteases" 10 and 17. *Int J Cancer, 133*(7), 1557-1566. doi: 10.1002/ijc.28174

Chiu, J., Ernst, D. M., & Keating, A. (2018). Acquired Natural Killer Cell Dysfunction in the Tumor Microenvironment of Classic Hodgkin Lymphoma. *Front Immunol, 9*, 267. doi: 10.3389/fimmu.2018.00267

Chou, T. C. (2010). Drug combination studies and their synergy quantification using the Chou-Talalay method. *Cancer Res, 70*(2), 440-446. doi: 10.1158/0008-5472.CAN-09-1947

Chow, J., & Poon, R. Y. (2010). DNA damage and polyploidization. *Adv Exp Med Biol, 676*, 57-71.

Davoli, T., & de Lange, T. (2011). The causes and consequences of polyploidy in normal development and cancer. *Annu Rev Cell Dev Biol, 27*, 585-610. doi: 10.1146/annurev-cellbio-092910-154234

de Visser, K. E., Eichten, A., & Coussens, L. M. (2006). Paradoxical roles of the immune system during cancer development. *Nat Rev Cancer, 6*(1), 24-37. doi: 10.1038/nrc1782

Dougan, M., Dranoff, G., & Dougan, S. K. (2019). Cancer Immunotherapy: Beyond Checkpoint Blockade. *Annual Review of Cancer Biology, 3*(1), 55-75. doi: 10.1146/annurev-cancerbio-030518-055552

Dreger, P., Ghia, P., Schetelig, J., van Gelder, M., Kimby, E., Michallet, M., . . . Marrow, T. (2018). High-risk chronic lymphocytic leukemia in the era of pathway inhibitors: integrating molecular and cellular therapies. *Blood, 132*(9), 892-902. doi: 10.1182/blood-2018-01-826008

Duhren-von Minden, M., Ubelhart, R., Schneider, D., Wossning, T., Bach, M. P., Buchner, M., . . . Jumaa, H. (2012). Chronic lymphocytic leukaemia is driven by antigen-independent cell-autonomous signalling. *Nature, 489*(7415), 309-312. doi: 10.1038/nature11309

Dunn, G. P., Bruce, A. T., Ikeda, H., Old, L. J., & Schreiber, R. D. (2002). Cancer immunoediting: from immunosurveillance to tumor escape. *Nat Immunol, 3*(11), 991-998. doi: 10.1038/ni1102-991

Fabbri, G., & Dalla-Favera, R. (2016). The molecular pathogenesis of chronic lymphocytic leukaemia. *Nat Rev Cancer, 16*(3), 145-162. doi: 10.1038/nrc.2016.8

Ferreira, P. G., Jares, P., Rico, D., Gomez-Lopez, G., Martinez-Trillos, A., Villamor, N., . . . Guigo, R. (2014). Transcriptome characterization by RNA sequencing identifies a major molecular and clinical subdivision in chronic lymphocytic leukemia. *Genome Res, 24*(2), 212-226. doi: 10.1101/gr.152132.112

Fillatreau, S., Sweenie, C. H., McGeachy, M. J., Gray, D., & Anderton, S. M. (2002). B cells regulate autoimmunity by provision of IL-10. *Nat Immunol, 3*(10), 944-950. doi: 10.1038/ni833

Garg, A. D., Krysko, D. V., Verfaillie, T., Kaczmarek, A., Ferreira, G. B., Marysael, T., . . . Agostinis, P. (2012). A novel pathway combining calreticulin exposure and ATP secretion in immunogenic cancer cell death. *EMBO J, 31*(5), 1062-1079. doi: 10.1038/emboj.2011.497

Gasser, S., Orsulic, S., Brown, E. J., & Raulet, D. H. (2005). The DNA damage pathway regulates innate immune system ligands of the NKG2D receptor. *Nature, 436*(7054), 1186-1190. doi: 10.1038/nature03884

Gilfillan, S., Chan, C. J., Cella, M., Haynes, N. M., Rapaport, A. S., Boles, K. S., . . . Colonna, M. (2008). DNAM-1 promotes activation of cytotoxic lymphocytes by nonprofessional antigen-presenting cells and tumors. *J Exp Med, 205*(13), 2965-2973. doi: 10.1084/jem.20081752

Gordon, D. J., Resio, B., & Pellman, D. (2012). Causes and consequences of aneuploidy in cancer. *Nat Rev Genet, 13*(3), 189-203. doi: 10.1038/nrg3123

Green, D. R., Ferguson, T., Zitvogel, L., & Kroemer, G. (2009). Immunogenic and tolerogenic cell death. *Nat Rev Immunol, 9*(5), 353-363. doi: 10.1038/nri2545

Green, L., & Donehower, R. C. (1984). Hepatic toxicity of low doses of mithramycin in hypercalcemia. *Cancer Treat Rep, 68*(11), 1379-1381.

Grivennikov, S. I., Greten, F. R., & Karin, M. (2010). Immunity, inflammation, and cancer. *Cell, 140*(6), 883-899. doi: 10.1016/j.cell.2010.01.025

Groh, V., Wu, J., Yee, C., & Spies, T. (2002). Tumour-derived soluble MIC ligands impair expression of NKG2D and T-cell activation. *Nature, 419*(6908), 734-738. doi: 10.1038/nature01112

Guerra, N., Tan, Y. X., Joncker, N. T., Choy, A., Gallardo, F., Xiong, N., . . . Raulet, D. H. (2008). NKG2D-deficient mice are defective in tumor surveillance in models of spontaneous malignancy. *Immunity, 28*(4), 571-580. doi: 10.1016/j.immuni.2008.02.016

Guillerey, C., Harjunpaa, H., Carrie, N., Kassem, S., Teo, T., Miles, K., . . . Smyth, M. J. (2018). TIGIT immune checkpoint blockade restores CD8(+) T-cell immunity against multiple myeloma. *Blood, 132*(16), 1689-1694. doi: 10.1182/blood-2018-01-825265

Hallek, M., Cheson, B. D., Catovsky, D., Caligaris-Cappio, F., Dighiero, G., Dohner, H., . . . Kipps, T. J. (2018). iwCLL guidelines for diagnosis, indications for treatment, response assessment, and supportive management of CLL. *Blood, 131*(25), 2745-2760. doi: 10.1182/blood-2017-09-806398

Hallek, M., Shanafelt, T. D., & Eichhorst, B. (2018). Chronic lymphocytic leukaemia. *Lancet, 391*(10129), 1524-1537. doi: 10.1016/S0140-6736(18)30422-7

Hanahan, D., & Weinberg, R. A. (2000). The hallmarks of cancer. *Cell, 100*(1), 57-70.

Hanahan, D., & Weinberg, R. A. (2011). Hallmarks of cancer: the next generation. *Cell, 144*(5), 646-674. doi: 10.1016/j.cell.2011.02.013

Hata, A. N., Engelman, J. A., & Faber, A. C. (2015). The BCL2 Family: Key Mediators of the Apoptotic Response to Targeted Anticancer Therapeutics. *Cancer Discov, 5*(5), 475-487. doi: 10.1158/2159-8290.CD-15-0011

Henney, C. S., Kuribayashi, K., Kern, D. E., & Gillis, S. (1981). Interleukin-2 augments natural killer cell activity. *Nature, 291*(5813), 335-338.

Herman, S. E., Gordon, A. L., Hertlein, E., Ramanunni, A., Zhang, X., Jaglowski, S., . . . Byrd, J. C. (2011). Bruton tyrosine kinase represents a promising therapeutic target for treatment of chronic lymphocytic leukemia and is effectively targeted by PCI-32765. *Blood, 117*(23), 6287-6296. doi: 10.1182/blood-2011-01-328484

Herman, S. E., Gordon, A. L., Wagner, A. J., Heerema, N. A., Zhao, W., Flynn, J. M., . . . Johnson, A. J. (2010). Phosphatidylinositol 3-kinase-delta inhibitor CAL-101 shows promising preclinical activity in chronic lymphocytic leukemia by antagonizing intrinsic and extrinsic cellular survival signals. *Blood, 116*(12), 2078-2088. doi: 10.1182/blood-2010-02-271171

Highlights in chronic lymphocytic leukemia from the 2018 American Society of Clinical Oncology annual meeting. (2018). *Clin Adv Hematol Oncol, 16 Suppl 12*(7), 1-24.

Hodge, J. W., Garnett, C. T., Farsaci, B., Palena, C., Tsang, K. Y., Ferrone, S., & Gameiro, S. R. (2013). Chemotherapy-induced immunogenic modulation of tumor cells enhances killing by cytotoxic T lymphocytes and is distinct from immunogenic cell death. *Int J Cancer, 133*(3), 624-636. doi: 10.1002/ijc.28070

Hoogeboom, R., van Kessel, K. P., Hochstenbach, F., Wormhoudt, T. A., Reinten, R. J., Wagner, K., . . . van Noesel, C. J. (2013). A mutated B cell chronic lymphocytic leukemia subset that recognizes and responds to fungi. *J Exp Med, 210*(1), 59-70. doi: 10.1084/jem.20121801

Huang, R. Y., Francois, A., McGray, A. R., Miliotto, A., & Odunsi, K. (2017). Compensatory upregulation of PD-1, LAG-3, and CTLA-4 limits the efficacy of single-agent checkpoint blockade in metastatic ovarian cancer. *Oncoimmunology, 6*(1), e1249561. doi: 10.1080/2162402X.2016.1249561

Huergo-Zapico, L., Acebes-Huerta, A., Gonzalez-Rodriguez, A. P., Contesti, J., Gonzalez-Garcia, E., Payer, A. R., . . . Gonzalez, S. (2014). Expansion of NK cells and reduction of NKG2D expression in chronic lymphocytic leukemia. Correlation with progressive disease. *PLoS One, 9*(10), e108326. doi: 10.1371/journal.pone.0108326

Huergo-Zapico, L., Acebes-Huerta, A., Lopez-Soto, A., Villa-Alvarez, M., Gonzalez-Rodriguez, A. P., & Gonzalez, S. (2014). Molecular Bases for the Regulation of NKG2D Ligands in Cancer. *Front Immunol, 5*, 106. doi: 10.3389/fimmu.2014.00106

Hussain, S. R., Cheney, C. M., Johnson, A. J., Lin, T. S., Grever, M. R., Caligiuri, M. A., . . . Byrd, J. C. (2007). Mcl-1 is a relevant therapeutic target in acute and chronic lymphoid malignancies: down-regulation enhances rituximab-mediated apoptosis and complement-dependent cytotoxicity. *Clin Cancer Res, 13*(7), 2144-2150. doi: 10.1158/1078-0432.CCR-06-2294

Iannello, A., Thompson, T. W., Ardolino, M., Lowe, S. W., & Raulet, D. H. (2013). p53-dependent chemokine production by senescent tumor cells supports NKG2D-dependent tumor elimination by natural killer cells. *J Exp Med, 210*(10), 2057-2069. doi: 10.1084/jem.20130783

Ibrahim, S., Keating, M., Do, K. A., O'Brien, S., Huh, Y. O., Jilani, I., . . . Albitar, M. (2001). CD38 expression as an important prognostic factor in B-cell chronic lymphocytic leukemia. *Blood, 98*(1), 181-186.

Iguchi-Manaka, A., Kai, H., Yamashita, Y., Shibata, K., Tahara-Hanaoka, S., Honda, S., . . . Shibuya, A. (2008). Accelerated tumor growth in mice deficient in DNAM-1 receptor. *J Exp Med, 205*(13), 2959-2964. doi: 10.1084/jem.20081611

Johnston, R. J., Yu, X., & Grogan, J. L. (2015). The checkpoint inhibitor TIGIT limits antitumor and antiviral CD8(+) T cell responses. *Oncoimmunology, 4*(9), e1036214. doi: 10.1080/2162402X.2015.1036214

Jung, H., Hsiung, B., Pestal, K., Procyk, E., & Raulet, D. H. (2012). RAE-1 ligands for the NKG2D receptor are regulated by E2F transcription factors, which control cell cycle entry. *J Exp Med, 209*(13), 2409-2422. doi: 10.1084/jem.20120565

Kalampokis, I., Yoshizaki, A., & Tedder, T. F. (2013). IL-10-producing regulatory B cells (B10 cells) in autoimmune disease. *Arthritis Res Ther, 15 Suppl 1*, S1. doi: 10.1186/ar3907

Kastenhuber, E. R., & Lowe, S. W. (2017). Putting p53 in Context. *Cell, 170*(6), 1062-1078. doi: 10.1016/j.cell.2017.08.028

Keating, M. J., O'Brien, S., Albitar, M., Lerner, S., Plunkett, W., Giles, F., . . . Kantarjian, H. (2005). Early results of a chemoimmunotherapy regimen of fludarabine, cyclophosphamide, and rituximab as initial therapy for chronic lymphocytic leukemia. *J Clin Oncol, 23*(18), 4079-4088. doi: 10.1200/JCO.2005.12.051

Keating, M. J., O'Brien, S., Lerner, S., Koller, C., Beran, M., Robertson, L. E., . . . Kantarjian, H. (1998). Long-term follow-up of patients with chronic lymphocytic leukemia (CLL) receiving fludarabine regimens as initial therapy. *Blood, 92*(4), 1165-1171.

Kepp, O., Menger, L., Vacchelli, E., Locher, C., Adjemian, S., Yamazaki, T., . . . Zitvogel, L. (2013). Crosstalk between ER stress and immunogenic cell death. *Cytokine Growth Factor Rev, 24*(4), 311-318. doi: 10.1016/j.cytogfr.2013.05.001

Kimiz-Gebologlu, I., Gulce-Iz, S., & Biray-Avci, C. (2018). Monoclonal antibodies in cancer immunotherapy. *Mol Biol Rep, 45*(6), 2935-2940. doi: 10.1007/s11033-018-4427-x

King, M. C., Marks, J. H., Mandell, J. B., & New York Breast Cancer Study, G. (2003). Breast and ovarian cancer risks due to inherited mutations in BRCA1 and BRCA2. *Science, 302*(5645), 643-646. doi: 10.1126/science.1088759

Kipps, T. J., Stevenson, F. K., Wu, C. J., Croce, C. M., Packham, G., Wierda, W. G., . . . Rai, K. (2017). Chronic lymphocytic leukaemia. *Nat Rev Dis Primers, 3*, 16096. doi: 10.1038/nrdp.2016.96

Klinker, M. W., & Lundy, S. K. (2012). Multiple mechanisms of immune suppression by B lymphocytes. *Mol Med, 18*, 123-137. doi: 10.2119/molmed.2011.00333

Koehrer, S., & Burger, J. A. (2016). B-cell receptor signaling in chronic lymphocytic leukemia and other B-cell malignancies. *Clin Adv Hematol Oncol, 14*(1), 55-65.

Kroemer, G., Galluzzi, L., Kepp, O., & Zitvogel, L. (2013). Immunogenic cell death in cancer therapy. *Annu Rev Immunol, 31*, 51-72. doi: 10.1146/annurev-immunol-032712-100008

Kruse, P. H., Matta, J., Ugolini, S., & Vivier, E. (2014). Natural cytotoxicity receptors and their ligands. *Immunol Cell Biol, 92*(3), 221-229. doi: 10.1038/icb.2013.98

Kulis, M., Heath, S., Bibikova, M., Queiros, A. C., Navarro, A., Clot, G., . . . Martin-Subero, J. I. (2012). Epigenomic analysis detects widespread gene-body DNA hypomethylation in chronic lymphocytic leukemia. *Nat Genet, 44*(11), 1236-1242. doi: 10.1038/ng.2443

Lakshmikanth, T., Burke, S., Ali, T. H., Kimpfler, S., Ursini, F., Ruggeri, L., . . . Colucci, F. (2009). NCRs and DNAM-1 mediate NK cell recognition and lysis of human and mouse melanoma cell lines in vitro and in vivo. *J Clin Invest, 119*(5), 1251-1263. doi: 10.1172/JCI36022

Lanemo Myhrinder, A., Hellqvist, E., Sidorova, E., Soderberg, A., Baxendale, H., Dahle, C., . . . Rosen, A. (2008). A new perspective: molecular motifs on oxidized LDL, apoptotic cells, and bacteria are targets for chronic lymphocytic leukemia antibodies. *Blood, 111*(7), 3838-3848. doi: 10.1182/blood-2007-11-125450

Lee, J. C., Lee, K. M., Kim, D. W., & Heo, D. S. (2004). Elevated TGF-beta1 secretion and down-modulation of NKG2D underlies impaired NK cytotoxicity in cancer patients. *J Immunol, 172*(12), 7335-7340. doi: 10.4049/jimmunol.172.12.7335

Lissa, D., Senovilla, L., Rello-Varona, S., Vitale, I., Michaud, M., Pietrocola, F., . . . Kroemer, G. (2014). Resveratrol and aspirin eliminate tetraploid cells for anticancer chemoprevention. *Proc Natl Acad Sci U S A, 111*(8), 3020-3025. doi: 10.1073/pnas.1318440111

Liu, G., Atteridge, C. L., Wang, X., Lundgren, A. D., & Wu, J. D. (2010). The membrane type matrix metalloproteinase MMP14 mediates constitutive shedding of MHC class I chain-related molecule A independent of A disintegrin and metalloproteinases. *J Immunol, 184*(7), 3346-3350. doi: 10.4049/jimmunol.0903789

Livak, K. J., & Schmittgen, T. D. (2001). Analysis of relative gene expression data using real-time quantitative PCR and the 2(-Delta Delta C(T)) Method. *Methods, 25*(4), 402-408. doi: 10.1006/meth.2001.1262

Lopez-Soto, A., Gonzalez, S., Smyth, M. J., & Galluzzi, L. (2017). Control of Metastasis by NK Cells. *Cancer Cell, 32*(2), 135-154. doi: 10.1016/j.ccell.2017.06.009

Lopez-Soto, A., Huergo-Zapico, L., Acebes-Huerta, A., Villa-Alvarez, M., & Gonzalez, S. (2015). NKG2D signaling in cancer immunosurveillance. *Int J Cancer, 136*(8), 1741-1750. doi: 10.1002/ijc.28775

Lopez-Soto, A., Huergo-Zapico, L., Galvan, J. A., Rodrigo, L., de Herreros, A. G., Astudillo, A., & Gonzalez, S. (2013). Epithelial-mesenchymal transition induces an antitumor immune response mediated by NKG2D receptor. *J Immunol, 190*(8), 4408-4419. doi: 10.4049/jimmunol.1202950

Lorenzo-Herrero, S., Sordo-Bahamonde, C., Gonzalez, S., & Lopez-Soto, A. (2019a). CD107a Degranulation Assay to Evaluate Immune Cell Antitumor Activity. *Methods Mol Biol, 1884*, 119-130. doi: 10.1007/978-1-4939-8885-3_7

Lorenzo-Herrero, S., Sordo-Bahamonde, C., Gonzalez, S., & Lopez-Soto, A. (2019b). A Flow Cytometric NK Cell-Mediated Cytotoxicity Assay to Evaluate Anticancer Immune Responses In Vitro. *Methods Mol Biol, 1884*, 131-139. doi: 10.1007/978-1-4939-8885-3_8

Love, M. I., Huber, W., & Anders, S. (2014). Moderated estimation of fold change and dispersion for RNA-seq data with DESeq2. *Genome Biol, 15*(12), 550. doi: 10.1186/s13059-014-0550-8

Lundholm, M., Schroder, M., Nagaeva, O., Baranov, V., Widmark, A., Mincheva-Nilsson, L., & Wikstrom, P. (2014). Prostate tumor-derived exosomes down-regulate NKG2D expression on natural killer cells and CD8+ T cells: mechanism of immune evasion. *PLoS One, 9*(9), e108925. doi: 10.1371/journal.pone.0108925

Malek, A., Nunez, L. E., Magistri, M., Brambilla, L., Jovic, S., Carbone, G. M., . . . Catapano, C. V. (2012). Modulation of the activity of Sp transcription factors by mithramycin analogues as a new strategy for treatment of metastatic prostate cancer. *PLoS One, 7*(4), e35130. doi: 10.1371/journal.pone.0035130

Maleki, Y., Alahbakhshi, Z., Heidari, Z., Moradi, M. T., Rahimi, Z., Yari, K., . . . Bahremand, F. (2019). NOTCH1, SF3B1, MDM2 and MYD88 mutations in patients with chronic lymphocytic leukemia. *Oncol Lett, 17*(4), 4016-4023. doi: 10.3892/ol.2019.10048

Melisi, D., Ishiyama, S., Sclabas, G. M., Fleming, J. B., Xia, Q., Tortora, G., . . . Chiao, P. J. (2008). LY2109761, a novel transforming growth factor beta receptor type I and type II dual inhibitor, as a therapeutic approach to suppressing pancreatic cancer metastasis. *Mol Cancer Ther, 7*(4), 829-840. doi: 10.1158/1535-7163.MCT-07-0337

Miliotou, A. N., & Papadopoulou, L. C. (2018). CAR T-cell Therapy: A New Era in Cancer Immunotherapy. *Curr Pharm Biotechnol, 19*(1), 5-18. doi: 10.2174/1389201019666180418095526

Moen, M. D., McKeage, K., Plosker, G. L., & Siddiqui, M. A. (2007). Imatinib: a review of its use in chronic myeloid leukaemia. *Drugs, 67*(2), 299-320. doi: 10.2165/00003495-200767020-00010

Morvan, M. G., & Lanier, L. L. (2016). NK cells and cancer: you can teach innate cells new tricks. *Nat Rev Cancer, 16*(1), 7-19. doi: 10.1038/nrc.2015.5

Myklebust, J. H., Brody, J., Kohrt, H. E., Kolstad, A., Czerwinski, D. K., Walchli, S., . . . Levy, R. (2017). Distinct patterns of B-cell receptor signaling in non-Hodgkin lymphomas identified by single-cell profiling. *Blood, 129*(6), 759-770. doi: 10.1182/blood-2016-05-718494

Niemann, C. U., & Wiestner, A. (2013). B-cell receptor signaling as a driver of lymphoma development and evolution. *Semin Cancer Biol, 23*(6), 410-421. doi: 10.1016/j.semcancer.2013.09.001

O'Brien, S., Furman, R. R., Coutre, S., Flinn, I. W., Burger, J. A., Blum, K., . . . Byrd, J. C. (2018). Single-agent ibrutinib in treatment-naive and relapsed/refractory chronic lymphocytic leukemia: a 5-year experience. *Blood, 131*(17), 1910-1919. doi: 10.1182/blood-2017-10-810044

Obeid, M., Tesniere, A., Ghiringhelli, F., Fimia, G. M., Apetoh, L., Perfettini, J. L., . . . Kroemer, G. (2007). Calreticulin exposure dictates the immunogenicity of cancer cell death. *Nat Med, 13*(1), 54-61. doi: 10.1038/nm1523

Osgood, C. L., Maloney, N., Kidd, C. G., Kitchen-Goosen, S., Segars, L., Gebregiorgis, M., . . . Grohar, P. J. (2016). Identification of Mithramycin Analogues with Improved Targeting of the EWS-FLI1 Transcription Factor. *Clin Cancer Res, 22*(16), 4105-4118. doi: 10.1158/1078-0432.CCR-15-2624

Otegbeye, F., Ojo, E., Moreton, S., Mackowski, N., Lee, D. A., de Lima, M., & Wald, D. N. (2018). Inhibiting TGF-beta signaling preserves the function of highly activated, in vitro expanded

natural killer cells in AML and colon cancer models. *PLoS One, 13*(1), e0191358. doi: 10.1371/journal.pone.0191358

Ozaki, T., & Nakagawara, A. (2011). Role of p53 in Cell Death and Human Cancers. *Cancers (Basel), 3*(1), 994-1013. doi: 10.3390/cancers3010994

Packham, G., Krysov, S., Allen, A., Savelyeva, N., Steele, A. J., Forconi, F., & Stevenson, F. K. (2014). The outcome of B-cell receptor signaling in chronic lymphocytic leukemia: proliferation or anergy. *Haematologica, 99*(7), 1138-1148. doi: 10.3324/haematol.2013.098384

Packham, G., & Stevenson, F. K. (2005). Bodyguards and assassins: Bcl-2 family proteins and apoptosis control in chronic lymphocytic leukaemia. *Immunology, 114*(4), 441-449. doi: 10.1111/j.1365-2567.2005.02117.x

Panaretakis, T., Joza, N., Modjtahedi, N., Tesniere, A., Vitale, I., Durchschlag, M., . . . Kroemer, G. (2008). The co-translocation of ERp57 and calreticulin determines the immunogenicity of cell death. *Cell Death Differ, 15*(9), 1499-1509. doi: 10.1038/cdd.2008.67

Panaretakis, T., Kepp, O., Brockmeier, U., Tesniere, A., Bjorklund, A. C., Chapman, D. C., . . . Kroemer, G. (2009). Mechanisms of pre-apoptotic calreticulin exposure in immunogenic cell death. *EMBO J, 28*(5), 578-590. doi: 10.1038/emboj.2009.1

Park, Y. J., Kuen, D. S., & Chung, Y. (2018). Future prospects of immune checkpoint blockade in cancer: from response prediction to overcoming resistance. *Exp Mol Med, 50*(8), 109. doi: 10.1038/s12276-018-0130-1

Parry, H. M., Stevens, T., Oldreive, C., Zadran, B., McSkeane, T., Rudzki, Z., . . . Moss, P. (2016). NK cell function is markedly impaired in patients with chronic lymphocytic leukaemia but is preserved in patients with small lymphocytic lymphoma. *Oncotarget, 7*(42), 68513-68526. doi: 10.18632/oncotarget.12097

Patro, R., Duggal, G., Love, M. I., Irizarry, R. A., & Kingsford, C. (2017). Salmon provides fast and bias-aware quantification of transcript expression. *Nat Methods, 14*(4), 417-419. doi: 10.1038/nmeth.4197

Pavlova, N. N., & Thompson, C. B. (2016). The Emerging Hallmarks of Cancer Metabolism. *Cell Metab, 23*(1), 27-47. doi: 10.1016/j.cmet.2015.12.006

Pegram, H. J., Andrews, D. M., Smyth, M. J., Darcy, P. K., & Kershaw, M. H. (2011). Activating and inhibitory receptors of natural killer cells. *Immunol Cell Biol, 89*(2), 216-224. doi: 10.1038/icb.2010.78

Pende, D., Parolini, S., Pessino, A., Sivori, S., Augugliaro, R., Morelli, L., . . . Moretta, A. (1999). Identification and molecular characterization of NKp30, a novel triggering receptor involved in natural cytotoxicity mediated by human natural killer cells. *J Exp Med, 190*(10), 1505-1516. doi: 10.1084/jem.190.10.1505

Perez, M. C., Miura, J. T., Naqvi, S. M. H., Kim, Y., Holstein, A., Lee, D., . . . Zager, J. S. (2018). Talimogene Laherparepvec (TVEC) for the Treatment of Advanced Melanoma: A Single-Institution Experience. *Ann Surg Oncol, 25*(13), 3960-3965. doi: 10.1245/s10434-018-6803-0

Pesce, S., Tabellini, G., Cantoni, C., Patrizi, O., Coltrini, D., Rampinelli, F., . . . Marcenaro, E. (2015). B7-H6-mediated downregulation of NKp30 in NK cells contributes to ovarian carcinoma immune escape. *Oncoimmunology, 4*(4), e1001224. doi: 10.1080/2162402X.2014.1001224

Pogge von Strandmann, E., Simhadri, V. R., von Tresckow, B., Sasse, S., Reiners, K. S., Hansen, H. P., . . . Engert, A. (2007). Human leukocyte antigen-B-associated transcript 3 is released

from tumor cells and engages the NKp30 receptor on natural killer cells. *Immunity, 27*(6), 965-974. doi: 10.1016/j.immuni.2007.10.010

Puente, X. S., Pinyol, M., Quesada, V., Conde, L., Ordonez, G. R., Villamor, N., . . . Campo, E. (2011). Whole-genome sequencing identifies recurrent mutations in chronic lymphocytic leukaemia. *Nature, 475*(7354), 101-105. doi: 10.1038/nature10113

Queiros, A. C., Villamor, N., Clot, G., Martinez-Trillos, A., Kulis, M., Navarro, A., . . . Martin-Subero, J. I. (2015). A B-cell epigenetic signature defines three biologic subgroups of chronic lymphocytic leukemia with clinical impact. *Leukemia, 29*(3), 598-605. doi: 10.1038/leu.2014.252

Quesada, V., Conde, L., Villamor, N., Ordonez, G. R., Jares, P., Bassaganyas, L., . . . Lopez-Otin, C. (2011). Exome sequencing identifies recurrent mutations of the splicing factor SF3B1 gene in chronic lymphocytic leukemia. *Nat Genet, 44*(1), 47-52. doi: 10.1038/ng.1032

Quezada, S. A., Peggs, K. S., Simpson, T. R., & Allison, J. P. (2011). Shifting the equilibrium in cancer immunoediting: from tumor tolerance to eradication. *Immunol Rev, 241*(1), 104-118. doi: 10.1111/j.1600-065X.2011.01007.x

Rai, K. R., Sawitsky, A., Cronkite, E. P., Chanana, A. D., Levy, R. N., & Pasternack, B. S. (1975). Clinical staging of chronic lymphocytic leukemia. *Blood, 46*(2), 219-234.

Ramsay, A. J., Quesada, V., Foronda, M., Conde, L., Martinez-Trillos, A., Villamor, N., . . . Lopez-Otin, C. (2013). POT1 mutations cause telomere dysfunction in chronic lymphocytic leukemia. *Nat Genet, 45*(5), 526-530. doi: 10.1038/ng.2584

Raulet, D. H. (2003). Roles of the NKG2D immunoreceptor and its ligands. *Nat Rev Immunol, 3*(10), 781-790. doi: 10.1038/nri1199

Raulet, D. H., Gasser, S., Gowen, B. G., Deng, W., & Jung, H. (2013). Regulation of ligands for the NKG2D activating receptor. *Annu Rev Immunol, 31*, 413-441. doi: 10.1146/annurev-immunol-032712-095951

Raval, A., Tanner, S. M., Byrd, J. C., Angerman, E. B., Perko, J. D., Chen, S. S., . . . Plass, C. (2007). Downregulation of death-associated protein kinase 1 (DAPK1) in chronic lymphocytic leukemia. *Cell, 129*(5), 879-890. doi: 10.1016/j.cell.2007.03.043

Reiners, K. S., Topolar, D., Henke, A., Simhadri, V. R., Kessler, J., Sauer, M., . . . Pogge von Strandmann, E. (2013). Soluble ligands for NK cell receptors promote evasion of chronic lymphocytic leukemia cells from NK cell anti-tumor activity. *Blood, 121*(18), 3658-3665. doi: 10.1182/blood-2013-01-476606

Remsing, L. L., Gonzalez, A. M., Nur-e-Alam, M., Fernandez-Lozano, M. J., Brana, A. F., Rix, U., . . . Rohr, J. (2003). Mithramycin SK, a novel antitumor drug with improved therapeutic index, mithramycin SA, and demycarosyl-mithramycin SK: three new products generated in the mithramycin producer Streptomyces argillaceus through combinatorial biosynthesis. *J Am Chem Soc, 125*(19), 5745-5753. doi: 10.1021/ja034162h

Ribas, A., & Wolchok, J. D. (2018). Cancer immunotherapy using checkpoint blockade. *Science, 359*(6382), 1350-1355. doi: 10.1126/science.aar4060

Rickert, R. C. (2013). New insights into pre-BCR and BCR signalling with relevance to B cell malignancies. *Nat Rev Immunol, 13*(8), 578-591. doi: 10.1038/nri3487

Roberts, A. W., Davids, M. S., Pagel, J. M., Kahl, B. S., Puvvada, S. D., Gerecitano, J. F., . . . Seymour, J. F. (2016). Targeting BCL2 with Venetoclax in Relapsed Chronic Lymphocytic Leukemia. *N Engl J Med, 374*(4), 311-322. doi: 10.1056/NEJMoa1513257

Robertson, L. E., Plunkett, W., McConnell, K., Keating, M. J., & McDonnell, T. J. (1996). Bcl-2 expression in chronic lymphocytic leukemia and its correlation with the induction of apoptosis and clinical outcome. *Leukemia, 10*(3), 456-459.

Rogakou, E. P., Nieves-Neira, W., Boon, C., Pommier, Y., & Bonner, W. M. (2000). Initiation of DNA fragmentation during apoptosis induces phosphorylation of H2AX histone at serine 139. *J Biol Chem, 275*(13), 9390-9395. doi: 10.1074/jbc.275.13.9390

Rosen, A., Murray, F., Evaldsson, C., & Rosenquist, R. (2010). Antigens in chronic lymphocytic leukemia--implications for cell origin and leukemogenesis. *Semin Cancer Biol, 20*(6), 400-409. doi: 10.1016/j.semcancer.2010.09.004

Salih, H. R., Rammensee, H. G., & Steinle, A. (2002). Cutting edge: down-regulation of MICA on human tumors by proteolytic shedding. *J Immunol, 169*(8), 4098-4102. doi: 10.4049/jimmunol.169.8.4098

Schlecker, E., Fiegler, N., Arnold, A., Altevogt, P., Rose-John, S., Moldenhauer, G., . . . Cerwenka, A. (2014). Metalloprotease-mediated tumor cell shedding of B7-H6, the ligand of the natural killer cell-activating receptor NKp30. *Cancer Res, 74*(13), 3429-3440. doi: 10.1158/0008-5472.CAN-13-3017

Schreiber, R. D., Old, L. J., & Smyth, M. J. (2011). Cancer immunoediting: integrating immunity's roles in cancer suppression and promotion. *Science, 331*(6024), 1565-1570. doi: 10.1126/science.1203486

Semeraro, M., Rusakiewicz, S., Minard-Colin, V., Delahaye, N. F., Enot, D., Vely, F., . . . Zitvogel, L. (2015). Clinical impact of the NKp30/B7-H6 axis in high-risk neuroblastoma patients. *Sci Transl Med, 7*(283), 283ra255. doi: 10.1126/scitranslmed.aaa2327

Senovilla, L., Vitale, I., Martins, I., Tailler, M., Pailleret, C., Michaud, M., . . . Kroemer, G. (2012). An immunosurveillance mechanism controls cancer cell ploidy. *Science, 337*(6102), 1678-1684. doi: 10.1126/science.1224922

Seymour, J. F., Kipps, T. J., Eichhorst, B., Hillmen, P., D'Rozario, J., Assouline, S., . . . Kater, A. P. (2018). Venetoclax-Rituximab in Relapsed or Refractory Chronic Lymphocytic Leukemia. *N Engl J Med, 378*(12), 1107-1120. doi: 10.1056/NEJMoa1713976

Seymour, J. F., Ma, S., Brander, D. M., Choi, M. Y., Barrientos, J., Davids, M. S., . . . Roberts, A. W. (2017). Venetoclax plus rituximab in relapsed or refractory chronic lymphocytic leukaemia: a phase 1b study. *Lancet Oncol, 18*(2), 230-240. doi: 10.1016/S1470-2045(17)30012-8

Shayan, G., & Ferris, R. L. (2015). PD-1 blockade upregulate TIM-3 expression as a compensatory regulation of immune check point receptors in HNSCC TIL. *Journal for ImmunoTherapy of Cancer, 3*(S2). doi: 10.1186/2051-1426-3-s2-p196

Sheppard, S., Guedes, J., Mroz, A., Zavitsanou, A. M., Kudo, H., Rothery, S. M., . . . Guerra, N. (2017). The immunoreceptor NKG2D promotes tumour growth in a model of hepatocellular carcinoma. *Nat Commun, 8*, 13930. doi: 10.1038/ncomms13930

Sica, V., Maiuri, M. C., Kroemer, G., & Galluzzi, L. (2016). Detection of Apoptotic Versus Autophagic Cell Death by Flow Cytometry. *Methods Mol Biol, 1419*, 1-16. doi: 10.1007/978-1-4939-3581-9_1

Sivori, S., Vacca, P., Del Zotto, G., Munari, E., Mingari, M. C., & Moretta, L. (2019). Human NK cells: surface receptors, inhibitory checkpoints, and translational applications. *Cell Mol Immunol, 16*(5), 430-441. doi: 10.1038/s41423-019-0206-4

Smith, S. M., Pitcher, B. N., Jung, S. H., Bartlett, N. L., Wagner-Johnston, N., Park, S. I., . . . Leonard, J. P. (2017). Safety and tolerability of idelalisib, lenalidomide, and rituximab in relapsed and

refractory lymphoma: the Alliance for Clinical Trials in Oncology A051201 and A051202 phase 1 trials. *Lancet Haematol, 4*(4), e176-e182. doi: 10.1016/S2352-3026(17)30028-5

Song, H., Kim, J., Cosman, D., & Choi, I. (2006). Soluble ULBP suppresses natural killer cell activity via down-regulating NKG2D expression. *Cell Immunol, 239*(1), 22-30. doi: 10.1016/j.cellimm.2006.03.002

Soriani, A., Iannitto, M. L., Ricci, B., Fionda, C., Malgarini, G., Morrone, S., . . . Santoni, A. (2014). Reactive oxygen species- and DNA damage response-dependent NK cell activating ligand upregulation occurs at transcriptional levels and requires the transcriptional factor E2F1. *J Immunol, 193*(2), 950-960. doi: 10.4049/jimmunol.1400271

Soriani, A., Zingoni, A., Cerboni, C., Iannitto, M. L., Ricciardi, M. R., Di Gialleonardo, V., . . . Santoni, A. (2009). ATM-ATR-dependent up-regulation of DNAM-1 and NKG2D ligands on multiple myeloma cells by therapeutic agents results in enhanced NK-cell susceptibility and is associated with a senescent phenotype. *Blood, 113*(15), 3503-3511. doi: 10.1182/blood-2008-08-173914

Storchova, Z., & Pellman, D. (2004). From polyploidy to aneuploidy, genome instability and cancer. *Nat Rev Mol Cell Biol, 5*(1), 45-54. doi: 10.1038/nrm1276

Sun, C., Xu, J., Huang, Q., Huang, M., Wen, H., Zhang, C., . . . Tian, Z. (2017). High NKG2A expression contributes to NK cell exhaustion and predicts a poor prognosis of patients with liver cancer. *Oncoimmunology, 6*(1), e1264562. doi: 10.1080/2162402X.2016.1264562

Tees, M. T., & Flinn, I. W. (2017). Chronic lymphocytic leukemia and small lymphocytic lymphoma: two faces of the same disease. *Expert Rev Hematol, 10*(2), 137-146. doi: 10.1080/17474086.2017.1270203

ten Hacken, E., & Burger, J. A. (2014). Molecular pathways: targeting the microenvironment in chronic lymphocytic leukemia--focus on the B-cell receptor. *Clin Cancer Res, 20*(3), 548-556. doi: 10.1158/1078-0432.CCR-13-0226

Ten Hacken, E., & Burger, J. A. (2016). Microenvironment interactions and B-cell receptor signaling in Chronic Lymphocytic Leukemia: Implications for disease pathogenesis and treatment. *Biochim Biophys Acta, 1863*(3), 401-413. doi: 10.1016/j.bbamcr.2015.07.009

Textor, S., Fiegler, N., Arnold, A., Porgador, A., Hofmann, T. G., & Cerwenka, A. (2011). Human NK cells are alerted to induction of p53 in cancer cells by upregulation of the NKG2D ligands ULBP1 and ULBP2. *Cancer Res, 71*(18), 5998-6009. doi: 10.1158/0008-5472.CAN-10-3211

Torrance, C. J., Agrawal, V., Vogelstein, B., & Kinzler, K. W. (2001). Use of isogenic human cancer cells for high-throughput screening and drug discovery. *Nat Biotechnol, 19*(10), 940-945. doi: 10.1038/nbt1001-940

Trinchieri, G., Matsumoto-Kobayashi, M., Clark, S. C., Seehra, J., London, L., & Perussia, B. (1984). Response of resting human peripheral blood natural killer cells to interleukin 2. *J Exp Med, 160*(4), 1147-1169. doi: 10.1084/jem.160.4.1147

Tsavaris, N., Kosmas, C., Vadiaka, M., Kanelopoulos, P., & Boulamatsis, D. (2002). Immune changes in patients with advanced breast cancer undergoing chemotherapy with taxanes. *Br J Cancer, 87*(1), 21-27. doi: 10.1038/sj.bjc.6600347

Upshaw, J. L., Arneson, L. N., Schoon, R. A., Dick, C. J., Billadeau, D. D., & Leibson, P. J. (2006). NKG2D-mediated signaling requires a DAP10-bound Grb2-Vav1 intermediate and phosphatidylinositol-3-kinase in human natural killer cells. *Nat Immunol, 7*(5), 524-532. doi: 10.1038/ni1325

Vivier, E., Tomasello, E., Baratin, M., Walzer, T., & Ugolini, S. (2008). Functions of natural killer cells. *Nat Immunol, 9*(5), 503-510. doi: 10.1038/ni1582

Waldhauer, I., Goehlsdorf, D., Gieseke, F., Weinschenk, T., Wittenbrink, M., Ludwig, A., . . . Steinle, A. (2008). Tumor-associated MICA is shed by ADAM proteases. *Cancer Res, 68*(15), 6368-6376. doi: 10.1158/0008-5472.CAN-07-6768

Waldhauer, I., & Steinle, A. (2006). Proteolytic release of soluble UL16-binding protein 2 from tumor cells. *Cancer Res, 66*(5), 2520-2526. doi: 10.1158/0008-5472.CAN-05-2520

Walliser, C., Hermkes, E., Schade, A., Wiese, S., Deinzer, J., Zapatka, M., . . . Gierschik, P. (2016). The Phospholipase Cgamma2 Mutants R665W and L845F Identified in Ibrutinib-resistant Chronic Lymphocytic Leukemia Patients Are Hypersensitive to the Rho GTPase Rac2 Protein. *J Biol Chem, 291*(42), 22136-22148. doi: 10.1074/jbc.M116.746842

Wang, L., Shalek, A. K., Lawrence, M., Ding, R., Gaublomme, J. T., Pochet, N., . . . Wu, C. J. (2014). Somatic mutation as a mechanism of Wnt/beta-catenin pathway activation in CLL. *Blood, 124*(7), 1089-1098. doi: 10.1182/blood-2014-01-552067

Wei, S. C., Duffy, C. R., & Allison, J. P. (2018). Fundamental Mechanisms of Immune Checkpoint Blockade Therapy. *Cancer Discov, 8*(9), 1069-1086. doi: 10.1158/2159-8290.CD-18-0367

Wherry, E. J., & Kurachi, M. (2015). Molecular and cellular insights into T cell exhaustion. *Nat Rev Immunol, 15*(8), 486-499. doi: 10.1038/nri3862

Wierda, W., O'Brien, S., Wen, S., Faderl, S., Garcia-Manero, G., Thomas, D., . . . Keating, M. (2005). Chemoimmunotherapy with fludarabine, cyclophosphamide, and rituximab for relapsed and refractory chronic lymphocytic leukemia. *J Clin Oncol, 23*(18), 4070-4078. doi: 10.1200/JCO.2005.12.516

Wierz, M., Pierson, S., Guyonnet, L., Viry, E., Lequeux, A., Oudin, A., . . . Moussay, E. (2018). Dual PD1/LAG3 immune checkpoint blockade limits tumor development in a murine model of chronic lymphocytic leukemia. *Blood, 131*(14), 1617-1621. doi: 10.1182/blood-2017-06-792267

Wiestner, A., Rosenwald, A., Barry, T. S., Wright, G., Davis, R. E., Henrickson, S. E., . . . Staudt, L. M. (2003). ZAP-70 expression identifies a chronic lymphocytic leukemia subtype with unmutated immunoglobulin genes, inferior clinical outcome, and distinct gene expression profile. *Blood, 101*(12), 4944-4951. doi: 10.1182/blood-2002-10-3306

Wilson, E. B., El-Jawhari, J. J., Neilson, A. L., Hall, G. D., Melcher, A. A., Meade, J. L., & Cook, G. P. (2011). Human tumour immune evasion via TGF-beta blocks NK cell activation but not survival allowing therapeutic restoration of anti-tumour activity. *PLoS One, 6*(9), e22842. doi: 10.1371/journal.pone.0022842

Woyach, J. A., Furman, R. R., Liu, T. M., Ozer, H. G., Zapatka, M., Ruppert, A. S., . . . Byrd, J. C. (2014). Resistance mechanisms for the Bruton's tyrosine kinase inhibitor ibrutinib. *N Engl J Med, 370*(24), 2286-2294. doi: 10.1056/NEJMoa1400029

Woyach, J. A., Johnson, A. J., & Byrd, J. C. (2012). The B-cell receptor signaling pathway as a therapeutic target in CLL. *Blood, 120*(6), 1175-1184. doi: 10.1182/blood-2012-02-362624

Woyach, J. A., Ruppert, A. S., Heerema, N. A., Zhao, W., Booth, A. M., Ding, W., . . . Byrd, J. C. (2018). Ibrutinib Regimens versus Chemoimmunotherapy in Older Patients with Untreated CLL. *N Engl J Med, 379*(26), 2517-2528. doi: 10.1056/NEJMoa1812836

Zanetti, M., & Mahadevan, N. R. (2012). Cancer. Immune surveillance from chromosomal chaos? *Science, 337*(6102), 1616-1617. doi: 10.1126/science.1228464

Zhang, Z., Wu, N., Lu, Y., Davidson, D., Colonna, M., & Veillette, A. (2015). DNAM-1 controls NK cell activation via an ITT-like motif. *J Exp Med, 212*(12), 2165-2182. doi: 10.1084/jem.20150792

Zitvogel, L., Kepp, O., & Kroemer, G. (2011). Immune parameters affecting the efficacy of chemotherapeutic regimens. *Nat Rev Clin Oncol, 8*(3), 151-160. doi: 10.1038/nrclinonc.2010.223

SUPPLEMENTARY FIGURES

Supplementary Figure 1.1

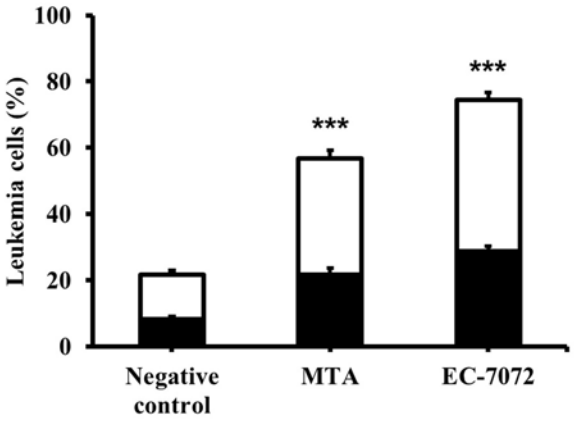

Supplementary Figure 1.1. EC-7072 has a cytotoxic effect similar to that of MTA. PBMCs from patients with CLL (n = 24) were treated with MTA (200 nM) or EC-7072 (200 nM) for 24 hours and leukemia cell death was evaluated by $DiOC_6(3)$/PI staining. Bars represent the mean percentages of apoptotic [$DiOC_6(3)^{low}$ PI^-] and dead [PI^+] cells. (Mean ± SEM; **p < 0.01; ***p < 0.001, Student's *t*-test).

Supplementary Figure 1.2

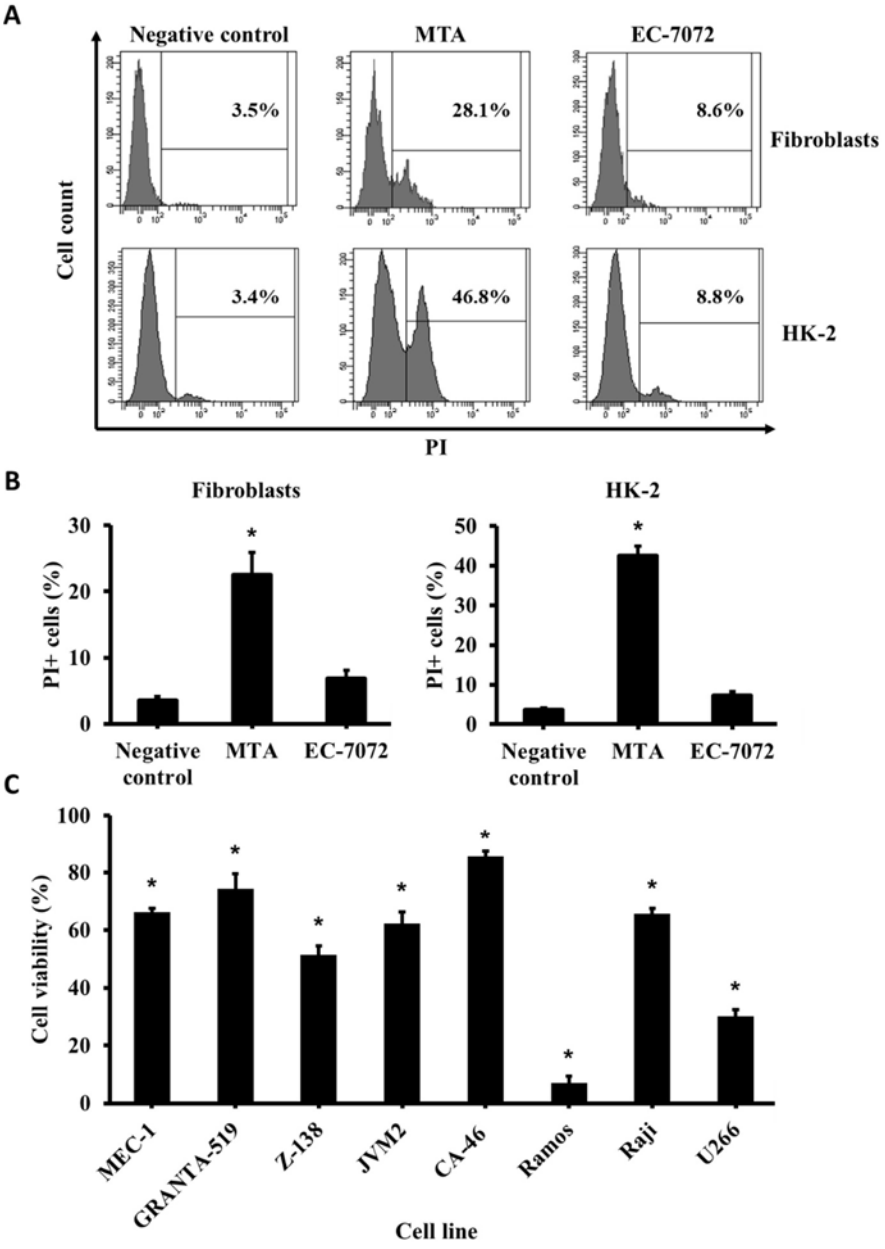

Supplementary Figure 1.2. EC-7072 does not markedly affect non-tumoral cells but is effective against different B-cell malignancies *in vitro*. Cell death was assessed by PI staining in primary fibroblasts from healthy donors (n = 4) and HK-2 cells (n = 3) incubated with MTA (200 nM) or EC-7072 (200 nM) for 24 hours. **A.** Histograms depict a representative experiment and percentages corresponding to dead cells [PI^+] are indicated for each panel. **B.** Bars represent the percentage of dead [PI^+] cells. **C.** Indicated cell lines were exposed to EC-7072 (500 nM) for 24 hours and cell viability was assessed by $DiOC_6(3)$/PI staining (n = 3). Bars represent the percentage of viable [$DiOC_6(3)^+$] cells normalized to control (DMSO) condition. (Mean ± SEM; *p < 0.05, Student's *t*-test).

Supplementary Figure 1.3

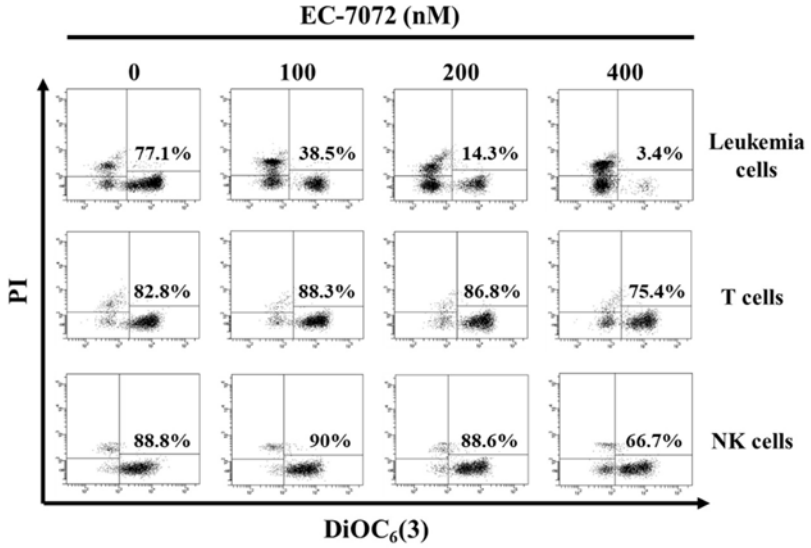

Supplementary Figure 1.3. EC-7072 negatively affect the viability of leukemia cells with no marked effect on healthy immune subsets. PBMCs from patients with CLL were exposed to increasing concentrations of EC-7072 (0-400 nM) and viability was determined for each immune subset by $DiOC_6(3)$/PI staining. Dot plots depict a representative experiment and percentage of viable [$DiOC_6(3)^+$] cells are indicated for each panel.

Supplementary Figure 1.4

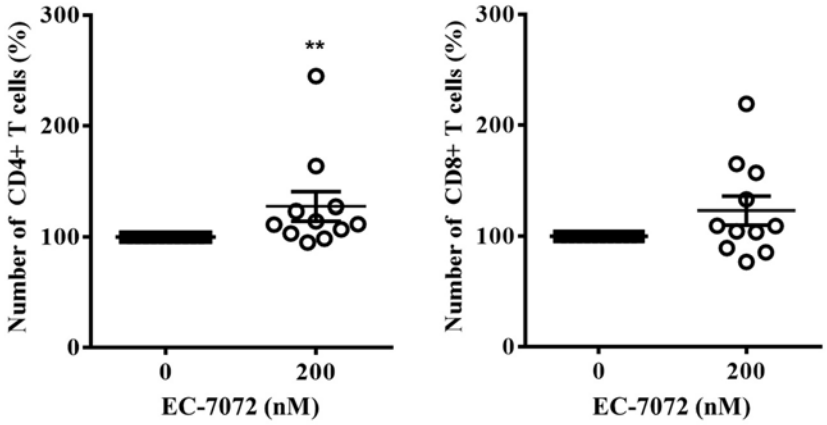

Supplementary Figure 1.4. The number of $CD8^+$ and $CD4^+$ T lymphocyte subsets from patients with CLL are not markedly altered by EC-7072. Numbers of $CD4^+$ and $CD8^+$ T cells were evaluated by flow cytometry in PBMCs from patients with CLL (n = 11) treated with EC-7072 (200 nM) for 24 hours. Graphs represent the normalized number of cells for each individual experiment. Dark lines correspond to mean ± SEM (**$p < 0.01$, Student's *t*-test).

Supplementary Figure 1.5

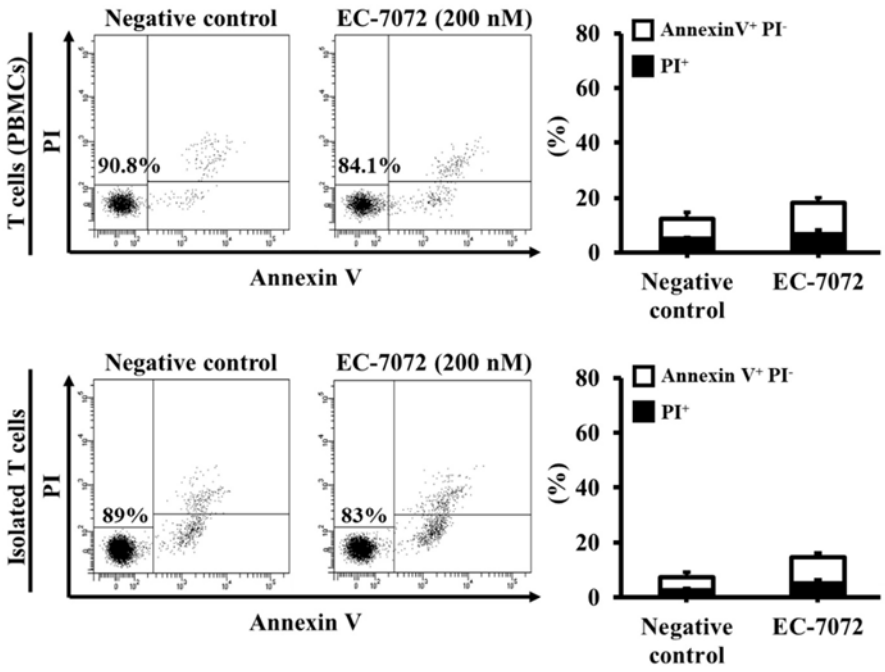

Supplementary Figure 1.5. EC-7072 does not significantly affect the viability of isolated T cells from patients with CLL. PBMCs and isolated T cells from patients with CLL (n = 3) were treated with EC-7072 (200 nM) for 24 hours and T cell apoptosis was assessed by Annexin V/PI staining. Dot plots show a representative patient and percentages within refer to viable [Annexin V^-] cells. Graphs depict the percentages of apoptotic [Annexin V^+ PI^-] and dead [PI^+] cells (mean ± SEM; Student's *t*-test).

Supplementary Figure 1.6

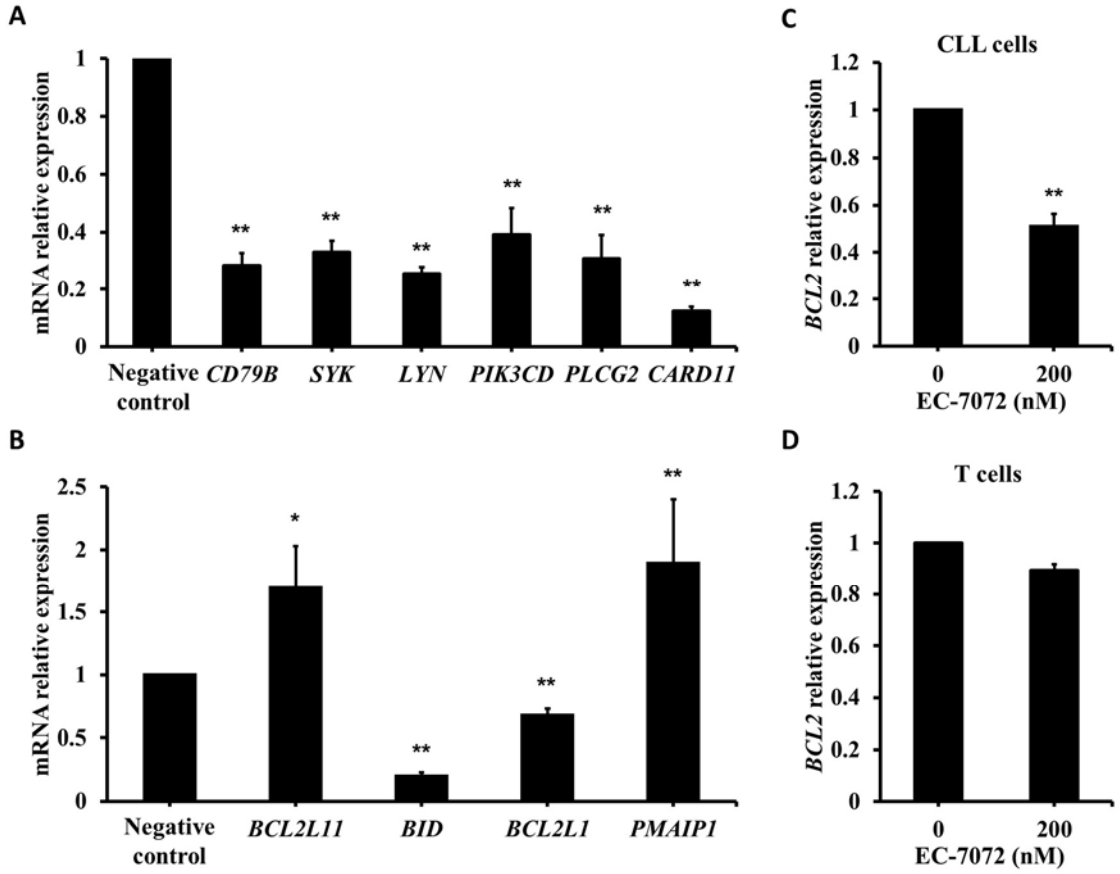

Supplementary Figure 1.6. EC-7072 modulates the transcriptome of primary CLL cells. Isolated CLL cells (n = 6) were treated with 200 nM EC-7072 for 6 hours. Total RNA was extracted and gene expression was analyzed by qPCR. **A.** Expression of BCR-related genes. **B.** Expression of relevant genes that regulate apoptosis in CLL. **C.** Expression of *BCL2*. **D.** Isolated T cells (n = 3) from patients with CLL were treated with EC-7072 (200 nM) for 6 hours and total RNA was extracted. Relative expression of *BLC2* was determined by qPCR. Graphs depict the relative gene expression normalized to the control (DMSO) condition. (Mean ± SEM; *p < 0.05; **p < 0.01, Student's *t*-test).

Supplementary Figure 1.7

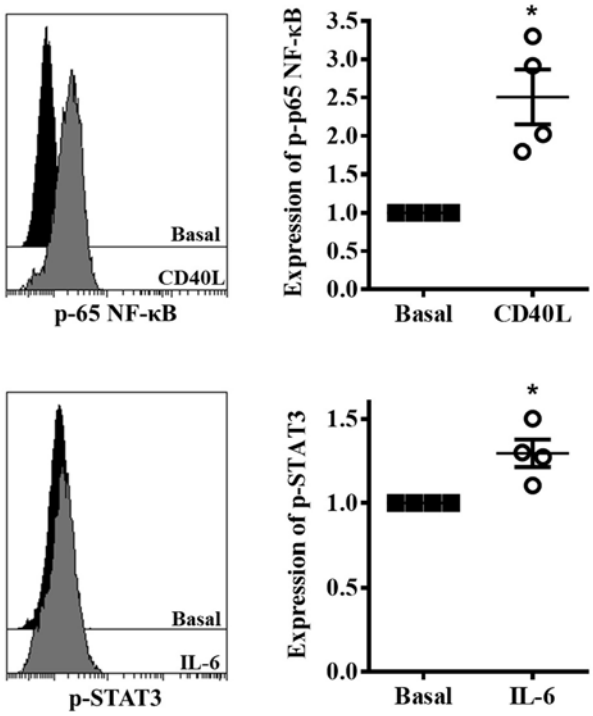

Supplementary Figure 1.7. Stimulation with specific activators enhances phosphorylation of BCR-related signaling nodes. Phosphorylation levels of p65 NF-κB and STAT3 were detected by phosphoflow in isolated CLL cells (n = 4) stimulated with CD40L (100 ng/mL) or IL-6 (40 ng/mL) for 15 minutes, respectively. Histograms show the MFI of a representative experiment. Graphs depict the normalized MFI for each individual patient and dark lines depict mean ± SEM (*p < 0.05, Student's *t*-test).

Supplementary Figure 1.8

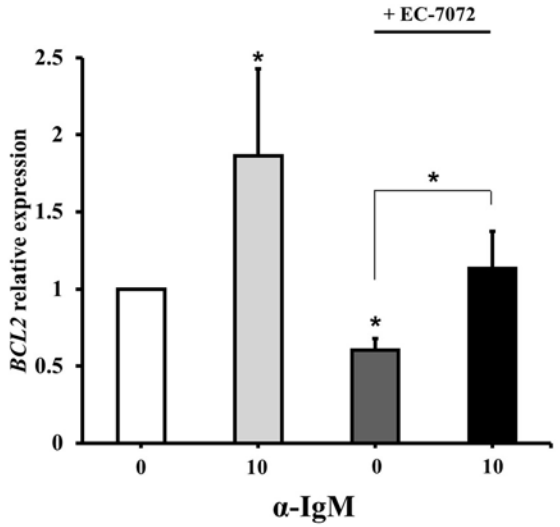

Supplementary Figure 1.8. BCR crosslinking restores the relative expression of *BCL2* to basal levels in the presence of EC-7072. Relative expression levels of *BCL2* were assessed by qPCR in isolated CLL cells incubated with EC-7072 (200 nM) and/or anti-IgM antibodies (10 µg/ml) for 6 hours. (Mean ± SEM; *p < 0.05, Student's *t*-test).

Supplementary Figure 1.9

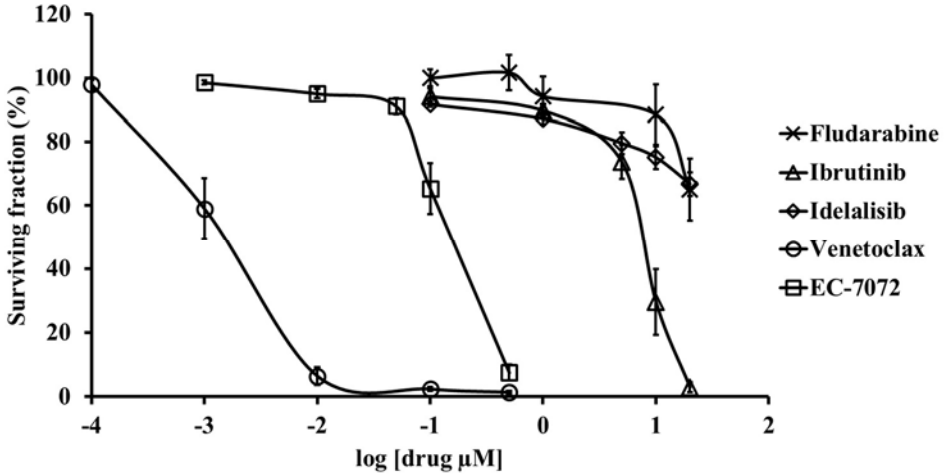

Supplementary Figure 1.9. The antileukemic activity of EC-7072 is comparable to that of therapies currently approved for CLL. Leukemia cell viability was determined in PBMCs from patients with CLL treated with increasing concentrations of EC-7072, fludarabine, ibrutinib, idelalisib or venetoclax. Dots represent the normalized percentage of viable [$DiOC_6(3)^+$] cells (Mean ± SEM).

Supplementary Figure 1.10

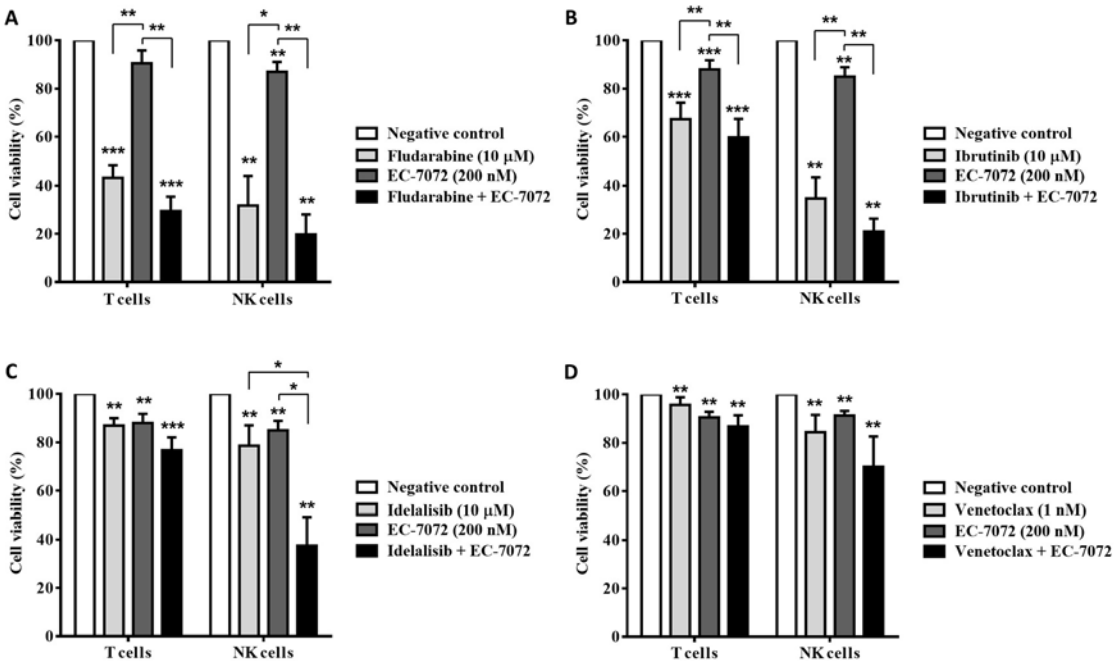

Supplementary Figure 2.10. Combination of EC-7072 with approved drugs results in increased toxicity to other immune subsets. PBMCs from patients with CLL were exposed to EC-7072 (200 nM) in combination with fludarabine (10 μM) (**A**), ibrutinib (10 μM) (**B**), idelalisib (10 μM) (**C**) or venetoclax (1 nM) (**D**) for 24 hours. Viability of T lymphocytes and NK cells was assessed by cytometric detection. Bars depict the normalized percentage of viable [$DiOC_6(3)^+$] cells. (Mean ± SEM; *p < 0.05, One-way ANOVA).

Supplementary Figure 2.1

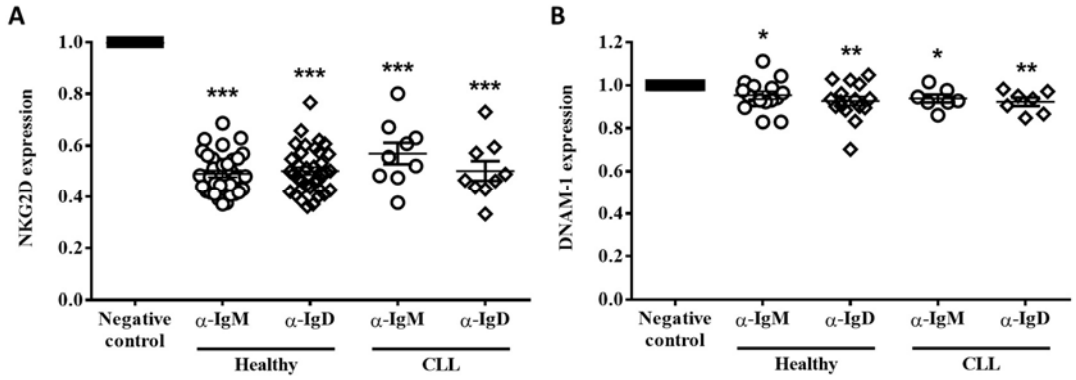

Supplementary Figure 2.1. BCR stimulation modulates the immunoreceptor profile of CD8$^+$ T cells. PMBCs from healthy donors (n = 16-36) or patients with CLL (n = 7-9) were incubated with F(ab')$_2$ anti-IgM (10 µg/mL) or anti-IgD (10 µg/mL) antibodies for 48 hours. Surface expression levels of NKG2D (**A**) and DNAM-1 (**B**) were evaluated in CD8$^+$ T cells by flow cytometry. Graphs depict the MFI for each receptor normalized to their respective control condition. (Mean ± SEM; *p < 0.05; **p < 0.01; ***p < 0.001, Student's t-test).

Supplementary Figure 2.2

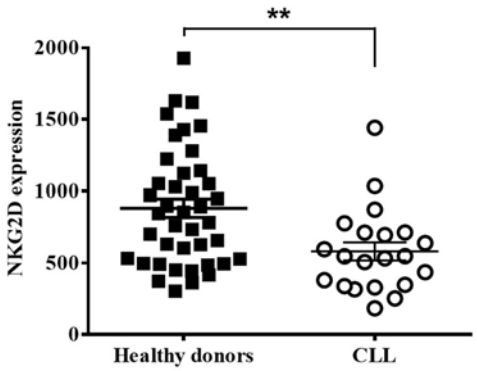

Supplementary Figure 2.2. NK cells from patients with CLL show reduced levels of NKG2D. NKG2D expression was determined in NK cells from healthy donors (n = 40) and patients with CLL (n = 21) by flow cytometry. The graph depicts the MFI for NKG2D. (Mean ± SEM; **p < 0.01, Mann-Whitney U test).

Supplementary Figure 2.3

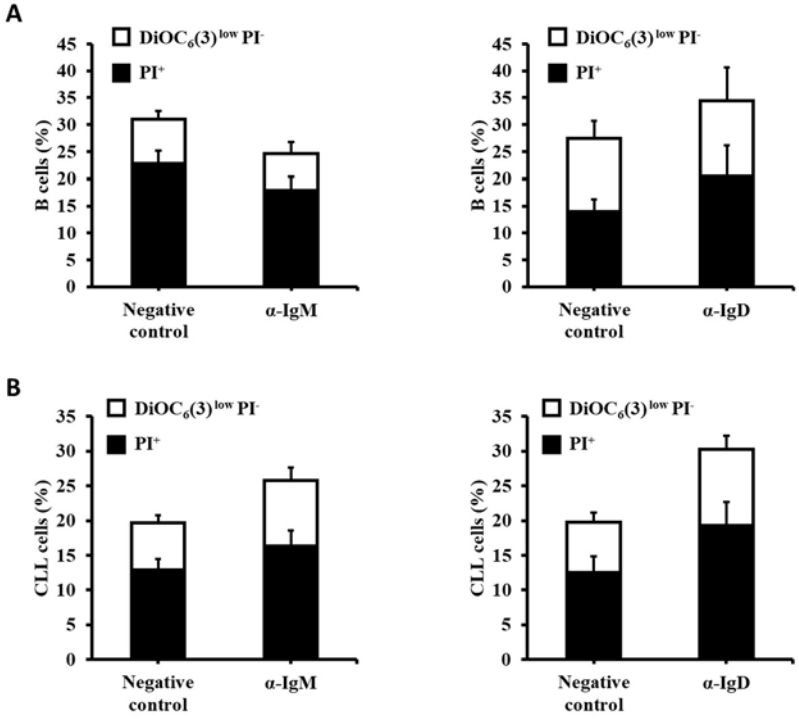

Supplementary Figure 2.3. BCR crosslinking does not affect B cell viability. PMBCs from healthy donors (n = 5-9) or patients with CLL (n = 5-9) were incubated with F(ab')$_2$ anti-IgM (10 µg/mL) or anti-IgD (10 µg/mL) antibodies for 48 hours. Cell death and apoptosis was evaluated in healthy B cells (**A**) and CLL cells (**B**) by cytofluorometric assessment of $DiOC_6(3)$/PI staining. Bars represent the normalized percentage of apoptotic [$DiOC_6(3)^{low}PI^-$] and dead cells [PI^+] for each receptor normalized to their respective control condition. (Mean ± SEM; Mann-Whitney U test).

Supplementary Figure 2.4

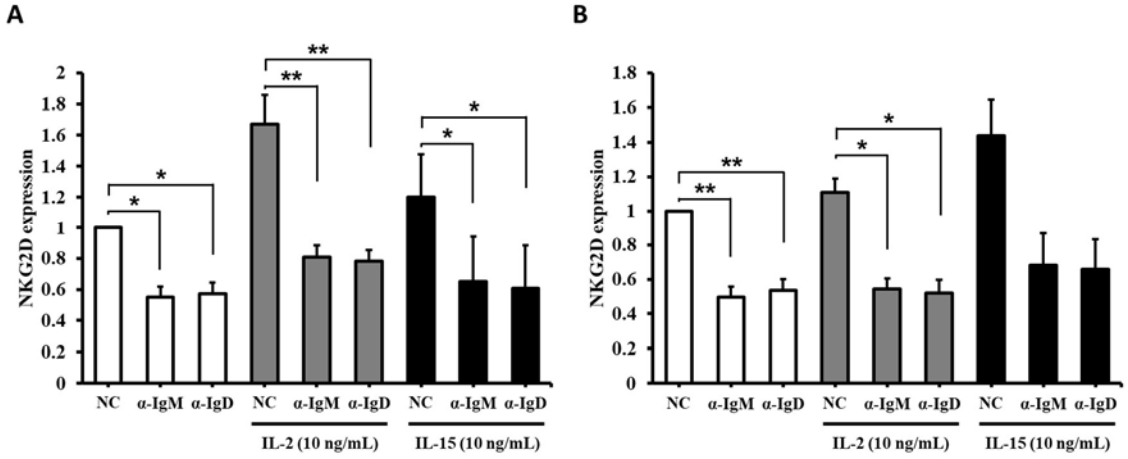

Supplementary Figure 2.4. Cytokine stimulation does not counteract the anti-BCR antibody-mediated downregulation of NKG2D. PMBCs from healthy donors (n = 4) were exposed F(ab')$_2$ anti-IgM or anti-IgD antibodies (10 µg/mL) with or without IL-2 (10 ng/mL) or IL-15 (25 ng/ml) for 48 hours. Surface expression levels of NKG2D were analyzed in NK cells (**A**) and CD8$^+$ T cells (**B**) by flow cytometry. Graphs represent the normalized MFI. (Mean ± SEM; *p < 0.05; **p < 0.01, One-way ANOVA).

Supplementary Figure 2.5

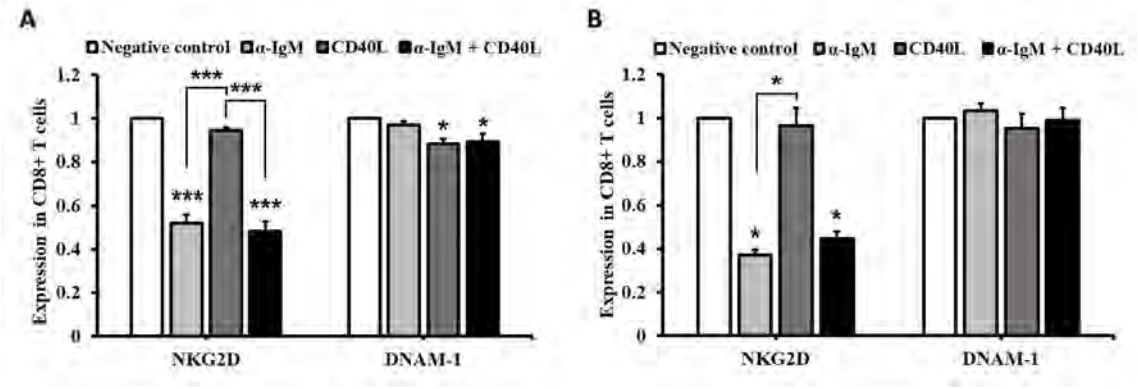

Supplementary Figure 2.5. Co-stimulation of B cells with CD40 ligand does not potentiate NKG2D downregulation in CD8$^+$ T cells. PMBCs from healthy donors (n = 4-6) (**A**) or patients with CLL (n = 3) (**B**) were incubated with F(ab')$_2$ anti-IgM antibodies (10 µg/mL) and/or CD40L (200 ng/mL) for 48 hours. Surface expression levels of NKG2D and DNAM-1 were determined in CD8$^+$ T cells by flow cytometry. Bars show the normalized MFI for each receptor. (Mean ± SEM; *p < 0.05; ***p < 0.001, One-way ANOVA).

Supplementary Figure 2.6

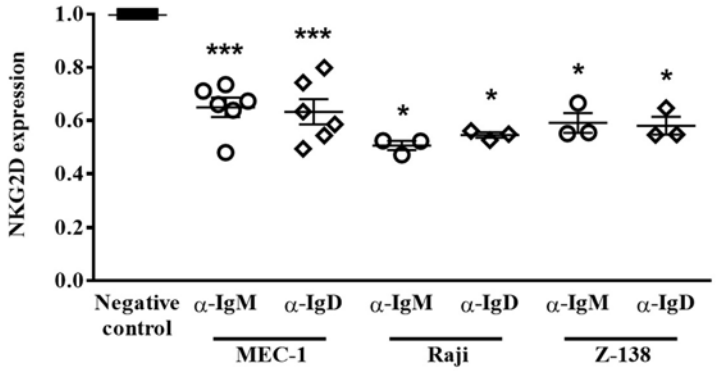

Supplementary Figure 2.6. NK cells suffer NKG2D downregulation after exposure to conditioned media from stimulated B cell malignant cell lines. MEC-1, Raji and Z-138 cells (n = 3-6) were treated with $F(ab')_2$ anti-IgM (10 µg/mL) or anti-IgD (10 µg/mL) antibodies for 48 hours and supernatants were collected. PBMCs from healthy donors were cultured in conditioned media for 48 hours and NKG2D expression was analyzed by flow cytometry. The graph depicts the normalized MFI for each experiment. (Mean ± SEM; *p < 0.05; ***p < 0.001, Student's t-test).

Supplementary Figure 3.1

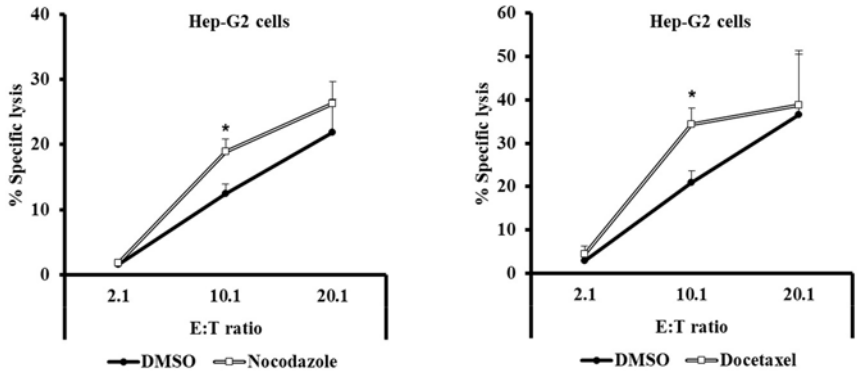

Supplementary Figure 3.1. Hyperploid tumor cells are more susceptible to NK cell-mediated lysis. Hep-G2 cells treated with 100 nM nocodazole or 3 nM docetaxel for 48 hours were cocultured with NKL cell line at three different E:T ratios and cytotoxicity was evaluated by flow cytometry. Graphs represent the percentage of specific lysis (mean ± SEM; *p < 0.05, Mann-Whitney U test).

Supplementary Figure 3.2

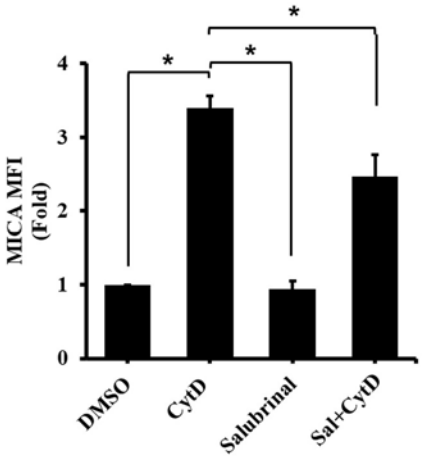

Supplementary Figure 3.2. ER stress is implicated in the upregulation of MICA in hyperploid tumor cells. HCT-116 cells were exposed to 0.6 µg/ml cytochalasin D (CytD) and or 20 µM salubrinal for 48 hours and MICA expression was evaluated by flow cytometry (n = 3). Graph shows the normalized MFI. (Mean ± SEM; *p < 0.05, Mann-Whitney U test).

Supplementary Figure 3.3

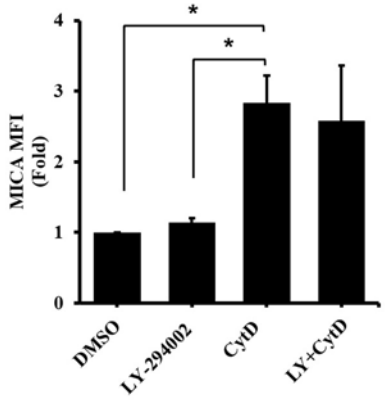

Supplementary Figure 3.3. PI3K blockade does not revert MICA upregulation in hyperploid cells. HCT-116 cells were exposed to 0.6 µg/ml cytochalasin D (CytD) and or 10 µM LY-294002 for 48 hours and MICA expression was analyzed by flow cytometry (n = 3). Graph shows the normalized MFI. (Mean ± SEM; *p < 0.05, Mann-Whitney U test).